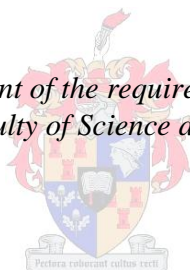


A study of isotope-effects in high-resolution ^{195}Pt NMR spectra of octahedral complexes of the type $[\text{PtCl}_{6-n}(\text{OH})_n]^{2-}$, $n = 0-6$, in water

by
Leon de Villiers Engelbrecht

*Thesis presented in fulfilment of the requirements for the degree of
Master of Science in the Faculty of Science at Stellenbosch University*



Supervisor: Prof Klaus R. Koch

March 2013

Declaration

By submitting this thesis/dissertation electronically, I declare that the entirety of the work contained therein is my own, original work, that I am the sole author thereof (save to the extent explicitly otherwise stated), that reproduction and publication thereof by Stellenbosch University will not infringe any third party rights and that I have not previously in its entirety or in part submitted it for obtaining any qualification.

Date: March 2013

Acknowledgements

I would like to express my sincere gratitude toward the following persons:

My supervisor, Prof Klaus Koch, for his enthusiasm, guidance and encouragement

Dr Wilhelmus Gerber, for his interest and for helpful discussion

AngloPlatinum and the University of Stellenbosch for financial support

Elsa Malherbe and Jaco Brand of the NMR facility

*Deidre Davids, Shafiek Mohammed and Roger Lawrence of the Analytical Chemistry
Division Staff*

The members of the PGM Research Group for their friendship and encouragement

Family and friends for their love and support

Abstract

The high-resolution ^{195}Pt NMR signals (128.8 MHz) of most of the octahedral mixed-ligand Pt(IV) complexes in the series $[\text{PtCl}_{6-n}(\text{OH})_n]^{2-}$, $n = 0-6$, have been recorded in aqueous solutions at 293 K. These signals show characteristic $^{35/37}\text{Cl}$ isotope-induced fine structure that results from the presence of several *isotopologues* in samples with a natural chlorine isotope distribution; each ^{37}Cl isotope incorporated into the Pt coordination sphere of one of these complexes affords a fixed upfield (low frequency) *isotope shift* of between 0.17 and 0.22 ppm, depending on the particular complex. This assignment is confirmed by the excellent agreement between the natural abundances of the various isotopologues and the relative contributions of the corresponding signals to the overall area of the experimental spectrum of the particular isotopologue set, obtained by a non-linear least-squares line fitting procedure. These results confirm that the ^{195}Pt magnetic shielding in *isotopomers* differing only in the combination of the two chlorine isotopes coordinated in sites *trans* to hydroxido-ligands are indistinguishable under these experimental conditions, unlike those of similar isotopomers in the related series of *aqua*-complexes $[\text{PtCl}_n(\text{H}_2\text{O})_{6-n}]^{4-n}$, $n = 3-5$, as reported by Koch and co-workers. Moreover, the order of ^{195}Pt shielding for the members of all stereoisomer pairs in the series of hydroxido-complexes is the reverse of that reported for the corresponding pairs in the aqua-series. These and other observations are interpreted qualitatively in terms of the relative strengths of the *trans*-influences of aqua-, hydroxido- and chlorido-ligands and the effect of these on bond displacements in these complexes. The ^{195}Pt NMR spectra of especially the complexes *cis*- $[\text{PtCl}_2(\text{OH})_4]^{2-}$ and $[\text{PtCl}(\text{OH})_5]^{2-}$ show remarkable fine structure in a *ca.* 45 % ^{18}O -enriched aqueous solution; apart from additional signals resulting from ^{18}O -containing isotopologues, the resonance signals of isotopomers differing in the combination of $^{16/18}\text{O}$ isotopes in sites *trans* to chlorido-ligands are partially resolved.

The effect of temperature on the $^{35/37}\text{Cl}$ isotope-induced fine structure in the ^{195}Pt signals of $[\text{PtCl}_6]^{2-}$ and $[\text{PtCl}(\text{OH})_5]^{2-}$ was investigated in the range 283-308 K; some interesting differences are observed. ^{195}Pt relaxation time measurements for $[\text{PtCl}_6]^{2-}$ in this temperature range reveal that line-broadening is at least partially responsible for the loss of resolution between the signals of isotopologues of this complex as the temperature is increased, possibly due to the spin-rotation relaxation mechanism. The temperature coefficient of ^{195}Pt shielding and the magnitude of isotope shifts in the spectra of the complexes in this series show

interesting correlations with the ^{195}Pt shielding itself; an interpretation of these observations is presented.

Opsomming

Die hoëresolusie ^{195}Pt NMR seine (128.8 MHz) van die oktaëdriese gemengde-ligand Pt(IV) komplekse in die reeks $[\text{PtCl}_{6-n}(\text{OH})_n]^{2-}$ is waargeneem in waterige oplossing by 'n temperatuur van 293 K. Hierdie seine toon 'n karakteristieke $^{35/37}\text{Cl}$ isotoop-geïnduseerde fynstruktuur as gevolg van die teenwoordigheid van verskeie isotopoloë in monsters met 'n natuurlike chloor isotoopverspreiding. Die verplasing van 'n ^{35}Cl isotoop deur 'n ^{37}Cl isotoop in die Pt koördinasiesfeer van hierdie komplekse lei tot 'n laefrekwensie isotoopverskuiwing van die ^{195}Pt resonansiesein van tussen 0.17 en 0.22 ppm, afhangend van die spesifieke kompleks. Die toekenning van resonansieseine in hierdie spektra word ondersteun deur die goeie ooreenstemming tussen die berekende natuurlike verspreiding van isotopoloë en die persentasie area bydrae van die ooreenstemmende pieke tot die area van volledige stel seine van die chemiese spesie, soos bepaal deur 'n nie-linieêre kleinste-kwadratiese passingsmetode. Hierdie resultate bevestig dat vir *isotopomere* waarvan slegs die kombinasie van chloorisotope wat in posisies *trans* tot hidroksido-ligande gekoördineer is 'n ononderskeibare ^{195}Pt magnetiese skerming waargeneem word, m.a.w. 'n enkele resonansiesein word vir hierdie isotopomere gemeet, anders as gerapporteer deur Koch en medewerkers vir die verwante aqua-komplekse $[\text{PtCl}_n(\text{H}_2\text{O})_{6-n}]^{4-n}$ waar $n = 3-5$. Verder is die order van ^{195}Pt magnetiese skerming vir stereoisomere in hierdie hidroksido-komplekse in elke stereoisomere paar die teenoorgestelde van dit waargeneem vir die ooreenstemmende aqua-komplekse. Hierdie waarnemings word kwalitatief geïnterpreteer in terme van die verskillende *trans*-invloede van die chlorido-, aqua- en hidroksido-ligande en die effekte daarvan op bindingslengtes in die komplekse. In 'n ongeveer 45 % ^{18}O -verrykte monster toon die ^{195}Pt seine van veral die komplekse *cis*- $[\text{PtCl}_2(\text{OH})_4]^{2-}$ en $[\text{PtCl}(\text{OH})_5]^{2-}$ uitsonderlike fynstruktuur vanweë die addisionele seine van ^{18}O -bevattende isotopoloë en die partiële resolusie van die seine van isotopomere wat verskil in die kombinasie van $^{16/18}\text{O}$ isotope wat *trans* tot chlorido-ligande gekoördineer is.

'n Studie is gemaak van die uitwerking van temperatuur op die $^{35/37}\text{Cl}$ isotoop-geïnduseerde fynstruktuur in die ^{195}Pt seine van die komplekse $[\text{PtCl}_6]^{2-}$ en $[\text{PtCl}(\text{OH})_5]^{2-}$ in die gebied 283-308 K; interessante verskille is waargeneem. ^{195}Pt magnetiese relaksasietyd metings vir die

kompleks $[\text{PtCl}_6]^{2-}$ in waterige oplossing in hierdie temperatuurgebied toon dat verbreding van resonansieseine ten minste gedeeltelik verantwoordelik is vir die waargenome verlies aan resolusie tussen die seine van isotopoloë namate die temperatuur styg; die verbreding van seine kan waarskynlik aan die spin-rotasie relaksasiemeganisme toegeskryf word. Die temperatuurkoëffisiënt van ^{195}Pt magnetiese skerming en die grootheid van isotoopverskuiwings in die spektra van die hidroksido-komplekse in hierdie reeks toon interessante korrelasies tot die ^{195}Pt magnetiese skerming; 'n interpretasie van hierdie waarnemings word voorgestel.

Contents

Declaration.....	ii
Acknowledgements.....	iii
Abstract.....	iv
Table of Contents.....	vii
List of Figures.....	ix
Abbreviations.....	xi

Chapter 1: Introduction

1.1 General Introduction	1
1.2 Applications of ^{195}Pt NMR spectroscopy.....	3
1.3 Isotope-effects in ^{195}Pt NMR spectroscopy.....	8
1.4 Objectives.....	18

Chapter 2: Experimental

2.1 ^{195}Pt NMR spectroscopy	19
2.2 Reagents and sample preparation.....	21

Chapter 3: Isotope-effects in the ^{195}Pt NMR spectra of the complexes $[\text{PtCl}_{6-n}(\text{OH})_n]^{2-}$, $n = 0-6$

3.1 Ligand substitution reactions	23
3.2 Results and Discussion.....	26
3.2.1 $^{35/37}\text{Cl}$ isotope-effects in ^{195}Pt NMR spectra.....	26
3.2.2 $^{16/18}\text{O}$ isotope-effects in ^{195}Pt NMR spectra.....	37
3.3 Temperature dependence of isotope-induced fine structure	47

Chapter 4: ^{195}Pt nuclear magnetic relaxation in the complexes $[\text{PtCl}_{6-n}(\text{OH})_n]^{2-}$, $n = 0-6$

4.1 Introduction	56
4.2 Results and Discussion.....	63
Chapter 5: Conclusions	78
References.....	81
Appendix.....	87

List of Figures

- Figure 1.1** Molecular structures of $[\text{PtCl}_6]^{2-}$, $[\text{PtCl}_5(\text{OH})]^-$ and $\text{cis-}[\text{PtCl}_4(\text{OH})_2]^0$.
- Figure 1.2** Schematic representation of the basic modes of adsorption of $[\text{PtCl}_6]^{2-}$ to alumina surface in aqueous solution.
- Figure 1.3** Schematic representation of the mechanism of spin-orbit coupling contribution to nuclear magnetic shielding.
- Figure 1.4** ^{195}Pt NMR spectra of $[\text{PtCl}_6]^{2-}$ in aqueous solution at 294 K at 1.4, 4.7 and 9.4 T magnetic fields (reproduced from Sadler *et al.*¹⁹).
- Figure 1.5** ^{195}Pt NMR spectra of $[\text{PtCl}_5(\text{H}_2\text{O})]^-$ and $\text{cis-}[\text{PtCl}_4(\text{H}_2\text{O})_2]^0$ in aqueous solution at 293 K (reproduced from Murray *et al.*³⁷) with molecular structures.
- Figure 1.6** ^{195}Pt NMR spectra of the stereoisomers $\text{cis/trans-}[\text{PtCl}_2(\text{H}_2\text{O})_4]^{2+}$ in aqueous solution at 293 K with molecular structures (reproduced from Murray *et al.*³⁸).
- Figure 1.7** ^{195}Pt NMR spectra of $\text{cis-}[\text{PtCl}_4(\text{H}_2\text{O})_2]^0$ and $\text{cis-}[\text{PtCl}_2(\text{H}_2\text{O})_4]^{2+}$ in ^{18}O -enriched aqueous solution at 293 K (reproduced from Murray *et al.*³⁸).
- Figure 2.1** Example of ^{195}Pt T_1 and T_2 measurements (14.1 T) for $[\text{PtCl}_6]^{2-}$ anion in aqueous solution at 273 K.
- Figure 2.2** Plots of T_1 and T_2 data for $[\text{PtCl}_6]^{2-}$ with exponential functions fitted.
- Figure 3.1** Full ^{195}Pt NMR spectrum (14.1 T) of the series of complexes $[\text{PtCl}_{6-n}(\text{OH})_n]^{2-}$, $n = 0-6$, in aqueous solution at 293 K.
- Figure 3.2** Plot of ^{195}Pt chemical shift as a function of number of hydroxido-ligands in Pt coordination sphere for the series of complexes $[\text{PtCl}_{6-n}(\text{OH})_n]^{2-}$, $n = 0-6$; ‘chemical shift trend-analysis’.
- Figure 3.3** ^{195}Pt NMR signals of complexes in the series $[\text{PtCl}_{6-n}(\text{OH})_n]^{2-}$, $n = 0-6$, in aqueous solution at 293 K showing isotope-induced fine structure, with model functions fitted.
- Figure 3.4** Molecular structures of complexes $\text{cis-}[\text{PtCl}_4(\text{H}_2\text{O})_2]^0$ and $\text{cis-}[\text{PtCl}_4(\text{OH})_2]^{2-}$ showing positions of expected Pt-Cl bond contraction and extension.
- Figure 3.5** Molecular structures of stereoisomer pairs $\text{cis/trans-}[\text{PtCl}_2(\text{H}_2\text{O})_4]^{2+}$ and $\text{cis/trans-}[\text{PtCl}_2(\text{OH})_4]^{2-}$ showing expected bond contraction and extension.

- Figure 3.6** ^{195}Pt NMR spectra of complexes $[\text{PtCl}_5(\text{OH})]^{2-}$, $\text{cis-}[\text{PtCl}_4(\text{OH})_2]^{2-}$, $\text{fac-}[\text{PtCl}_3(\text{OH})_3]^{2-}$, $\text{trans/cis-}[\text{PtCl}_2(\text{OH})_4]^{2-}$, $[\text{PtCl}(\text{OH})_5]^{2-}$ and $[\text{Pt}(\text{OH})_6]^{2-}$ in ^{18}O -enriched aqueous solution at 293 K, with model functions fitted.
- Figure 3.7** Molecular structures of $\text{cis-}[\text{PtCl}_4(\text{H}_2\text{O})_2]^0$ and $\text{cis-}[\text{PtCl}_2(\text{OH})_4]^{2-}$ showing respectively Pt-Cl and Pt-O bond contraction; structures of isotopomers assigned to Signals 1 and 2 in Figure 3.6.
- Figure 3.8** Molecular structures of isotopomers assigned to Signals 3 and 4 in Figure 3.6; structures of $[\text{PtCl}(\text{OH})_5]^{2-}$ and $\text{cis-}[\text{PtCl}_2(\text{H}_2\text{O})_4]^{2-}$ showing positions of expected Pt-O bond contraction and extension.
- Figure 3.9** ^{195}Pt NMR signals of $[\text{PtCl}_6]^{2-}$ and $[\text{PtCl}(\text{OH})_5]^{2-}$ in aqueous solutions at various temperatures between 283 and 308 K.
- Figure 3.10** ^{195}Pt chemical shifts of $[\text{PtCl}_6]^{2-}$ and $[\text{PtCl}(\text{OH})_5]^{2-}$ plotted as function of temperature in range 283 to 313 K with linear trends fitted.
- Figure 3.11** $^{35/37}\text{Cl}$ and $^{16/18}\text{O}$ isotope shifts in ^{195}Pt signals of complexes $[\text{PtCl}_{6-n}(\text{OH})_n]^{2-}$, $n = 0-6$, plotted as function of ^{195}Pt chemical shift with linear trends.
- Figure 3.12** ^{195}Pt signals of $\text{fac-}[\text{PtCl}_3(\text{OH})_3]^{2-}$ in aqueous solution at 293 and 278 K; ^1H signals of $\text{H}_2\text{O}/\text{HDO}$ in same solution at 278 K.
- Figure 4.1** Logarithmic plot of ^{195}Pt T_1 and T_2 data for $[\text{PtCl}_6]^{2-}$ in aqueous solution plotted as a function of inverse absolute temperature with linear trends fitted.
- Figure 4.2** ^{195}Pt T_1 and T_2 data for $[\text{PtCl}_6]^{2-}$ in aqueous solution plotted as a function of inverse absolute temperature.
- Figure 4.3** ^{195}Pt R_1 and R_2 data for $[\text{PtCl}_6]^{2-}$ in aqueous solution plotted as a function of inverse absolute temperature.
- Figure 4.4** Molecular model of microsolvated cluster $[\text{PtCl}_5(\text{H}_2\text{O})]^- \cdot 2\text{H}_2\text{O}$ showing hydrogen bonding interactions (reproduced from Davis *et al.*⁴⁹).

Abbreviations

acac	acetylacetonato (ligand)
COSMO	continuum solvent model
CPCM	conductor-like polarizable continuum model
CPMG	Carr-Purcell-Meiboom-Gill (pulse sequence)
CSA	chemical shift anisotropy
DD	dipole-dipole
DFT	density functional theory
DOSY	diffusion-ordered spectroscopy
EFG	electric field gradient
<i>n.o.</i>	not observed
NOE	nuclear Overhauser effect
PBE	Perdew-Burke-Ernzerhof (functional)
PGMs	platinum group metals
PGSE	pulsed gradient spin-echo
rf	radio frequency
SC	scalar coupling
SO	spin-orbit
SR	spin-rotation
SRFK	scalar relaxation of the first kind
SRSK	scalar relaxation of the second kind
UV-vis	ultraviolet-visible
ZORA	zeroth-order regular approximation

1

Introduction

1.1 General Introduction

South Africa is the world's leading primary producer of platinum group metals (PGMs: Pt, Pd, Rh, Ru, Ir and Os), supplying annually more than three quarters of the world's total platinum production.¹ Especially platinum and rhodium are in great demand as they are used in automobile emission control devices and in other catalytic conversion schemes in the chemical industry.² PGM refining typically involves dissolution of crude PGM mixtures in highly acidic oxidising aqueous solutions, followed by selective extraction (separation) of the various PGMs from these process solutions; while this last step may seem trivial, efficient recovery of precious metals on a large scale is of critical importance to these industries and extensive research efforts are devoted to optimisation of recovery schemes.^{2,3}

Modern PGM recovery schemes typically employ solvent extraction or anion exchange methods and, more recently, methods based on supramolecular recognition of PGM anions by alkylamine-type compounds to transfer these PGM anions from aqueous process solutions to non-aqueous receptor phases.^{3,4} In the case of platinum recovery, these methods generally exploit the favourable properties of the octahedral Pt(IV) chlorido-complex, $[\text{PtCl}_6]^{2-}$; the hydrolysis product $[\text{PtCl}_5(\text{H}_2\text{O})]^{2-}$ has been demonstrated to be less readily extracted by these methods.^{2,3} (See Figure 1.1.) Depending on the solution conditions (platinum and halide content, acidity and temperature) a number of mixed-ligand complexes of the type $[\text{PtCl}_n(\text{H}_2\text{O})_{6-n}]^{4-n}$ and their deprotonated analogues $[\text{PtCl}_{6-n}(\text{OH})_n]^{2-}$, $n = 1-6$, may be present in solution and these are similarly thought to be less extractable.⁵ It follows that a detailed knowledge of the chemical 'species' present in these solutions is of great importance when

1 Introduction

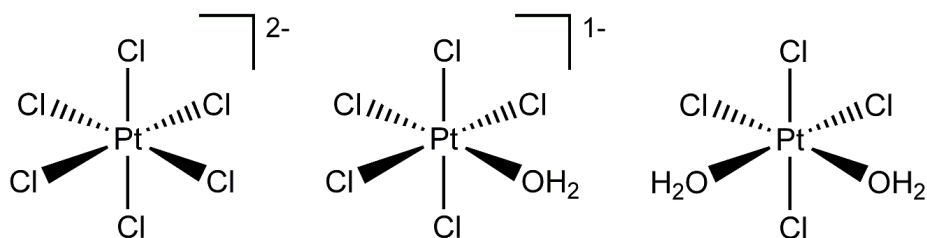


Figure 1.1 Molecular structures of the octahedral complexes $[\text{PtCl}_6]^{2-}$, $[\text{PtCl}_5(\text{H}_2\text{O})]^{-}$ and *cis*- $[\text{PtCl}_4(\text{H}_2\text{O})_2]^0$, typically present in dilute acidic aqueous solutions of a salt of $[\text{PtCl}_6]^{2-}$.

pursuing efficient recovery of platinum from process solutions and in the development of more efficient recovery schemes. These so-called ‘speciation’ studies and related studies of the kinetics of these hydrolysis reactions were initially undertaken largely by UV-visible spectrophotometry, but these methodologies are limited primarily by the low resolution inherent to this technique.^{6,7}

The speciation of the $[\text{PtCl}_6]^{2-}$ anion in aqueous solutions is also of particular importance to the supported catalyst preparation industry; support materials are typically wetted/immersed in dilute aqueous solutions of H_2PtCl_6 , which are usually mildly acidic, during the preparation of supported platinum catalysts for use in the naphtha refining industry.^{8,9} During this wetting period, platinum complexes are adsorbed on the large surface of the support material; initial interaction of these complexes with the support is thought to be of an electrostatic nature (the surfaces of these support materials are usually charged in solution, typically by protonation or pre-treatment with chloride; Figure 1.2A), while specific interactions, e.g. hydrogen bonding, may also contribute.¹⁰ These initial modes of interaction are thought to be followed by slower thermally activated ‘grafting’ which involves changes in the primary coordination sphere of the platinum complex at the solution-support interface (Figure 1.2).

Depending on the zero-charge point of the support, however, the pH of these solutions may change significantly during wetting of the support and this could have an effect on the chemical species present in this so-called impregnation solution; it has been suggested that complexes containing O donor atoms (aqua- and hydroxido-complexes) interact differently with high surface area alumina supports compared to $[\text{PtCl}_6]^{2-}$ and this, in turn, has a significant effect on the metal deposition properties of the final supported catalyst.¹⁰ The distribution of metallic platinum clusters on the support is of critical importance in this industry since it determines the efficiency of the supported platinum catalyst; numerous

1 Introduction

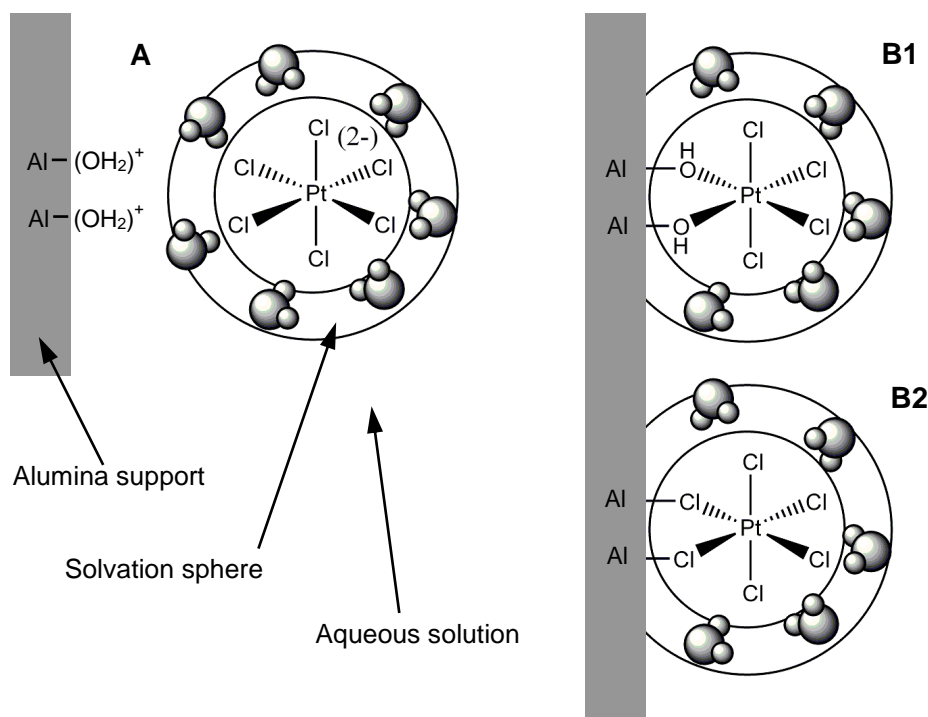


Figure 1.2 Scheme showing the basic models of adsorption of $[\text{PtCl}_6]^{2-}$ to alumina surface in an aqueous solution of H_2PtCl_6 : electrostatic adsorption of the solvated anionic complex (A) and two proposed modes of grafting ('inner-sphere complex formation') (B1 and B2). Grey space-filling units represent water molecules in the solvation sphere of the complex. Note that this scheme is not intended to convey accurate information regarding the true nature or composition of the solvation sphere; scheme drawn after Shelimov *et al.*¹⁰

research efforts have been aimed at producing highly dispersed supported platinum catalysts with small metal clusters since these make for most efficient catalysts (high surface area and best utilisation of precious metal)¹¹ In fact, it has been suggested that while a great many empirical observations have been reported regarding the effect of a large number of variables, e.g. temperature and pH, on the properties of supported platinum catalysts,¹² until very recently these phenomena were only poorly understood on a molecular mechanistic level.¹¹

1.2 Applications of ^{195}Pt NMR spectroscopy

The fairly abundant (*ca.* 34 %) ^{195}Pt isotope is a useful nuclear magnetic resonance (NMR) probe owing to favourable magnetic properties ($I = 1/2$, $\gamma = 5.768 \times 10^7 \text{ rad}\cdot\text{s}^{-1}\cdot\text{T}^{-1}$) and the exceptional sensitivity of magnetic shielding (σ) to chemical changes; the known ^{195}Pt chemical shift (δ) range in solution is greater than 12 000 ppm.¹³ (Note convention: $\delta = \sigma_{\text{ref}} - \sigma$, where σ_{ref} is the shielding of a reference nucleus) ^{195}Pt NMR has long been used to study complexes of this metal in solution¹³, the first direct observation of ^{195}Pt magnetic resonance

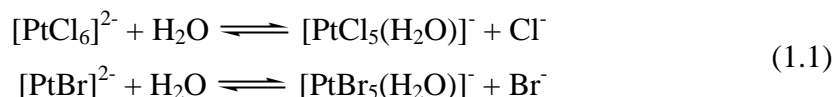
1 Introduction

having been reported by Proctor and Yu some sixty years ago in an aqueous solution of H_2PtCl_6 .¹⁴ A survey of the literature soon reveals that these studies are numerous, with a number of reviews having been published over the years (in fact, ^{195}Pt is among the most often studied transition metal nuclei), and that the vast majority of ^{195}Pt NMR work has been performed on square-planar Pt(II) complexes, owing largely to the additional interest in these compounds as biologically-active agents and catalysts.^{13,15,16} ^{195}Pt chemical shifts and large 1J and 2J scalar coupling of ^{195}Pt to especially ^1H , ^{13}C , ^{15}N and ^{31}P was found to be extremely useful in the characterisation of novel platinum complexes in solution; measurement of these properties are still very popular in the study of the interaction of Pt(II) agents with DNA and in other biological processes, as exemplified by the work Aldrich-Wright and co-workers.¹⁶ Early ^{195}Pt NMR studies of simple octahedral Pt(IV) complexes in solution, notably by van Zelewsky¹⁷, Pesek and Mason¹⁸ and Sadler and co-workers¹⁹, have demonstrated that these complexes could be similarly characterised, while the large effect of temperature changes and isotopic substitution (mass) of ligating atoms on ^{195}Pt chemical shifts also emerged from these studies, stimulating theoretical work aimed at understanding these phenomena.^{20,21}

On a more practical front, Goodfellow *et al.*²² have demonstrated that the 10 complexes in the series $[\text{PtCl}_{6-n}(\text{OH})_n]^{2-}$ with $n = 0-6$, including all stereoisomers, could be resolved and identified from ^{195}Pt chemical shifts in alkaline aqueous solutions; the replacement of chloride by hydroxide ion in the Pt coordination sphere was found to result in approximately additive incremental decreases in ^{195}Pt shielding of about 500 ppm, with stereoisomers separated by only about 21 ppm. Similar observations were reported by these authors for the related series of complexes $[\text{PtCl}_n(\text{H}_2\text{O})_{6-n}]^{4-n}$, where $n = 2-6$, formed upon acidification of the alkaline solutions mentioned above. More recently, Shelimov and co-workers have used ^{195}Pt NMR in a similar fashion to study the chemical speciation of platinum in aqueous solutions of H_2PtCl_6 as relevant to the supported platinum catalyst preparation industry.^{8,10} By the joint use of ^{195}Pt NMR and other spectroscopic techniques (UV-vis, Raman and X-ray absorption spectroscopies), these workers were able to study the modes of interaction of these octahedral Pt(IV) complexes with industrial alumina supports during the initial stages of catalyst preparation; the information provided by ^{195}Pt NMR regarding changes in the primary Pt coordination sphere and the mobility of adsorbed complexes was found to be indispensable.

1 Introduction

Koch and co-workers have in the last decade extensively studied the speciation of platinum in aqueous solutions of H_2PtCl_6 , H_2PtBr_6 and mixtures of these salts as well as their disodium analogues (Na_2PtCl_6 and Na_2PtBr_6) using ^{195}Pt NMR spectroscopy. Kramer and Koch have determined the equilibrium constants of the ligand substitution reactions ('aquation constants') of $[\text{PtCl}_6]^{2-}$ and $[\text{PtBr}_6]^{2-}$ with water to yield $[\text{PtCl}_5(\text{H}_2\text{O})]^-$ and $[\text{PtBr}_5(\text{H}_2\text{O})]^-$ in aqueous perchloric acid solutions at 303 K as 1.75 ± 0.05 and 2.71 ± 0.15 , respectively.²³



These authors also reported the ^{195}Pt NMR spectrum of an aqueous solution of a mixture of H_2PtCl_6 and H_2PtBr_6 and were able to detect and assign the ^{195}Pt resonance signals of all possible complexes (12 in total) of the type $[\text{PtCl}_{5-n}\text{Br}_n(\text{H}_2\text{O})]^-$ where $n = 0-5$; this assignment was facilitated by remarkable second-order linear correlation that was found between the ^{195}Pt chemical shift of these complexes and n , the number of bromide ions in the Pt coordination sphere.²³ It is interesting to note also that the chemical shifts of stereoisomers differing only in the halide ion (chloride or bromide) coordinated in the site directly opposite (*trans*) to the coordinated water molecule were found to be different, the Pt centres of stereoisomers with bromide ion in this site being more shielded throughout the series.²³ This ^{195}Pt *chemical shift trend-analysis* could be used to rapidly assign signals of complexes of this type in industrial process solutions. The preferential extraction of $[\text{PtCl}_6]^{2-}$ over $[\text{PtCl}_5(\text{H}_2\text{O})]^-$ from these acidic aqueous solutions by conventional silica-based diethylene triamine anion exchangers was also demonstrated: ^{195}Pt NMR spectra of these solutions collected after contact with the anion exchanger clearly shows a decrease in the intensity of the $[\text{PtCl}_6]^{2-}$ signal, while that of $[\text{PtCl}_5(\text{H}_2\text{O})]^-$ remains unaffected. The ^{195}Pt chemical shift trend-analysis approach was extended by these authors to the assignment of the 56 complexes in the series $[\text{PtCl}_{6-m-n}\text{Br}_m(\text{OH})_n]^{2-}$, where $m, n = 0-6$, formed by dissolution of mixtures of H_2PtCl_6 and H_2PtBr_6 in alkaline aqueous solutions.²⁴ As mentioned previously, especially the complexes $[\text{PtCl}_{5-n}\text{Br}_n(\text{H}_2\text{O})]^-$ are of particular interest to the platinum refining industry since these are produced during the industrial oxidation of Pt(II) complexes with sodium chlorate and bromate in acidic aqueous process streams; in this context, Murray and Koch have investigated the products and reaction kinetics of these oxidation reactions and this work relied largely on ^{195}Pt NMR spectroscopy as a means of characterising platinum complexes in solution.²⁵

1 Introduction

Koch *et al.* have also explored the use of experimental ^{195}Pt NMR spectroscopy and a combination of density functional theory (DFT) -based ^{195}Pt shielding tensor computations and molecular dynamics (MD) simulations as a means of characterising the structure of the solvation shells of $[\text{PtCl}_6]^{2-}$ in binary solvent systems as well as to study the formation of $\{\text{Na}^+[\text{PtCl}_6]^{2-}\}$ ion pairs in methanol and acetonitrile.²⁶ ^{195}Pt chemical shift measurements, for example, have enabled these workers to demonstrate a preferential solvation of $[\text{PtCl}_6]^{2-}$ by methanol in water/methanol mixtures. Pregosin *et al.* have recently used pulsed gradient spin-echo (PGSE) diffusion measurements with ^{195}Pt as probe-nucleus to study the ion-pairing/aggregation of the $[\text{PtCl}_6]^{2-}$ dianion in solutions of Na_2PtCl_6 and H_2PtCl_6 in water and methanol.²⁷ This study constitutes the first reported realisation of the ^{195}Pt PGSE experiment and confirmed that, while in water the Na^+ and $[\text{PtCl}_6]^{2-}$ ions are most probably separated, some form of ion-pairing or aggregation is certainly prevalent in methanol.

A detailed knowledge of the solvation structure of a platinum complex in a particular solution is of considerable importance when pursuing accurate *ab initio* quantum-chemical calculations of the ^{195}Pt chemical shift. Autschbach and co-workers^{28,29} have stressed the importance of incorporating implicit (bulk solvent electrostatic) and explicit solvation models when optimising chemical structures as a basis for relativistic DFT calculations of ^{195}Pt chemical shifts. They have demonstrated that when computing the ^{195}Pt chemical shift of complexes in solution the choice of reference compound has a marked effect on the achievable agreement between computed and experimental shifts; satisfactory agreement between experimental and calculated ^{195}Pt chemical shifts could only be obtained when the Pt centre of the reference compound occupied a very similar chemical environment compared to that of the probe-nucleus. In fact, these authors have suggested that the excellent agreement between experimental ^{195}Pt chemical shifts and those calculated by Penka Fowe *et al.*³⁰, using a relativistic DFT method, for members of the series of octahedral Pt(IV) complexes $[\text{PtCl}_{6-n}\text{Br}_n]^{2-}$, $n = 0-6$, when using the $[\text{PtCl}_6]^{2-}$ complex (a member of this series) as reference should be attributed largely to this phenomenon; it turns out that error cancellation is responsible.²⁹ (Note: $\delta = \sigma_{\text{ref}} - \sigma$, where σ_{ref} is the shielding of a reference nucleus) These errors result from the approximations made regarding basis sets and difficulty in treating electron correlation and relativistic effects for these heavy nuclei (large number of electrons); when the reference nucleus is situated in an electronic environment similar to that of the probe nucleus a certain degree of error cancellation is afforded.²⁹ This was also noted by Koch *et al.* when attempting to compute ^{195}Pt chemical shifts for members of the series

1 Introduction

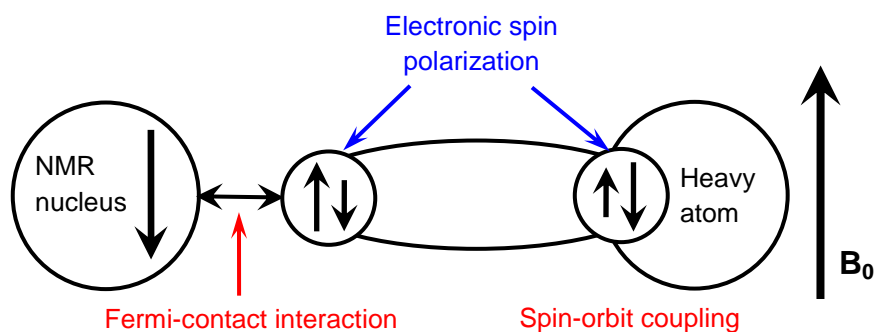


Figure 1.3 Scheme illustrating qualitatively the mechanism of spin-orbit coupling contribution to the magnetic shielding of an NMR probe nucleus by a directly bonded heavy nucleus in the presence of an applied magnetic field (B_0); scheme, showing *negative* SO-shielding, drawn after Kaupp *et al.*³²

$[\text{PtCl}_{6-n}(\text{OH})_n]^{2-}$ ($n = 0-6$) in aqueous solution (again with $[\text{PtCl}_6]^{2-}$ as reference): the discrepancy between experimental and DFT predicted chemical shifts increased as more hydroxide ions were introduced in the Pt coordination sphere, ultimately reaching about 20 % difference for $[\text{Pt}(\text{OH})_6]^{2-}$ (COSMO).²⁶

Ziegler and co-workers pioneered relativistic DFT-based predictions of ^{195}Pt nuclear magnetic shielding tensors of platinum complexes in solution in the late 1990s.³¹ They demonstrated the importance of explicitly including the relativistic spin-orbit coupling contribution, σ^{SO} (electron spin-polarization transmitted by Fermi-contact mechanism,³² Figure 1.3), to the overall heavy metal shielding; the overall nuclear shielding can then be represented as a sum of three terms,

$$\sigma = \sigma^{\text{d}} + \sigma^{\text{p}} + \sigma^{\text{SO}} \quad (1.2)$$

where σ^{d} and σ^{p} are respectively the ordinary diamagnetic and paramagnetic shielding contributions. The important effect of magnetic coupling between electronic orbitals on the paramagnetic shielding term (excited electronic states also contribute to paramagnetic nuclear shielding, which is negative, or ‘deshielding’) was also demonstrated and parallels were drawn to the early work on the interpretation of ^{195}Pt shielding in square planar Pt(II) complexes by Dean and Green³³ and by Pidcock *et al.*³⁴ in the late 60s (These were developed from the original paramagnetic shielding theory of Ramsey³⁵). More recently, Koch *et al.* reported relativistic computations of ^{195}Pt shifts in binary mixed-halide octahedral Pt(IV) complexes in aqueous solution³⁶; they confirmed the importance of both the paramagnetic *and* spin-orbit coupling contributions to the shift, especially for the heavier-

1 Introduction

halide complexes $[\text{PtCl}_{6-n}\text{Br}_n]^{2-}$ and $[\text{PtBr}_{6-n}\text{I}_n]^{2-}$. (Note that while the diamagnetic current contribution to ^{195}Pt shielding is not small in an absolute sense, its contribution to the *chemical shift* from the $[\text{PtCl}_6]^{2-}$ reference is negligible compared to that of the paramagnetic and spin-orbit terms.) While the ^{195}Pt shifts and trends calculated by these workers were generally in good agreement with experiment, it is interesting to note that considerably larger discrepancies were found for complexes deviating significantly from the ideal octahedral geometry and for the fluoride-containing complexes; these observations were thought to result from inadequate modelling of solvent interactions and especially specific/explicit interactions (hydrogen-bonding) by F ligands since these interactions are likely to affect metal-ligand bond displacements and other electronic properties of these complexes, which in turn affect the metal shielding. Clearly, the accurate prediction of ^{195}Pt chemical shifts of platinum complexes in solution remains a non-trivial task in general.

1.3 Isotope-effects in ^{195}Pt NMR spectroscopy

In recent years, Koch and co-workers have become interested in the use of isotope-effects in the ^{195}Pt NMR signals of complexes of the type $[\text{PtCl}_n(\text{H}_2\text{O})_{6-n}]^{4-n}$ ($n = 2-6$) in aqueous solutions as a means of unambiguous identification.^{37,38} These isotope-induced NMR frequency shifts, or simply isotope shifts, were first detected in the high-resolution spectra of simple covalent molecules, e.g. H_2 , CH_4 and halomethanes, in the 50s and 60s.³⁹ In the ^{13}C spectrum of CH_4 , for example, substitution of a proton by a deuteron (i.e. a ^1H nucleus is displaced by a ^2H nucleus) results in a small upfield (low-frequency) shift in the ^{13}C resonance frequency of *ca.* 0.19 ppm, i.e. the carbon nucleus is slightly *more shielded* following this isotopic substitution.⁴⁰ This phenomenon was quite general; introduction of a heavier isotope in the molecule almost invariably resulted in the nearby probe nucleus experiencing greater magnetic shielding.³⁹ These isotope shifts were also found to be at least approximately additive for all practical reasons, i.e. introduction of two deuterons in CH_4 produces twice the amount of additional ^{13}C shielding resulting from only one such isotopic substitution (in some cases, however, extremely small systematic deviations from perfect additivity are found and these have been studied in some detail⁴¹).

Interestingly, isotope shifts were also observed in the NMR signals of transition metal nuclei situated in complexes in solution and these shifts were generally found to be larger compared to those in the spectra of the preceding molecules. Lauterbur,⁴² for example, was one of the

1 Introduction

early investigators who observed large $^{12/13}\text{C}$ and $^{14/15}\text{N}$ isotope-induced shifts in the ^{59}Co resonance signal of the cyano-complex $[\text{Co}(\text{CN})_6]^{3-}$ in an aqueous solution of $\text{K}_3\text{Co}(\text{CN})_6$; other transition metal nuclei for which isotope shifts were subsequently studied include ^{51}V , ^{195}Pt and ^{199}Hg .^{20,21,43} Isotope shifts resulting from substitution at positions separated from the probe nucleus by two chemical bonds ('two-bond isotope shifts') have often been observed, but are generally found to be significantly smaller than shifts produced by isotopic substitution of directly bonded nuclei (or then, one-bond isotope shifts);³⁹ e.g. substitution of a single ^{12}C nucleus by ^{13}C in the above cobalt complex results in a *ca.* 0.914 ppm upfield shift of the ^{59}Co resonance (i.e. -0.914 ppm shift), while that produced by substitution of a ^{14}N by ^{15}N is only -0.197 ppm.⁴² In some cases, however, these two-bond isotope shifts can be quite large; in fact, one of the largest isotope shifts reported is that produced by $^{1/2}\text{H}$ substitution in the ^{59}Co spectrum of the $[\text{Co}(\text{NH}_3)_6]^{3-}$ complex (-5.2 ppm per deuteron introduced).⁴⁴

This large ^{59}Co isotope shift nicely illustrates two other important general features of isotope shifts: the magnitude of the isotope shift is dependent on the nature of the probe nucleus in that nuclei having large chemical shift ranges, e.g. ^{19}F , ^{31}P and transition metal nuclei, are also found to have large isotope shifts; secondly, the larger the *fractional change in mass* accompanying isotopic substitution, the greater the isotope shift (e.g. the one-bond ^{19}F isotope shift produced by $^{1/2}\text{H}$ substitution is larger than that produced by $^{12/13}\text{C}$ substitution).³⁹ It was recognised already at an early stage that isotope shifts should originate from small changes in the vibrational and rotational state of the molecule following isotopic substitution; these dynamic changes affect the electron distribution in the molecule and the shielding of the nuclei.⁴⁵ Several theories have been presented in an attempt to account for the sign and magnitude of isotope shifts and to allow for their accurate prediction.³⁹ Jameson and co-workers, in particular, have extensively studied the theoretical aspects of NMR isotope shifts for nuclei in polyatomic molecules, including transition metal nuclei in complexes;^{20,21,46} some of these theories will be considered in more detail later.

About 30 years ago, Sadler *et al.*¹⁹ reported that at high magnetic fields (9.4 T) the normally broad and asymmetric ^{195}Pt NMR signal of the complex anion $[\text{PtCl}_6]^{2-}$ in a concentrated aqueous solution of its sodium salt at 294 K appeared to resolve to a characteristic fine structure (Figure 1.4). Drawing on theoretical work on the origin of isotope shifts in NMR spectroscopy by Jameson⁴⁷, and consulting the known natural abundances of the two

1 Introduction

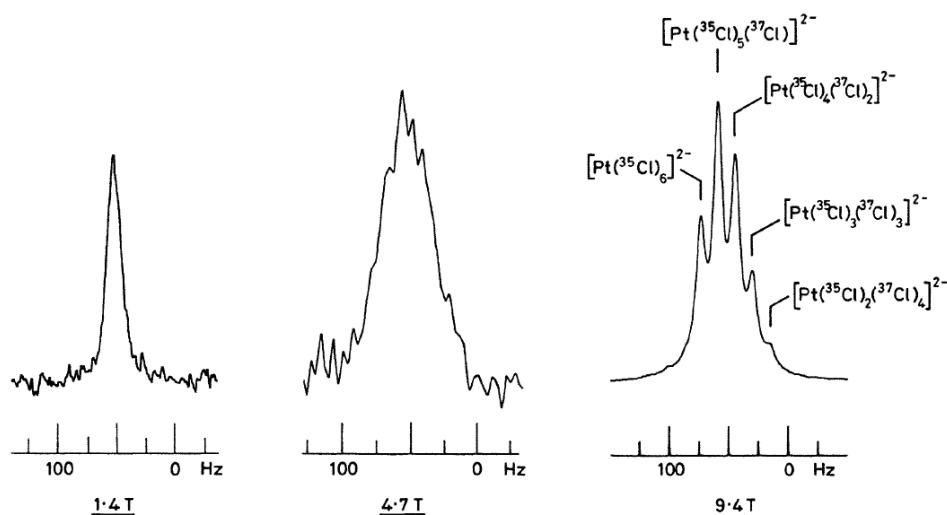


Figure 1.4 ^{195}Pt NMR spectrum of $[\text{PtCl}_6]^{2-}$ in a 2 mol.dm^{-3} solution of Na_2PtCl_6 salt in D_2O collected at 294 K at 1.4, 4.7 and 9.4 T fields. (Image reproduced from Sadler *et al.*¹⁹)

common chlorine isotopes, ^{35}Cl and ^{37}Cl , they were able to establish that these additional partially-resolved peaks were the resonance signals of the seven co-existing isotopic analogues, commonly termed *isotopologues*, of the octahedral Pt complex, i.e. the series $[\text{Pt}^{35}\text{Cl}_{6-n}^{37}\text{Cl}_n]^{2-}$ where $n = 0-6$. Each ^{37}Cl isotope incorporated into the coordination sphere of the metal afforded an upfield isotope shift of *ca.* 0.167 ppm and the *relative* intensities of these partially resolved ^{195}Pt signals were found to be in good agreement with that expected based on natural abundances of the isotopologues to which they were attributed. (Recall that the *relative areas* of NMR signals in a uniformly pulsed/excited frequency range are directly proportional to the number of equivalent nuclei that give rise to them; this translates to relative signal intensities only if the widths of all signals are identical.) Similar observations were reported for $[\text{PtBr}_6]^{2-}$ ($^{79/81}\text{Br}$ isotope shifts) and the mixed-halide complex $[\text{PtClBr}_5]^{2-}$.¹⁹

Subsequent fundamental work by Jameson and co-workers^{20,21} on the effect of isotopic substitution and temperature on the magnetic shielding of nuclei at the centre of octahedral MX_6 type molecules demonstrated that the magnitude of the M-nucleus isotope shift resulting from X-isotope substitution should be directly proportional to a mass factor $(m'-m)/m'$, where m' and m are the masses of the two X-isotopes in question. This work involved calculation of the mean M-X bond displacements for various pairs of isotopologues using *L*-tensor and Bartell methods⁴⁸ with anharmonic force fields; the magnitude of experimental NMR isotope shifts were found to be directly proportional to the difference between the mean M-X bond displacement of isotopologues (which in turn is directly proportional to the above mass

1 Introduction

factor), confirming that changes in metal-to-ligand bond distance upon isotopic substitution are responsible for the observed isotope shifts.

More recently, Koch and co-workers³⁷ have reported high-resolution (14.1 T) ^{195}Pt resonance signals of the complexes $[\text{PtCl}_5(\text{H}_2\text{O})]^-$ and $\text{cis-}[\text{PtCl}_4(\text{H}_2\text{O})_2]^0$ in an acidic aqueous solution (Figure 1.5); these are formed by ligand exchange reactions in the Pt coordination sphere of the $[\text{PtCl}_6]^{2-}$ anion upon dissolution of suitable salt or can be produced in higher concentration by oxidation of square-planar Pt(II) complexes in an aqueous solution of K_2PtCl_4 (typically $[\text{PtCl}_4]^{2-}$ and $[\text{PtCl}_3(\text{H}_2\text{O})]^-$) by some industrial oxidants e.g. hydrogen peroxide or sodium chlorate. These workers were interested in observing the isotope-induced fine structure in the above ^{195}Pt signals; the signal profiles of these two complexes would be different, and different to that of $[\text{PtCl}_6]^{2-}$ (also present in their solutions), since the three complexes exist as different numbers of isotopologues produced by the natural $^{35/37}\text{Cl}$ isotope abundances ($n+1$ isotopologues, where n is the number of chlorido-ligands) and so their ^{195}Pt resonance signals could provide unique ‘spectroscopic fingerprints’ for the characterisation of these complexes in solution. The ^{195}Pt spectrum of the complexes $[\text{Pt}^{35/37}\text{Cl}_6]^{2-}$ was found to resemble that reported by Sadler *et al.*¹⁹, consisting of at least five partially-resolved and uniformly spaced isotopologue signals; a non-linear least-squared fit of a sum function of the expected seven uniformly spaced Lorentzian peaks (one for each isotopologue) of equal line width to the spectroscopic data yielded an excellent fit and, as confirmation of this assignment, the relative areas of these peaks were found to be in excellent agreement with the expected natural abundances of the corresponding $[\text{Pt}^{35/37}\text{Cl}]^{2-}$ isotopologues (note that, owing to the low natural abundance of the isotopologues $[\text{Pt}^{35}\text{Cl}^{37}\text{Cl}_5]^{2-}$ and $[\text{Pt}^{37}\text{Cl}_6]^{2-}$ their ^{195}Pt signals are expected to be of relatively low intensity and as a result these are not readily detectable).

Interestingly, the ^{195}Pt signals of the isotopologues $[\text{Pt}^{35/37}\text{Cl}_5(\text{H}_2^{16}\text{O})]^-$ (Figure 1.5A) appeared to be more complex than the expected six uniformly spaced Lorentzian peaks (of variable intensity, of course); the *isotopologue model* that had been fitted to the spectrum of $[\text{Pt}^{35/37}\text{Cl}_6]^{2-}$ was clearly not appropriate. (Note that since the ^{18}O isotope has a very low natural abundance the signals of ^{18}O containing isotopologues cannot be detected.) The deviations of the profile of signals of the $\text{cis-}[\text{Pt}^{35/37}\text{Cl}_4(\text{H}_2^{16}\text{O})_2]$ isotopologues (Figure 1.5B) from that predicted by the isotopologue model was even more apparent: some of the isotopologue signals appeared to resolve to multiplets. Since it is known that ^{195}Pt shielding

1 Introduction

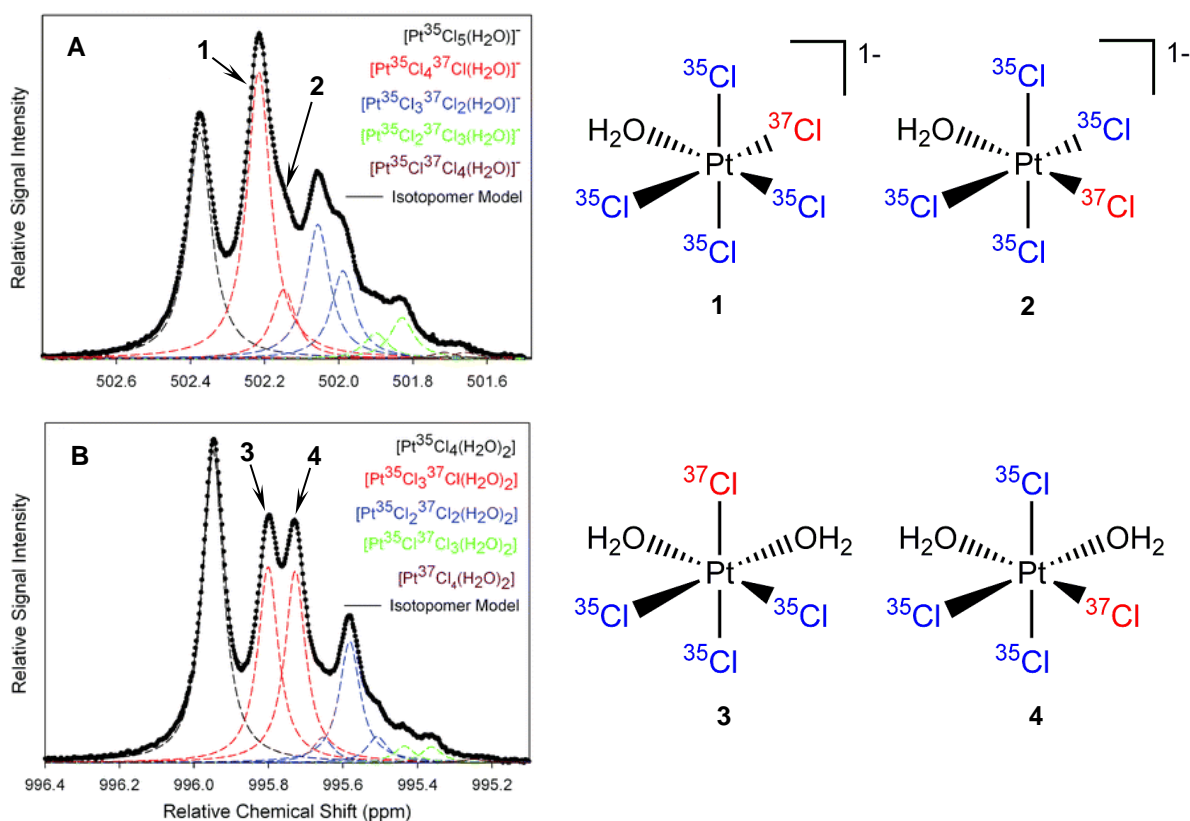


Figure 1.5 128.8 MHz ^{195}Pt NMR spectra of the complexes $[\text{PtCl}_5(\text{H}_2\text{O})]^-$ (A) and $\text{cis}-[\text{PtCl}_4(\text{H}_2\text{O})_2]^0$ (B) in acidic aqueous solution at 293 K; molecular structures on the right show structure of isotopomers assigned to signals 1-4. (NMR spectra reproduced from Koch *et al.*³⁷) The different colours of the chlorine isotopes in the structures are for the purposes of clarity only and are in no way connected to similar colours in the fitted spectra of Koch *et al.*

can be extremely sensitive to subtle changes in the electronic environment of the Pt nucleus¹⁹, it was proposed that these additional peaks should be assigned to isotopic stereoisomers, or *isotopomers*, that are possible for some of these isotopologues. (Note that these ‘multiplets’ are not actual multiplets produced by spin coupling; no time averaged spin-spin coupling between ^{195}Pt and either of the two chlorine isotopes is observed in the ^{195}Pt spectra of these complexes, as evidenced by the $[\text{PtCl}_6]^{2-}$ spectrum: starting from the $2I+1$ rule for coupling patterns we would expect significantly more peaks from the quadrupolar chlorine isotopes, both having $I = 3/2$; see Figure 1.5.)

It was postulated by these workers that the ^{195}Pt nuclei of isotopomers with ^{37}Cl coordinated *trans* to a water molecule were slightly more shielded than those of isotopomers having ^{35}Cl in this site: the $\text{cis}-[\text{Pt}^{35}\text{Cl}_3^{37}\text{Cl}(\text{H}_2\text{O})_2]$ isotopologue, for example, exists as two isotopomers; one in which the ^{37}Cl isotope is coordinated *trans* to the water molecule and another where this isotope is *trans* to a ^{35}Cl chloride ion and these should exist in equal abundance

1 Introduction

(statistically, based on the geometry of these complexes), consistent with the equal experimental signal intensities. (Signals 3 and 4 and corresponding molecular structures in Figure 1.5.) Moreover, these shielding differences appeared to be additive: two ^{37}Cl nuclei *trans* to coordinated water molecules afforded twice the amount of Pt shielding produced by one ^{37}Cl and ^{35}Cl in these sites. Since the set of $[\text{Pt}^{35/37}\text{Cl}_6]^{2-}$ signals did not show any apparent deviations from the isotopologue model, it was assumed that it is of little consequence to the ^{195}Pt shielding which combinations of chlorine isotopes were bound *trans* to one another. (It was noted that it might be possible to resolve the signals of these isotopomers at higher magnetic fields; these experiments were conducted at 14.1 T.) The resulting *isotopomer model*, which allowed different chemical shifts for ^{195}Pt signals of isotopologues and isotopomers of the type described above, was fitted to the experimental spectra of these complexes with great success: a non-linear least-squares fit of this function to the data produced an excellent fit and the relative areas of the Lorentzian peaks constituting the function corresponded very well to the statistically calculated abundances of the corresponding isotopologues and isotopomers. (These fits and the individual isotopologue and isotopomer signals are shown in Figure 1.5.) It was also noted by these workers that optimal resolution of this spectral fine structure could only be attained at carefully controlled temperatures in a relatively narrow range (*ca.* 10 degrees K) centred at about 293 K and this was tentatively ascribed to line broadening by the spin-rotation relaxation mechanism thought to be important in these platinum complexes and/or scalar coupling to the quadrupolar chlorine nuclei.¹⁸

Recent theoretical work by Davis and Bühl⁴⁹ has been aimed at computation of the ^{195}Pt nuclear shielding tensors for $[\text{Pt}^{35}\text{Cl}_6]^{2-}$, $[\text{Pt}^{37}\text{Cl}_6]^{2-}$ and for the isotopologues and isotopomers in the series $[\text{Pt}^{35}\text{Cl}_{5-n}^{37}\text{Cl}_n(\text{H}_2\text{O})]^-$ ($n = 0-5$), *cis*- $[\text{Pt}^{35}\text{Cl}_{4-n}^{37}\text{Cl}_n(\text{H}_2\text{O})_2]$ ($n = 0-4$) and *fac*- $[\text{Pt}^{35}\text{Cl}_{3-n}^{37}\text{Cl}_n(\text{H}_2\text{O})_3]^+$ ($n = 0-3$) using relativistic ZORA-SO (zero-order regular approximation, spin-orbit⁵⁰) DFT methods and attempting to model solvent interactions by implementing the CPCM continuum solvent model (*Gaussian09*⁵¹) in structure optimizations. These attempts have been successful in the sense that isotope-shift trends are reproduced reasonably well and these can be computed to at least the order of magnitude of the experimental values. Quantitative agreement of calculated shifts with experiment is not yet realized, however, underscoring the fact that accurate calculation of ^{195}Pt chemical shifts for even these simple complexes in solution remains a challenge (approximations including

1 Introduction

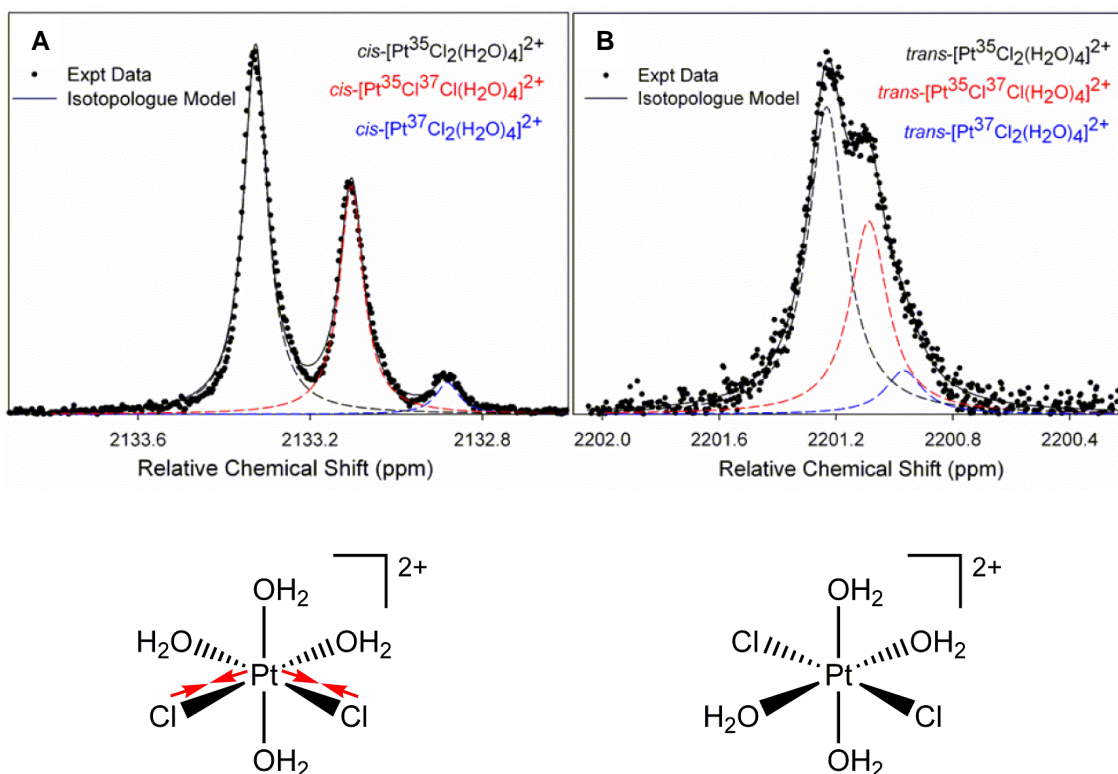


Figure 1.6 128.8 MHz ^{195}Pt NMR spectra of the stereoisomers *cis*- and *trans*- $[\text{PtCl}_2(\text{H}_2\text{O})_4]^{2+}$ (**A** and **B**, respectively) in acidic aqueous solution at 293 K; molecular structures are shown below their corresponding spectra. Red arrows show the expected contraction of bonds as discussed in the text and are not ‘chemical’ symbols. (Spectra reproduced from Koch *et al.*³⁸)

basis sets and treatment of electron correlation and relativistic effects, and inability to model solvent effects by continuum models are thought to be important²⁹). They conclude that isotope-effects on the Pt shielding in these complexes are produced by extremely small changes in bond displacement, on the order of femtometers, following isotopic substitution (isotopologues) and changes in the position of these isotopes relative to coordinated water molecules (isotopomers).

In a recent paper, Koch and co-workers³⁸ have demonstrated that in the high-resolution ^{195}Pt spectra of the stereoisomers *cis/trans*- $[\text{PtCl}_2(\text{H}_2\text{O})_4]^{2+}$, for which no $^{35/37}\text{Cl}$ isotopomers are possible, the $^{35/37}\text{Cl}$ isotope shifts are not of the same magnitude: the *cis*- $[\text{PtCl}_2(\text{H}_2\text{O})_4]^{2+}$ isomer, having a more shielded Pt nucleus, also shows significantly better resolved isotopologue signals, owing to larger isotope shifts, compared to that of the *trans*-isomer (Figure 1.6). Similar observations were reported for the other stereoisomer pairs in this series, *cis/trans*- $[\text{PtCl}_4(\text{H}_2\text{O})_2]$ and *fac/mer*- $[\text{PtCl}_3(\text{H}_2\text{O})_3]^+$, in which the isomers having more chlorido-ligands coordinated in sites *trans* to water molecules (i.e. *cis*- $[\text{PtCl}_4(\text{H}_2\text{O})_2]$ and *fac*-

1 Introduction

$[\text{PtCl}_3(\text{H}_2\text{O})_3]^+$) contained more shielded centres and appeared to display larger isotope shifts. These observations were rationalised by comparing the relative strengths of the *trans*-influence of the two ligands and the differing effects of these on mean Pt-Cl bond displacements in the stereoisomer pairs. Here the *trans*-influence of a ligand refers to the ability of this ligand to reduce the dissociation energy of a chemical bond to the metal in the *trans*-position, which is expected to be accompanied by some degree of elongation/extension of this latter bond; for two different groups in these positions, the relative *trans*-influence is important, where the bond to the metal of the ligand having the weaker *trans*-influence will be longer compared to the bonding situation where two of these ligands occupy these same sites.⁵² Conversely, the bond between the metal and the stronger *trans*-influencing ligand will be relatively shortened/contracted. Considering the dichlorido-stereoisomer pair, *cis/trans*- $[\text{PtCl}_2(\text{H}_2\text{O})_4]^{2+}$, for example, they suggest that where the two water molecules, having the *relatively* weaker *trans*-influence in Pt complexes, are coordinated *trans* to the two chlorido-ligands in the *cis*-stereoisomer, these Pt-Cl bonds should be slightly shorter relative to those in the *trans*-stereoisomer, and this slight contraction was thought to produce the greater Pt shielding observed for this stereoisomer, as would be predicted by the earlier theoretical work (see molecular structures in Figure 1.6). Moreover, the larger average Pt-Cl bond displacement in the *trans*-isomer probably results in the shielding afforded to the Pt centre by coordinated ³⁵Cl and ³⁷Cl isotopes to be more comparable than in the case of the *cis*-isomer, which could again explain the observed differences in the magnitude of ^{35/37}Cl isotope-induced shifts. It was recommended that more thorough theoretical work is needed to support these hypotheses, however, and they represent only a first attempt at explaining these subtle, but very useful and intriguing differences.

Koch and co-workers also report and discuss ^{16/18}O isotope-effects in the ¹⁹⁵Pt spectra of the complexes $[\text{PtCl}_5(\text{H}_2\text{O})]^-$, *cis*- $[\text{PtCl}_2(\text{H}_2\text{O})]$, *fac*- $[\text{PtCl}_3(\text{H}_2\text{O})_3]^+$ and *cis*- $[\text{PtCl}_2(\text{H}_2\text{O})_4]^{2+}$ in *ca.* 30% (v/v) ¹⁸O-enriched aqueous solution.³⁸ As was anticipated from the early work of Jameson and co-workers^{20,21}, they find that the ¹⁹⁵Pt shielding differences between ^{16/18}O isotopologues are significantly larger than those between ^{35/37}Cl isotopologues of the same complex and that these combined effects produce exquisitely complex fine structure in the signals of these complexes, with the larger ^{16/18}O isotope-effects essentially causing the ^{35/37}Cl isotope-induced patterns to multiply as a function of the number of O atoms in the Pt coordination sphere (see the accompanying spectra from the article in Figure 1.7). Interestingly, they find that, whereas for the first three complexes in the above series the

1 Introduction

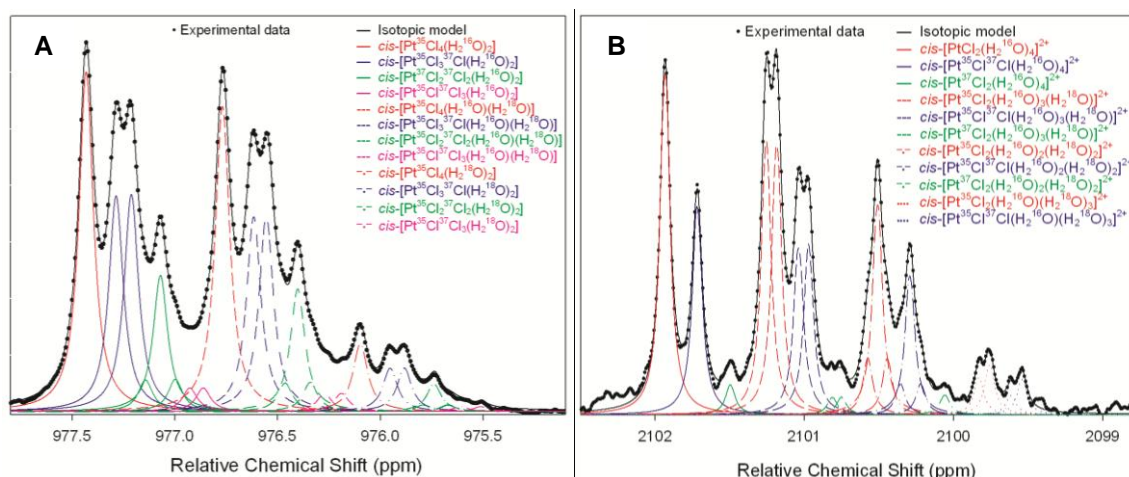


Figure 1.7 128.8 MHz ^{195}Pt NMR spectra of $\text{cis-}[\text{PtCl}_4(\text{H}_2\text{O})_2]^0$ (A) and $\text{cis-}[\text{PtCl}_2(\text{H}_2\text{O})_4]^{2+}$ (B) in an ^{18}O -enriched (30 %) aqueous sample at 293 K. Spectra have been reproduced from Koch *et al.*³⁸ and in both cases a model has been fitted to the data by the authors; see text for details.

$^{35/37}\text{Cl}$ isotope-induced profiles are simply reproduced in the signals of the various $^{16/18}\text{O}$ isotopologues (e.g. Figure 1.7A), this is not the case for the isotopologues of $\text{cis-}[\text{PtCl}_2(\text{H}_2\text{O})_4]^{2+}$ (Fig. 3.4B). Even though no $^{35/37}\text{Cl}$ isotopomers (of the ‘non-equivalent’ type considered previously, at least) are possible for any of the combinations $\text{cis-}[\text{Pt}^{35/37}\text{Cl}_2(\text{H}_2^{16/18}\text{O})_4]^{2+}$, it was suggested that the differential fine structure in the signals of the $^{16/18}\text{O}$ isotopologues should be assigned to certain $^{16/18}\text{O}$ isotopomers possible for some of these complexes (these are the isotopomers differing in the combination of $^{16/18}\text{O}$ isotopes coordinated in the two sites *trans* to the chloride ions *only*).

The signal of least shielded set of $^{35/37}\text{Cl}$ isotopologues, $[\text{Pt}^{35/37}\text{Cl}_2(\text{H}_2^{16}\text{O})_4]^{2+}$, simply consists of three lines, as expected since this is the same signal discussed earlier (no ^{18}O -containing analogues can be observed in the spectra of samples having a natural $^{16}\text{O}:$ ^{18}O ratio, owing to the low natural abundance of the ^{18}O isotope), while in the neighbouring set, assigned to $[\text{Pt}^{35/37}\text{Cl}_2(\text{H}_2^{16}\text{O})_3(\text{H}_2^{18}\text{O})]^{2+}$, these three isotopologue signals appear to be partially split, the two peaks having the same intensity throughout, at least within the experimental uncertainty of these measurements (lower signal-to-noise level). For the least shielded, most intense ‘doublet’ in this set the more upfield peak was assigned to the $\text{cis-}[\text{Pt}^{35}\text{Cl}_2(\text{H}_2^{16}\text{O})_3(\text{H}_2^{18}\text{O})]^{2+}$ isotopomer in which the ^{18}O isotope is coordinated *trans* to a chlorido-ligand; presumably this assignment was based on that previously described for the isotopomer signals of the complexes $\text{cis-}[\text{Pt}^{35/37}\text{Cl}_4(\text{H}_2^{16}\text{O})_2]^{2-}$ which, in a sense, can be considered an analogous problem. This hypothesis could also explain the equal intensities of the two peaks since for this particular complex we expect an equal probability of having two ^{16}O isotopes or one ^{16}O

1 Introduction

and one ^{18}O isotope coordinated *trans* to the two Cl ligands. This line of reasoning was extended to the other two isotopomer sets, with the more upfield of the two peaks being assigned to the isotopomer in which the ^{18}O isotope is situated *trans* to a Cl ligand (note that here the positions of Cl isotopes appear to be of little consequence to the Pt shielding).

Turning our attention to the third (central) set of $^{16/18}\text{O}$ isotopologue signals in Figure 1.7B, that assigned to $[\text{Pt}^{35/37}\text{Cl}_2(\text{H}_2^{16}\text{O})_2(\text{H}_2^{18}\text{O})_2]^{2+}$, we see that each of the three signals on its turn appears to be an approximately symmetrical combination of three poorly resolved peaks, the central peak having a much greater intensity than its two neighbours, which, in turn appear to have similar intensities. The authors follow reasoning similar to that described above to suggest that these triple-line patterns can be accounted for by the three isotopomers possible for each of the three $^{35/37}\text{Cl}$ isotopologues. The central peaks were assigned to the isotopomers in which one ^{16}O - and one ^{18}O -containing water molecule is coordinated *trans* to a chlorido-ligand, while the more upfield peaks are accounted for by the isotopomers having two ^{18}O isotopes *trans* to the two chlorido-ligands and the more downfield peaks by those with two ^{16}O isotopes in these sites. Again, this assignment is statistically consistent with the 1:4:1 intensity ratio observed for these peaks. The remaining two $^{16/18}\text{O}$ isotopologue sets, each with its own $^{35/37}\text{Cl}$ isotopologue and/or $^{16/18}\text{O}$ isotopomer distributions could, in principle, be assigned by similar analyses, however these signals are of much lower intensity as a result of the low ^{18}O enrichment level, the *cis*- $[\text{Pt}^{35/37}\text{Cl}_2(\text{H}_2^{18}\text{O})_4]^{2+}$ set escaping detection altogether.

Koch and co-workers⁵³ have recently reported the high-resolution ^{103}Rh NMR spectra of the octahedral complexes $[\text{RhCl}_n(\text{H}_2\text{O})_{6-n}]^{3-n}$, where $n = 3-6$, and have found natural $^{35/37}\text{Cl}$ isotope-induced patterns similar to those in the ^{195}Pt spectra of complexes in the series $[\text{PtCl}_n(\text{H}_2\text{O})_{6-n}]^{4-n}$, which they have been able to analyse in the same way, showing that this method of unambiguous identification is generally applicable to suitable metal complexes in solution.

1 Introduction

1.4 Objectives

The ^{195}Pt shielding of complexes in solution is extremely sensitive to changes in the Pt coordination sphere, even relatively subtle changes produced by isotopic substitution and changes in temperature. Koch and co-workers have shown that the ^{195}Pt NMR signals of isotopologues and even certain isotopomers of complexes in the series $[\text{PtCl}_n(\text{H}_2\text{O})_{6-n}]^{4-n}$, $n = 2-6$, in aqueous solutions can be resolved at temperatures in a narrow range about 293 K. In this context, the primary objectives of this study were as follows:

1. To generate all of the octahedral mixed-ligand Pt(IV) complexes in the related series $[\text{PtCl}_{6-n}(\text{OH})_n]^{2-}$, $n = 0-6$, in aqueous solution and to acquire high-resolution ^{195}Pt NMR spectra of these samples.
2. To investigate and interpret the $^{35/37}\text{Cl}$ and $^{16/18}\text{O}$ isotope-effects in the ^{195}Pt NMR signals of all of these complexes in order to allow for their unambiguous identification in solution. The ^{195}Pt signals will also be compared to those of the corresponding series of mixed aqua-chlorido-complexes $[\text{PtCl}_n(\text{H}_2\text{O})_{6-n}]^{4-n}$, $n = 2-5$, as reported by Koch and co-workers.^{37,38}
3. To investigate the effect of temperature on the isotope-induced fine-structure in high-resolution ^{195}Pt resonance signals of these complexes and to attempt an interpretation of the observations. This investigation will include the measurement of ^{195}Pt relaxation times for some of these complexes at various temperatures.

2

Experimental

2.1 ^{195}Pt NMR spectroscopy

128.8 MHz ^{195}Pt NMR spectra were recorded using a Varian INOVA 600 spectrometer equipped with a 5 mm broad-band probe; 85 MHz ^{195}Pt NMR spectra were recorded using a Varian INOVA 400 spectrometer equipped with a 5 mm dual broad-band probe (^2H field locking was employed throughout). Probe temperatures were calibrated using the standard methanol-ethylene glycol ^1H chemical shift technique; probe temperatures were controlled using the standard variable temperature unit of the instrument with a thermocouple in the probe head. ^{195}Pt chemical shifts are reported relative to that of $[\text{PtCl}_6]^{2-}$, commonly set as $\delta(^{195}\text{Pt}) = 0$ ppm, in an external reference solution (500 mg/cm^{-3} $\text{H}_2\text{PtCl}_6 \cdot 2\text{H}_2\text{O}$ in 30% (v/v) $\text{D}_2\text{O}/1\text{ M HCl}$) at 293 K. It is important to note that no proton decoupling was employed during these experiments as this produces temperature gradients and heating in our high ionic strength samples, which in turn is detrimental to the quality of ^{195}Pt spectra. Spectra were typically recorded using a 60° pulse (corresponding to a *ca.* 6 μs pulse duration) at maximum practical power (pwr = 52), employing an automatic receiver gain (gain = 60) and acquiring data for 0.5-1.0 s before allowing a relaxation delay of 1.0 s. The ^{195}Pt T_1 relaxation times of these complexes are reported to be shorter than about 150 ms in similar aqueous samples²⁴ (303 K); we have also performed some relaxation measurements and find that, in our samples, these T_1 relaxation times are typically shorter than 0.5 s, with the notable exception of $[\text{PtCl}_6]^{2-}$, for which this value is often closer to 1 s (note that our measurements were performed at 293 K). For many of these complexes relaxation time measurements are impractical since they have an only transient existence in these strongly alkaline solutions or since they are present in relatively low concentrations. Note that it is often necessary to

2 Experimental

collect several thousands of transients if the signal-to-noise ratio required for a satisfactory non-linear least-squares fit of functions describing isotope-effects is to be achieved (typically more than 20 000 transients).

Non-linear least-squares fits to the NMR spectra (initially processed using the *MestReNova 7.1.1* program © 2012 Mestrelab Research S.L.) were executed using the Marquart-Levenberg fitting algorithm of the computer program *SigmaPlot Ver. 11.0* (© 2008 Systat Software Inc.) Fitting of the ^{195}Pt spectra recorded from ^{18}O -enriched samples was performed using the *Line Fitting*-feature of *MestReNova*.

^{195}Pt T_1 measurements were performed using the standard inversion-recovery sequence and T_2 measurements using the Carr-Purcell-Meiboom-Gill (CPMG) echo sequence; pulse widths were optimised at each temperature after allowing at least one hour thermal equilibration. ^{195}Pt spectra were processed with a 10 Hz exponential line-broadening factor to ensure adequate signal-to-noise; relaxation data were processed using the standard exponential fitting routine of the *VnmrJ 2.2* software. Relaxation data were also processed manually; these relaxation times were in good agreement with those extracted using the spectrometer software. Representative ^{195}Pt NMR relaxation data are shown in Figure 2.1; the signal intensities are plotted as a function of the relaxation delay (τ) in Figure 2.2 and two-parameter exponential functions are fitted to these data using the Marquart-Levenberg non-linear least-squares fitting algorithm of *SigmaPlot*, relaxation times were calculated from these optimised parameters.

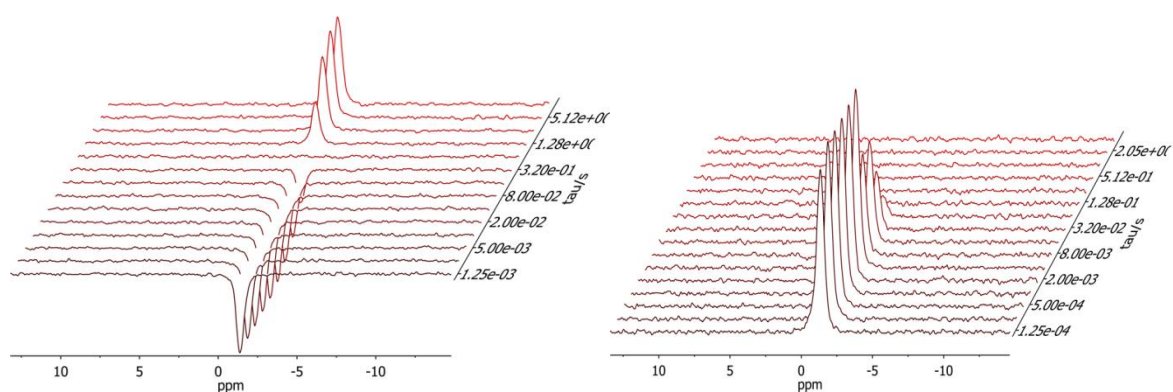


Figure 2.1 128.8 MHz ^{195}Pt T_1 (inversion-recovery) (left) and T_2 (CPMG echo) (right) measurements for $[\text{PtCl}_6]^{2-}$ in perchloric acid solution at 293 K (10 Hz exponential line broadening applied).

2 Experimental

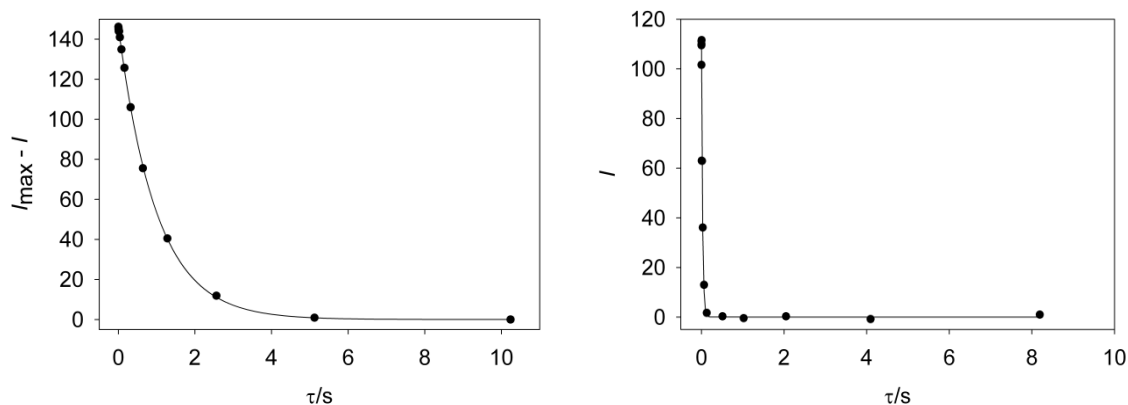


Figure 2.2 Plot of the difference between maximum signal intensity and the signal intensity at each time increment, $I_{\max} - I$, for the inversion-recovery experiment with exponential function fitted to data by non-linear least-squares analysis (left) and signal intensity versus time increment for the CPMG sequence (right), also with fitted exponential function.

2.2 Reagents and sample preparation

$\text{Na}_2\text{PtCl}_6 \cdot 6\text{H}_2\text{O}$ (Johnson Matthey PLC, Precious Metals Division) was of reagent grade and was dried *in vacuo* at *ca.* 333 K and stored in a desiccator prior to use. NMR samples were prepared by dissolving this Pt salt in alkaline solutions of NaOH (Aldrich) in ultra-pure Milli-Q water (electrical resistance greater than 18 M Ω). D_2O (99 %, Sigma-Aldrich) and H_2^{18}O (97 %, Isotec) were used as obtained; NMR samples typically contained about 50 % D_2O by volume for field locking purposes. ^{18}O enriched samples were prepared by dissolving the platinum salt in an alkaline solution of D_2O and H_2^{18}O (55:45 by volume). Initially all NMR samples were degassed by freeze-pump-thaw cycles, but this proved to have little effect on the achievable resolution. The bright orange solutions turn golden yellow, gradually changing to a more pale light yellow over the course of about 24 hours at room temperature, suggestive of chloride-ligand substitution reactions. ^{195}Pt NMR spectra were acquired from these samples over this period of active Pt ‘speciation’, i.e. before chemical equilibria are attained, as discussed by Kramer and Koch.²⁴

The acidic samples referred to in Chapter 4 were prepared by dissolving the Na_2PtCl_6 salt in a mixture of D_2O (99 %, Sigma-Aldrich) and concentrated HClO_4 (70 %) to produce a 1 mol.dm $^{-3}$ HClO_4 solution (*ca.* 90 % D_2O by volume). These golden yellow samples were degassed by freeze-pump-thaw cycles and sealed under Ar gas with rubber septa; this proved to have little effect on the ^{195}Pt relaxation times, however: at 298 K and 9.4 T the ^{195}Pt T_1 and

2 *Experimental*

T_2 relaxation times of the $[\text{PtCl}_6]^{2-}$ anion in a solution degassed by three freeze-pump-thaw cycles and sealed under Ar gas are 1.034 s and 28 ms, respectively, while in an essentially identical solution degassed only by ultrasound treatment the corresponding measurements were 990 ms and 27 ms.

3

Isotope-effects in the ^{195}Pt NMR spectra of complexes of the type $[\text{PtCl}_{6-n}(\text{OH})_n]^{2-}$, $n = 0-6$ *

3.1 Ligand substitution reactions

Although the methods by which the NMR samples were prepared in this study have been described in the previous experimental section, it is felt that a more general discussion of the chemical reactions in these alkaline solutions may be appropriate here, before presenting the results of the spectroscopy.

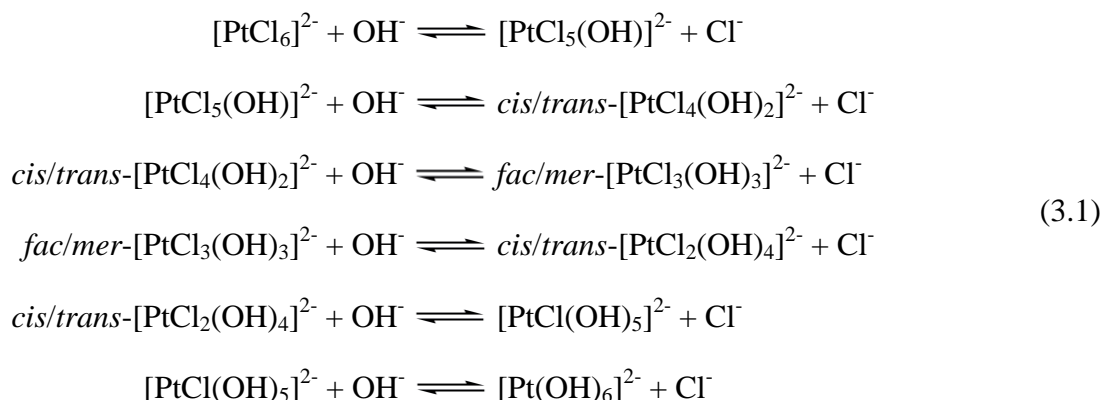
Goodfellow *et al.*²² initially produced all ten complexes of the type $[\text{PtCl}_{6-n}(\text{OH})_n]^{2-}$, $n = 0-6$, in aqueous solution by a combination of methods: the *homoleptic* complexes, $[\text{PtCl}_6]^{2-}$ and $[\text{Pt}(\text{OH})_6]^{2-}$, were prepared by simply dissolving the appropriate commercially available salts, Na_2PtCl_6 and $\text{Na}_2\text{Pt}(\text{OH})_6$, in aqueous solutions, while the five complexes $[\text{PtCl}_{6-n}(\text{OH})_n]^{2-}$ where $n = 5-3$ were generated by adding a further equivalent of Na_2PtCl_6 salt to an aqueous solution of Na_2PtCl_6 with five equivalents of sodium hydroxide that had been allowed to age for seven days at 288 K. The three remaining complexes, $[\text{PtCl}_5(\text{OH})]^{2-}$ and the stereoisomers *cis/trans*- $[\text{PtCl}_4(\text{OH})_2]^{2-}$, were produced by boiling a solution of Ag_2PtCl_6 in water and then adjusting to pH 10. It is interesting to note that, apparently, it is possible to isolate some of these complexes as pure salts.⁵⁴

In this study, however, it was decided to follow the general approach of Kramer and Koch:²⁴ adding an appropriate excess of sodium hydroxide to a concentrated aqueous solution (*ca.* 0.4 mol.dm^{-3}) of H_2PtCl_6 or Na_2PtCl_6 (or dissolving either of these in a sufficiently alkaline

* A paper based on these results is currently in preparation.

3 Isotope effects in ^{195}Pt NMR spectra of complexes

solution) results in an evolution of chemical species of the form $[\text{PtCl}_{6-n}(\text{OH})_n]^{2-}$, $n = 0-6$, according to the successive reaction equilibria in Equation 3.1:



While we have used Na_2PtCl_6 salt instead of the acid used by these authors and have added a larger excess of sodium hydroxide (10 molar equivalents), our observations are generally quite similar: the initially bright orange solutions turn golden yellow within a few minutes, and we find that these gradually change to a more pale light yellow over the course of a few days at room temperature.

^{195}Pt NMR spectra were collected from these fresh solutions, usually from within about 30 minutes of dissolving the salt, at 293 K over the course of about 24 hours and in different frequency ranges to produce the spectra reported here. Preliminary time-arrayed ^{195}Pt NMR spectra were collected from similar fresh solutions; these provide a *qualitative* view of the changes in the chemical species distribution in these solutions. During this time, the ligand substitution reactions in Equation 3.1 proceed to ultimately produce primarily the complexes *cis*- and *trans*- $[\text{PtCl}_2(\text{OH})_4]^{2-}$ and $[\text{PtCl}(\text{OH})_5]^{2-}$, with the $[\text{Pt}(\text{OH})_6]^{2-}$ complex forming slowly over time. In fact, we generally find that small amounts of fine, light yellow precipitate are produced from these solutions over the course of a few days at room temperature; we anticipate this to be the $\text{Na}_2\text{Pt}(\text{OH})_6$ salt (or some related formula), which is reported to be only sparingly soluble in water.²⁴ Before this happens, however, all of the complexes in this series are present in solution in reasonable concentrations, at least over some period of time, and their ^{195}Pt signals can be detected. As may be expected, the complexes containing fewer hydroxido-ligands ($n = 0-2$) have an only transient existence in these solutions and it is found that these are observable only during the first *ca.* 12 hours from the time of preparation.

3 Isotope effects in ^{195}Pt NMR spectra of complexes

Since the spectra reported here have been collected from these *equilibrating* solutions ('dynamic conditions'), in which the chemical species distribution is actively changing, no information regarding the equilibrium concentrations or the accurate relative stabilities of complexes should be inferred.²⁴ Attempts to produce stable solutions containing all of these complexes in reasonable concentrations for NMR measurements or only selected members of the series (we were especially interested in preparing both members of stereoisomer pairs) by adding small alkaline fractions to an aqueous solution of Na_2PtCl_6 have met with little success; the composition of these solutions tend to change significantly over the course of a few days at room temperature and some stereoisomers are still not produced in good concentration (especially not the *trans*- $[\text{PtCl}_4(\text{OH})_2]^{2-}$ complex), even when protected from ambient light.²³ At any rate, a detailed investigation of the reaction equilibria in Equation 3.1 has been beyond the scope of our study; the interested reader is referred to the work of Regalbuto and co-workers⁹, Shelimov *et al.*^{8,10} and Kramer and Koch.²⁴ Alternative synthetic methods of preparation could also be investigated in future work, e.g. oxidation of appropriate Pt(II) complexes and the methods described by Goodfellow *et al.*²²

3 Isotope effects in ^{195}Pt NMR spectra of complexes

3.2 Results and Discussion

3.2.1 $^{35/37}\text{Cl}$ isotope-effects in the ^{195}Pt NMR spectra of the complexes $[\text{PtCl}_{6-n}(\text{OH})_n]^{2-}$

The full 128.8 MHz ^{195}Pt NMR spectrum of the series of complexes $[\text{PtCl}_{6-n}(\text{OH})_n]^{2-}$, $n = 0-6$, recorded at 293K is shown in Figure 3.1. At first glance, this spectrum appears rather similar to that reported by Koch *et al.* for the series of *aqua*-complexes, $[\text{PtCl}_n(\text{H}_2\text{O})_{6-n}]^{4-n}$ where $n = 2-5$ (apart from the presence of the two most downfield signals in Figure 3.1);³⁸ the signals are well separated by large and approximately uniform spacing (mind the ‘breaks’ in the chemical shift scale), with a smaller separation between what appears to be the signals of stereoisomers. However, we do note a larger average separation of about 600 ppm between the ^{195}Pt signals of complexes differing in the number of hydroxido-ligands in the Pt coordination sphere compared to the corresponding separation reported for the *aqua*-series of about 500 ppm per water molecule. This observation is also consistent with the earlier work of Kramer and Koch²⁴, taking into account that their spectra were recorded at 303K and assuming a linear downfield shift of up to *ca.* 1 ppm per degree K increase in temperature.^{20,55}

The ^{195}Pt chemical shift trend-analysis approach of Kramer and Koch can be used to tentatively assign the spectrum in Figure 3.1; interestingly, the order of ^{195}Pt shielding suggested by these authors for the members of stereoisomer pairs in this series of hydroxido-complexes is in each case the reversed of that determined for the corresponding pairs in the *aqua*-series: the shielding of the *trans*- $[\text{PtCl}_4(\text{OH})_2]^{2-}$ complex, for example, is greater than that of the *cis*-stereoisomer, while Koch *et al.*³⁸ have shown that for the *cis/trans*-

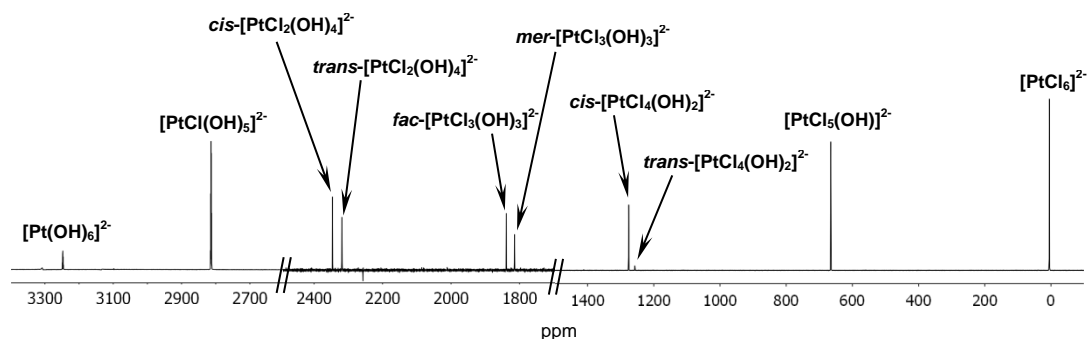


Figure 3.1 Full 128.8 MHz ^{195}Pt NMR spectrum of the complexes $[\text{PtCl}_{6-n}(\text{OH})_n]^{2-}$, $n = 0-6$, in an alkaline aqueous solution of Na_2PtCl_6 salt at 293 K. (Note the ‘breaks’ in the chemical shift values)

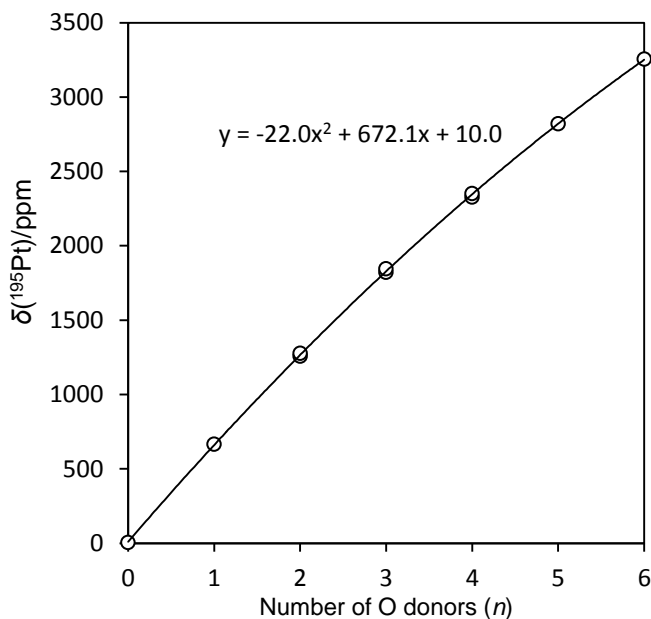
3 Isotope effects in ^{195}Pt NMR spectra of complexes

Figure 3.2 ^{195}Pt chemical shifts of the complexes $[\text{PtCl}_{6-n}(\text{OH})_n]^{2-}$, $n = 0-6$, at 293 K plotted as a function of the number of O atoms in Pt coordination sphere, n , with second-order trend.

$[\text{PtCl}_4(\text{H}_2\text{O})_2]^0$ stereoisomer pair, the *cis*-stereoisomer contains the more shielded Pt centre (Note that our initial assignment of stereoisomer signals is based entirely on the assignment of Kramer and Koch²⁴). Further, the ^{195}Pt shielding differences between stereoisomers in this hydroxido-series appear to be significantly smaller at about 25 ppm compared to the *ca.* 100 ppm differences in the aqua-series.³⁸ To our knowledge, no detailed theoretical studies have been reported regarding the interpretation of the shielding of stereoisomers in these series of octahedral Pt(IV) complexes. However, a simple rationalisation of these phenomena will be developed later in the text by considering the likely effects of the differing relative *trans*-influence of these ligands on metal-to-ligand bond displacements and Pt shielding in these complexes.

The expanded ^{195}Pt signals of most of the complexes in the series $[\text{PtCl}_{6-n}(\text{OH})_n]^{2-}$, $n = 0-6$, are reported in Figure 3.3, showing the expected $^{35/37}\text{Cl}$ isotope effects. Unfortunately, the complexes *trans*- $[\text{PtCl}_4(\text{OH})_2]^{2-}$ and *mer*- $[\text{PtCl}_3(\text{OH})_3]^{2-}$ were always present in relatively low concentrations in our solutions (the former disappears over the course of a few hours) and as a result satisfactory spectra could not be obtained within a reasonable amount of time. Nevertheless, the signal assigned to $[\text{PtCl}_6]^{2-}$ clearly shows the expected $^{35/37}\text{Cl}$ isotope-induced fine structure profile reported in the literature,^{18,37,38} we can readily detect five isotopologue signals. It is reasonable to expect the signals of the isotopologues $[\text{Pt}^{35}\text{Cl}^{37}\text{Cl}_5]^{2-}$ and $[\text{Pt}^{37}\text{Cl}_6]^{2-}$ to be of very low intensity since these complexes have a low natural

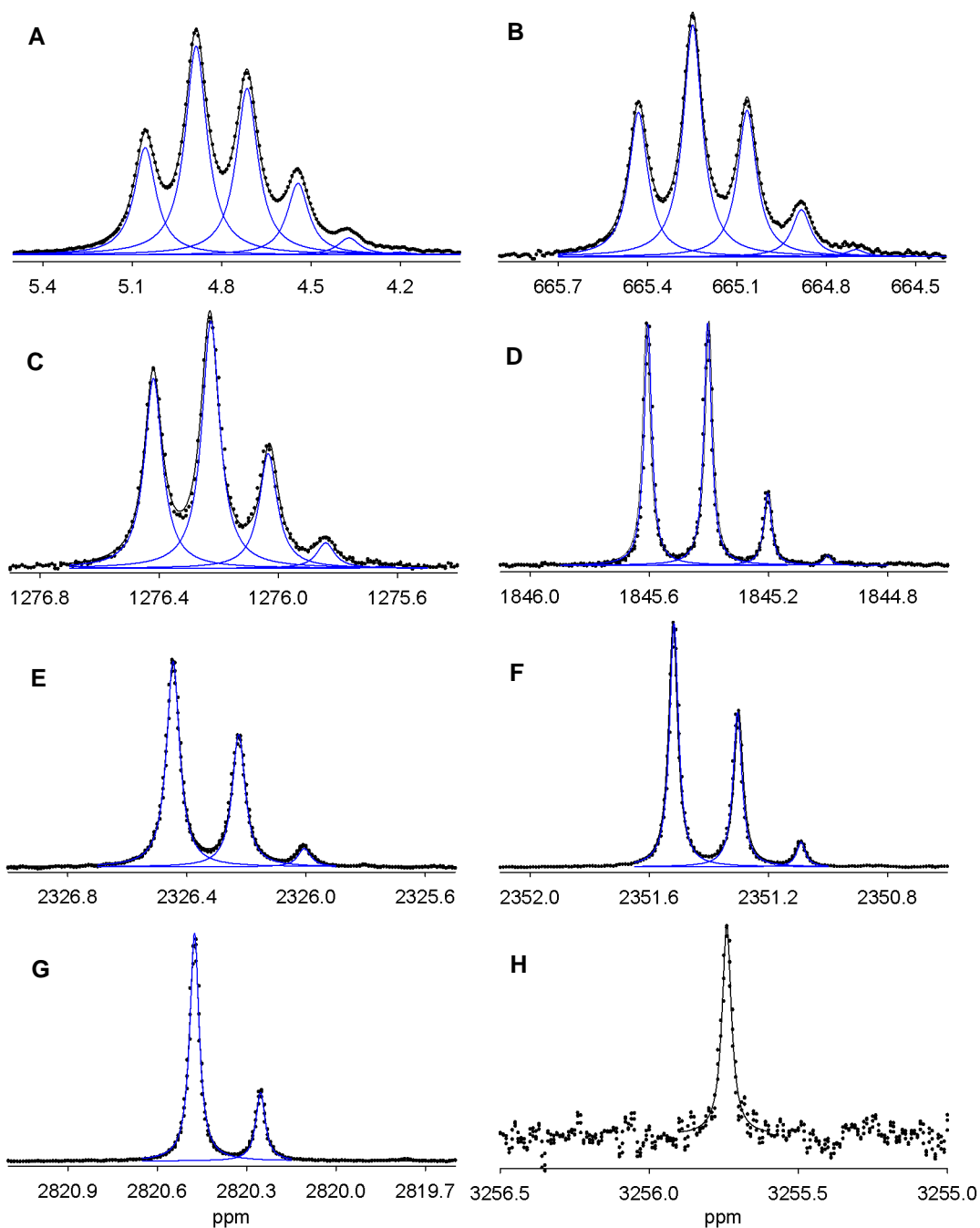
3 Isotope effects in ^{195}Pt NMR spectra of complexes

Figure 3.3 128.8 MHz ^{195}Pt NMR spectra (black dots) of the complexes $[\text{PtCl}_6]^{2-}$ (A), $[\text{PtCl}_5(\text{OH})]^{2-}$ (B), *cis*- $[\text{PtCl}_4(\text{OH})_2]^{2-}$ (C), *fac*- $[\text{PtCl}_3(\text{OH})_3]^{2-}$ (D), *cis*- and *trans*- $[\text{PtCl}_2(\text{OH})_4]^{2-}$ (E and F, respectively), $[\text{PtCl}(\text{OH})_5]^{2-}$ (G) and $[\text{Pt}(\text{OH})_6]^{2-}$ (H) in alkaline aqueous solution of Na_2PtCl_6 at 293 K. Solid black line shows the non-linear least-squares fit of an *isotopologue* model to these data, while the blue lines represent the signals of individual isotopologues. See text for details of fitting procedure.

3 Isotope effects in ^{195}Pt NMR spectra of complexes

abundance; these signals are obscured by rf noise. An *isotopologue model*, which in this case is a sum function of seven uniformly spaced Lorentzian peaks of equal width (one peak for each of the isotopologues in the series $[\text{Pt}^{35}\text{Cl}_{6-n}^{37}\text{Cl}_n]^{2-}$, $n = 0-6$), yields an excellent non-linear least-squares fit to the experimental signals of these complexes, as shown in Figure 3.3A. The fitting procedure returns the following optimised parameters: an absolute $^{35/37}\text{Cl}$ isotope shift of 0.171 ppm (i.e. -0.171 ppm shift per ^{37}Cl incorporated) and line widths at half-height of 10 Hz (^{195}Pt NMR signals are typically much broader than ^1H signals due to the faster spin relaxation characteristics of ^{195}Pt nuclei in most situations). Note that the constraints imposed on this model are based largely on experimental observations; isotope shifts in transition metal NMR spectra are generally found to be approximately additive and we assume that the line widths the ^{195}Pt resonance signals of all the isotopologues are equal.²⁰ These optimised parameters have been used to plot (in blue) in Figure 3.3A the seven individual Lorentzian peaks representing the signals of the various isotopologues. It has been shown that the natural fractional abundances of the $^{35/37}\text{Cl}$ isotopologues of complexes of this type can be calculated using the following equation:

$$P(n) = \sum_{n=0}^{n+r} \binom{n+r}{n} \alpha_{^{35}\text{Cl}}^n \alpha_{^{37}\text{Cl}}^r \quad (3.1)$$

where $\alpha(^{35}\text{Cl}) = 0.7553$ and $\alpha(^{37}\text{Cl}) = 0.2447$ (the fractional natural abundances of the two chlorine isotopes) and where n and r represent respectively the number of ^{35}Cl and ^{37}Cl isotopes in the Pt coordination sphere.³⁷ The percentage contributions of each of the Lorentzian peaks to the total area of the fitted function are shown in Table 3.1, together with the calculated natural abundances of the corresponding isotopologues calculated using Equation 3.1. The agreement between these area contributions (i.e. experimental isotopologue abundances) and statistically calculated values is very good for most isotopologues, confirming unambiguously the assignment of this set of signals. Note that as the intensity of the peaks (concentrations of the corresponding complexes in solution) decrease the agreement with the predicted value deteriorates; this is a result of the larger uncertainty/error in the areas of peaks with a lower signal-noise ratio.

Considering the expansion of the signal assigned by chemical shift trend-analysis to $[\text{PtCl}_5(\text{OH})]^{2-}$, we can distinguish five partially resolved peaks (Figure 3.3B). These are separated by about 0.18 ppm, similar to the separation between the $^{35/37}\text{Cl}$ isotopologues in

3 Isotope effects in ^{195}Pt NMR spectra of complexes**Table 3.1** Calculated natural abundances of isotopologues and percentage area contribution by corresponding resonance signals (determined from non-linear least-squares fitting procedure) for complexes the $[\text{Pt}^{35/37}\text{Cl}_{6-n}(\text{}^{16}\text{OH})_n]^{2-}$, $n=0-6$

Isotopologue	Natural statistical abundance	Percentage area (<i>fit</i>)
$[\text{Pt}^{35}\text{Cl}_6]^{2-}$	18.57	18.66
$[\text{Pt}^{35}\text{Cl}_5^{37}\text{Cl}]^{2-}$	36.09	36.33
$[\text{Pt}^{35}\text{Cl}_4^{37}\text{Cl}_2]^{2-}$	29.23	28.97
$[\text{Pt}^{35}\text{Cl}_3^{37}\text{Cl}_3]^{2-}$	12.63	12.46
$[\text{Pt}^{35}\text{Cl}_2^{37}\text{Cl}_4]^{2-}$	3.07	2.96
$[\text{Pt}^{35}\text{Cl}^{37}\text{Cl}_5]^{2-}$	0.40	0.49
$[\text{Pt}^{37}\text{Cl}_5]^{2-}$	0.02	0.12
$[\text{Pt}^{35}\text{Cl}_5(\text{}^{16}\text{OH})]^{2-}$	24.58	24.99
$[\text{Pt}^{35}\text{Cl}_4^{37}\text{Cl}(\text{}^{16}\text{OH})]^{2-}$	39.82	40.13
$[\text{Pt}^{35}\text{Cl}_3^{37}\text{Cl}_2(\text{}^{16}\text{OH})]^{2-}$	25.80	25.36
$[\text{Pt}^{35}\text{Cl}_2^{37}\text{Cl}_3(\text{}^{16}\text{OH})]^{2-}$	8.36	8.13
$[\text{Pt}^{35}\text{Cl}^{37}\text{Cl}_4(\text{}^{16}\text{OH})]^{2-}$	1.35	1.24
$[\text{Pt}^{37}\text{Cl}_5(\text{}^{16}\text{OH})]^{2-}$	0.08	0.16
<i>cis</i> - $[\text{Pt}^{35}\text{Cl}_4(\text{}^{16}\text{OH})_2]^{2-}$	32.54	32.79
<i>cis</i> - $[\text{Pt}^{35}\text{Cl}_3^{37}\text{Cl}(\text{}^{16}\text{OH})_2]^{2-}$	42.17	42.64
<i>cis</i> - $[\text{Pt}^{35}\text{Cl}_2^{37}\text{Cl}_2(\text{}^{16}\text{OH})_2]^{2-}$	20.50	19.80
<i>cis</i> - $[\text{Pt}^{35}\text{Cl}^{37}\text{Cl}_3(\text{}^{16}\text{OH})_2]^{2-}$	4.43	4.40
<i>cis</i> - $[\text{Pt}^{37}\text{Cl}_4(\text{}^{16}\text{OH})_2]^{2-}$	0.36	0.36
<i>fac</i> - $[\text{Pt}^{35}\text{Cl}_3(\text{}^{16}\text{OH})_3]^{2-}$	43.09	42.60
<i>fac</i> - $[\text{Pt}^{35}\text{Cl}_2^{37}\text{Cl}(\text{}^{16}\text{OH})_3]^{2-}$	41.88	42.87
<i>fac</i> - $[\text{Pt}^{35}\text{Cl}^{37}\text{Cl}_2(\text{}^{16}\text{OH})_3]^{2-}$	13.57	12.80
<i>fac</i> - $[\text{Pt}^{37}\text{Cl}_3(\text{}^{16}\text{OH})_3]^{2-}$	1.47	1.73
<i>cis</i> - $[\text{Pt}^{35}\text{Cl}_2(\text{}^{16}\text{OH})_4]^{2-}$	57.05	57.61
<i>cis</i> - $[\text{Pt}^{35}\text{Cl}^{37}\text{Cl}(\text{}^{16}\text{OH})_4]^{2-}$	36.96	36.54
<i>cis</i> - $[\text{Pt}^{37}\text{Cl}_2(\text{}^{16}\text{OH})_4]^{2-}$	5.99	5.85
$[\text{Pt}^{35}\text{Cl}(\text{}^{16}\text{OH})_5]^{2-}$	75.53	76.89
$[\text{Pt}^{37}\text{Cl}(\text{}^{16}\text{OH})_5]^{2-}$	24.47	23.11

the spectrum of $[\text{PtCl}_6]^{2-}$, and so it seems reasonable to assume that these peaks can be assigned to the $^{35/37}\text{Cl}$ isotopologues of $[\text{PtCl}_5(\text{OH})]^{2-}$ (while we expect to see an additional signal due to the $[\text{Pt}^{37}\text{Cl}_5(\text{OH})]^{2-}$ isotopologue, this complex has a very low natural abundance and as a result it cannot be readily detected within a reasonable spectral acquisition time). Indeed, we find that the non-linear least-squares fit of an isotopologue model consisting of six uniformly spaced Lorentzian peaks of equal line width to the experimental spectrum is excellent and that the relative area contributions of these isotopologue peaks match the expected natural abundances very well, similar to that described above for $[\text{PtCl}_6]^{2-}$ (Figure 3.3A). The results of the fitting procedure and the calculated isotopologue abundances are

3 Isotope effects in ^{195}Pt NMR spectra of complexes

compared in Table 3.1. Note that while two-bond isotope-induced effects are certainly possible in general,^{20,21} we do not observe ^1H isotope shifts in the ^{195}Pt spectra of any of these hydroxido-complexes and we postulate that this is due to rapid exchange of protons and deuterons in solution under these conditions. A similar analysis can be performed for the signal assigned to the $\text{cis-}[\text{PtCl}_4(\text{OH})_2]^{2-}$ complex: a simple isotopologue model consisting of five uniformly spaced Lorentzian peaks of equal width yields an excellent least-squares fit to the experimental spectrum, as shown in Figure 3.3C and confirmed by the numerical results reported in Table 3.1.

As mentioned earlier, Koch *et al.* have shown that isotopomers differing only in whether ^{35}Cl or ^{37}Cl is situated in a site *trans* to a coordinated water molecule are separated by *ca.* 0.07 ppm in the signals of the complexes $[\text{PtCl}_5(\text{H}_2\text{O})]^-$ and $\text{cis-}[\text{PtCl}_4(\text{H}_2\text{O})_2]^0$, with the isotopomer having more ^{37}Cl in these sites afforded the larger Pt shielding. In contrast, the analysis of the $^{35/37}\text{Cl}$ isotope-induced effects in the signals of the complexes $[\text{PtCl}_5(\text{OH})]^{2-}$ and $\text{cis-}[\text{PtCl}_4(\text{OH})_2]^{2-}$ described above demonstrates convincingly that similar isotopomers, where only the combination of chlorine isotopes coordinated *trans* to hydroxido-ligands is different, have indistinguishable ^{195}Pt shielding, at least in the magnetic fields employed in this study, giving rise to a ‘single’ resonance signal. A rationalisation of these phenomena is presented here, based on the relative strengths of the *trans*-influence of the chlorido-, aqua- and hydroxido-ligands in these octahedral complexes.

Since the water molecule is expected to induce a smaller *trans*-influence compared to that of chloride ion, it is reasonable to assume that the average Pt-Cl bond displacement *trans* to a coordinated water molecule should be shorter than *trans* to a chlorido-ligand. This shorter Pt-Cl bond displacement may facilitate resolution of isotopomers in that the *difference* between Pt- ^{35}Cl and Pt- ^{37}Cl bond displacements in this site is expected to be larger than for the longer Pt-Cl bonds *trans* to a chlorido-ligand (Figure 3.4); this larger *difference in bond displacement* should result in a larger isotope shift for these isotopomers.³⁸ (See Jamesons.²⁰) While the above may be a simple, intuitive attempt at explaining the observations, as also mentioned by Koch *et al.*³⁸, the crystal structure of $[\text{PtCl}_5(\text{H}_2\text{O})]^-$, co-crystallised with 18-crown-6 clearly shows that the Pt-Cl bond *trans* to the water molecule is significantly shorter than the other four (2.273 and 2.310 Å respectively³⁷), lending some support for this hypothesis, as differences in Pt-Cl bond displacements of this magnitude have been used to account for observed shielding differences between isotopologues in the series of complexes

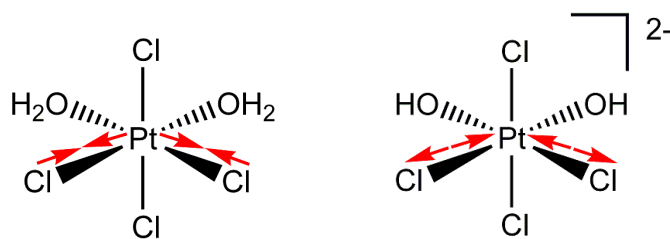
3 Isotope effects in ^{195}Pt NMR spectra of complexes

Figure 3.4 Molecular structures of $\text{cis-}[\text{PtCl}_4(\text{H}_2\text{O})_2]^0$ (left) and $\text{cis-}[\text{PtCl}_4(\text{OH})_2]^{2-}$ (right) with red arrows showing expected relative Pt-Cl bond compression (left) and extension (right).

$[\text{PtCl}_{6-n}(\text{H}_2\text{O})_n]^{4-n}$.⁴⁹ These bond displacements could also be reproduced very well computationally by high-level DFT structure optimisations with hybrid PBE functional on large basis sets incorporating the CPCM continuum solvent model.⁴⁹ This line of reasoning has also been extended to explain the shielding order of the stereoisomers in this series of complexes and also the observation that stereoisomers having more chloride ions coordinated in sites opposite water molecules display a larger separation between $^{35/37}\text{Cl}$ isotopologues, as explained earlier.³⁸ It is interesting to note that only the relative extension/contraction of Pt-Cl bonds are taken into account in these models; however, this seems reasonable considering the significantly greater Pt nuclear shielding afforded by a chlorido-ligand compared to that by a water molecule (*ca.* 500 ppm difference per ligand for these complexes).

The ^{195}Pt spectra of the corresponding hydroxido-complexes, $[\text{PtCl}_5(\text{OH})]^{2-}$ and $\text{cis-}[\text{PtCl}_4(\text{OH})_2]^{2-}$, however, show no resolution of $^{35/37}\text{Cl}$ isotopomer signals, and the Pt shielding order of all stereoisomer pairs (e.g. *cis-* and *trans-}[\text{PtCl}_4(\text{OH})_2]^{2-}) appear to be reversed compared to that reported for the corresponding aqua-complexes. These observations may be rationalised on the basis of the expectation that the Pt-Cl bonds *trans* to the stronger *trans*-influencing hydroxido-ligands be slightly elongated compared to those opposite chlorido-ligands⁵²: it seems unlikely that the former Pt-Cl bonds (those *trans* to the hydroxido-ligands) should be *contracted* relative to the latter (like Pt-Cl bonds *trans* to aqua-ligands in the related aqua-complexes) in a way that would increase the magnitude of the $^{35/37}\text{Cl}$ isotope shifts in these sites (Figure 3.4); this situation appears to be similar to that of the $[\text{Pt}^{35/37}\text{Cl}_6]^{2-}$ complexes where isotope shifts are uniform in magnitude for isotopic substitution in all sites (i.e. isotopic substitution *trans* to ^{35}Cl and ^{37}Cl yield similar shifts). This interpretation is supported by recent high-level DFT structure optimisations that predict a shorter Pt-Cl bond displacement *trans* to the hydroxido-ligand in $[\text{PtCl}_5(\text{OH})]^{2-}$ than in the other four sites (*ca.* 2.37 and 2.40 Å respectively); similar values were reported for other hydroxido-complexes.⁵⁶ It may also be reasonable to suggest that the greater Pt*

3 Isotope effects in ^{195}Pt NMR spectra of complexes

shielding of stereoisomers in which fewer chlorido-ligands are coordinated in the sites *trans* to the hydroxido-ligands may be attributed to the larger number of shorter *trans* Cl-Pt-Cl bond pairs. It must be emphasised, however, that these hypotheses constitute only a first step towards understanding these interesting observations and should benefit greatly from more rigorous theoretical work.

Regarding the shielding order of the stereoisomers, for example, we have suggested that elongation of the Pt-Cl bonds *trans* to the hydroxido-ligands in the *cis*- $[\text{PtCl}_4(\text{OH})_2]^{2-}$ stereoisomer results in the larger Pt chemical shift compared to that of the *trans*-stereoisomer, however the physical phenomena underlying this additional shift have not been established. We have mentioned that relativistic spin-orbit coupling-induced spin polarization at the ^{195}Pt nucleus in octahedral mixed-halide Pt(IV) complexes has been found to contribute significantly to the ^{195}Pt chemical shift,³⁶ with the magnitude of the spin-orbit shielding contribution afforded to the metal by the directly bonded halide being inversely dependent on the metal-to-halide bond displacement.³¹ In this light, it seems quite likely that spin-orbit shielding ‘transmitted’ through the shorter Pt-Cl bonds in the *trans*-stereoisomer might be greater compared to that in the *cis*-stereoisomer, which could also account for the observed shielding order.

Having mentioned this, however, we anticipate the paramagnetic shielding term to be rather more important to the chemical shifts in this series of complexes³⁶ (chlorine is a ‘lighter’ halide); the relative magnitudes of the paramagnetic shielding of these stereoisomers will be determined primarily by the balance between the energy gaps of the major electronic orbital transitions and the magnitude of the field-induced magnetic coupling between these orbitals (i.e. proportional to a factor $|\langle a|M_k|i\rangle|/\Delta E_{ai}$ for each transition, where ΔE_{ai} and $|\langle a|M_k|i\rangle|$ represent the magnitudes of the energy gap and the magnetic orbital coupling, respectively). While some general comments and approximations may be made here, this problem is best addressed by DFT calculations and a transition analysis as demonstrated by Gilbert and Ziegler.³¹ Such calculations have not yet been attempted by us and are beyond the scope of the current study, but this methodology will certainly be explored in future work. We anticipate that solvation and explicit hydrogen-bonding interactions may well be important here and will also have to be modelled in considerable detail in order to obtain good agreement with experiment.³⁶

3 Isotope effects in ^{195}Pt NMR spectra of complexes

No isotopomers of the type discussed above (i.e. complexes having the same isotopic composition, but differing only in whether a ^{35}Cl or ^{37}Cl isotope is coordinated *trans* to a hydroxido-ligand) are possible for the complexes *trans*- $[\text{PtCl}_4(\text{OH})_2]^{2-}$, *fac*- $[\text{PtCl}_3(\text{OH})_3]^{2-}$, *cis/trans*- $[\text{PtCl}_2(\text{OH})_4]^{2-}$ or $[\text{PtCl}(\text{OH})_5]^{2-}$. The expanded ^{195}Pt signals of most of these complexes are also reported in Figure 3.3 together with that of $[\text{Pt}(\text{OH})_6]^{2-}$. To each of these spectra is fitted an isotopologue model consisting of $n+1$ Lorentzian peaks, where n is the number of chlorido-ligands coordinated to the Pt centre, which yields good results in a manner similar to that described previously for the complexes $[\text{PtCl}_5(\text{OH})]^{2-}$ and *cis*- $[\text{PtCl}_4(\text{OH})_2]^{2-}$; numerical results are given in Table 3.1. Interestingly, comparison our signals of the stereoisomer pair *cis/trans*- $[\text{PtCl}_2(\text{OH})_4]^{2-}$ (Figure 3.3E and F) with that previously reported for the stereoisomers *cis/trans*- $[\text{PtCl}_2(\text{H}_2\text{O})_4]^{2+}$ in acidic solution (Figure 1.6) reveals that while the ^{195}Pt signals of this latter pair differ significantly (the three isotopologue signals of the *trans*-isomer overlap considerably as a result of smaller isotope shifts), the signals of the hydroxido-pair are well-resolved and essentially identical with only the overall chemical shift difference and the relative signal intensities affording some means of distinguishing between them. (Formation of the *cis*-isomer is expected to be more thermodynamically favourable.²⁴)

This observation is thought to originate from the larger *trans*-influence of the hydroxido-ligand⁵²: the mean Pt-Cl bond displacements in both of the stereoisomers *cis/trans*- $[\text{PtCl}_2(\text{OH})_4]^{2-}$ are relatively large and so we expect only minor differences in the change in Pt-Cl displacements accompanying $^{35/37}\text{Cl}$ isotopic substitution for these complexes, resulting in the very comparable magnitudes of the observed $^{35/37}\text{Cl}$ isotope shifts (Figure 3.5). Still, we find the strong visual difference between the Pt signals of the complexes *trans*- $[\text{PtCl}_2(\text{OH})_4]^{2-}$ and *trans*- $[\text{PtCl}_2(\text{H}_2\text{O})_4]^{2+}$ intriguing (in fact, also the striking similarity of the signals of *cis*- $[\text{PtCl}_2(\text{H}_2\text{O})_4]^{2+}$ to those of both *cis/trans*- $[\text{PtCl}_2(\text{OH})_4]^{2-}$); this probably arises from more subtle effects not considered in our previous theories, suggesting that while these arguments are certainly useful for our purposes, they appear to be inadequate for a fuller understanding of these phenomena. (Note that the actual isotope shift per ^{37}Cl substitution in the spectrum of *cis*- $[\text{PtCl}_2(\text{H}_2\text{O})_4]^{2-}$ was reported by Koch *et al.* to be -0.223 ppm, which is quite comparable to those of our *cis/trans*- $[\text{PtCl}_2(\text{OH})_4]^{2-}$ stereoisomers, while that of *trans*- $[\text{PtCl}_2(\text{H}_2\text{O})_4]^{2-}$ is certainly smaller at -0.144 ppm.³⁸)

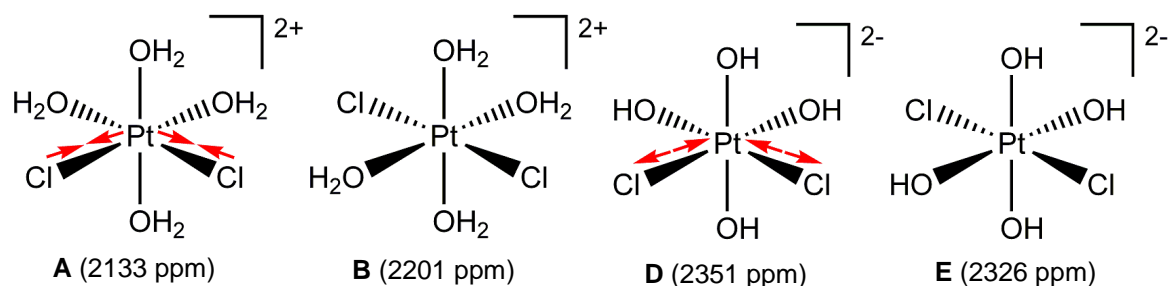
3 Isotope effects in ^{195}Pt NMR spectra of complexes

Figure 3.5 Molecular structures of the stereoisomer pairs $cis/trans$ - $[\text{PtCl}_2(\text{H}_2\text{O})_4]^{2+}$ (**A** and **B**) and $cis/trans$ - $[\text{PtCl}_2(\text{OH})_4]^{2-}$ (**C** and **D**) showing expected Pt-Cl bond contraction and extension; approximate ^{195}Pt chemical shifts are shown in brackets below structures.

Wasylishen and Burford⁵⁷ have reported one-bond $^{1/2}\text{H}$ isotope shifts in the ^{31}P and ^{119}Sn spectra of the two series of isoelectronic hydride-compounds PH_2^- , PH_3 , PH_4^+ and SnH_3^- , SnH_4 , SnH_3^+ finding that, within each series, the magnitude of the isotope shift is largest for the negatively charged ions and smallest for those having a positive charge. This was suggested to be the result of an increased sensitivity of the heavy nuclear shielding (^{31}P and ^{119}Sn) to changes in bond displacement as the gross charge on this atom becomes more negative, as has been predicted by earlier molecular orbital calculations for first- and second-row hydrides by Chesnut.⁵⁸ In the above series of tin hydrides a considerable change in geometry around the central tin nucleus results on going from SnH_4 to SnH_3^- and Wasylishen and Burford⁵⁷ have mentioned that this change may contribute to the observed difference in the one-bond $^{1/2}\text{H}$ isotope shifts (however, these contributions are likely to be small, as demonstrated by Chesnut⁵⁸). Nevertheless, our observations appear to be in qualitative agreement with this trend: the average $^{35/37}\text{Cl}$ isotope shift in the spectrum of the cationic $trans$ - $[\text{PtCl}_2(\text{H}_2\text{O})_4]^{2+}$ reported by Koch *et al.* (Figure 1.6) certainly appears to be smaller than that of the anions $cis/trans$ - $[\text{PtCl}_2(\text{OH})_4]^{2-}$ (Figure 3.3); still, the corresponding shifts for cis - $[\text{PtCl}_2(\text{H}_2\text{O})_4]^{2+}$ are quite comparable to those of these latter complexes and are probably the ‘special’ case, produced by Pt-Cl bond contraction, as described previously. Admittedly, though, the bonding situation in these Pt complexes is likely to be quite different to that in the simple ‘main-group’ hydrides mentioned above and we feel that a more thorough theoretical approach will certainly benefit a more general understanding of this phenomenon.⁵⁸

Finally, we note an interesting trend in the separations between the signals of stereoisomers in our series of complexes: the magnitude of this separation increases as more chloride ions are displaced from the Pt coordination sphere, from about 18 ppm for the $cis/trans$ - $[\text{PtCl}_4(\text{OH})_2]^{2-}$ pair to 24 ppm for fac/mer - $[\text{PtCl}_3(\text{OH})_3]^{2-}$ and ultimately 28 ppm for $cis/trans$ -

3 Isotope effects in ^{195}Pt NMR spectra of complexes

$[\text{PtCl}_2(\text{OH})_4]^{2-}$. At first glance, this seems quite reasonable considering that the first pair of stereoisomers (*cis/trans*- $[\text{PtCl}_4(\text{OH})_2]^{2-}$) share a common *trans*-set of Cl-Pt-Cl bonds and so we expect more comparable shielding, while this is not the case for the other two pairs. However, we find a general rationalisation of this trend based on our previous simple hypotheses regarding the effect of changes in average Pt-Cl bond displacements on Pt shielding more challenging; for now we can report that the Pt shielding differences (separation) between stereoisomers certainly increase as the average Pt shielding of these pairs decrease. It seems quite likely that this is a result of an increased sensitivity of metal shielding to changes in the average metal-to-ligand bond displacement as the shielding of the metal nucleus is decreased, as also reported and discussed by Jameson and co-workers for some octahedral vanadium carbonyl-complexes.²¹ (This is also consistent with the observed trend in the isotope shifts reported above.) Interestingly, when considering the spectra reported for the corresponding aqua-stereoisomer pairs, however, we find that here this trend is *reversed*: the shielding difference between stereoisomers in this series decrease as the average Pt shielding is decreased, from about 138 ppm for the *cis/trans*- $[\text{PtCl}_4(\text{H}_2\text{O})_2]^0$ pair to 68 ppm for *cis/trans*- $[\text{PtCl}_2(\text{H}_2\text{O})_4]^{2+}$ (recall also that the *shielding order* is reversed for all pairs of stereoisomers).³⁸

3 Isotope effects in ^{195}Pt NMR spectra of complexes3.2.2 $^{16/18}\text{O}$ isotope-effects in the ^{195}Pt NMR spectra of the complexes $[\text{PtCl}_{6-n}(\text{OH})_n]^{2-}$

The ^{195}Pt NMR signals of the complexes $[\text{PtCl}_{6-n}(\text{OH})_n]^{2-}$, $n = 0-6$, at 293 K in an aqueous $0.4 \text{ mol}\cdot\text{dm}^{-3}$ sodium hydroxide solution enriched with ^{18}O by addition of *ca.* 45% (v/v) H_2^{18}O are shown in Figure 3.6 (pages 38 and 39). Again, no resonances of sufficient intensity could be obtained for the complexes *trans*- $[\text{PtCl}_4(\text{OH})_2]^{2-}$ and *mer*- $[\text{PtCl}_3(\text{OH})_3]^{2-}$ within a reasonable acquisition time; as mentioned in the previous section, these complexes form in relatively low concentration and have an only transient existence in solution under these conditions. The ^{18}O -containing complexes were produced by dissolving the Na_2PtCl_6 salt in an ^{18}O -enriched sodium hydroxide solution; adding H_2^{18}O to a similar alkaline solution already containing these complexes, but with a natural $^{16/18}\text{O}$ -isotope ratio is a rather inefficient means of generating the ^{18}O -containing isotopologues since hydroxide ion exchange in the inner coordination sphere of these complexes was found to be very slow.

Koch and co-workers³⁸ have found that the ^{195}Pt resonances of the ^{18}O -enriched aqua-complexes $[\text{PtCl}_5(\text{H}_2\text{O})]^-$, *cis*- $[\text{PtCl}_4(\text{H}_2\text{O})_2]$, *fac*- $[\text{PtCl}_3(\text{H}_2\text{O})_3]^+$ and *cis*- $[\text{PtCl}_2(\text{H}_2\text{O})_4]^{2+}$ show well-resolved signals due to $^{16/18}\text{O}$ isotopologues of these complexes and that the separation between these are significantly larger than between those of $^{35/37}\text{Cl}$ isotopologues, resulting essentially in a multiplication of the $^{35/37}\text{Cl}$ isotope-induced signal profile as a function of the number of O nuclei in the Pt coordination sphere. Moreover, for these aqua-complexes the Pt centres of isotopomers of *cis*- $[\text{PtCl}_2(\text{H}_2\text{O})_4]^{2+}$ having a different number of ^{18}O isotopes coordinated in the sites *trans* to the two chlorido-ligands are not magnetically equivalent with each ^{18}O isotope introduced into one of these sites affording about 1 ppm shielding, resulting in remarkable fine structure. Note that while no $^{16/18}\text{O}$ isotopomers are possible for $[\text{PtCl}_5(\text{H}_2\text{O})]^-$, *cis*- $[\text{PtCl}_4(\text{H}_2\text{O})_2]$ and *fac*- $[\text{PtCl}_3(\text{H}_2\text{O})_3]^+$, partially resolved $^{35/37}\text{Cl}$ isotopomer signals are observed in all sets of $^{16/18}\text{O}$ isotopologues of the former two sets of complexes and these ‘isotopomer shifts’ appear to be of essentially uniform magnitude throughout each series. (See Figure 1.7A.)

The ^{195}Pt spectra of the isotopologue sets $[\text{Pt}^{35/37}\text{Cl}_5(^{16/18}\text{OH})]^{2-}$, *cis*- $[\text{Pt}^{35/37}\text{Cl}_4(^{16/18}\text{OH})_2]^{2-}$ and *fac*- $[\text{Pt}^{35/37}\text{Cl}_3(^{16/18}\text{OH})_3]^{2-}$ certainly show a similar multiplication of the $^{35/37}\text{Cl}$ isotope-induced profiles reported previously for the all ^{16}O isotopologues as a function of the number of O atoms in the Pt coordination sphere; note, however, that owing to the expansive $^{35/37}\text{Cl}$ isotope-effects in the spectra of some of these complexes the $^{16/18}\text{O}$ isotopologue sets overlap slightly. In Figure 3.6B the large $^{16/18}\text{O}$ and smaller $^{35/37}\text{Cl}$ isotope shifts in the expanded

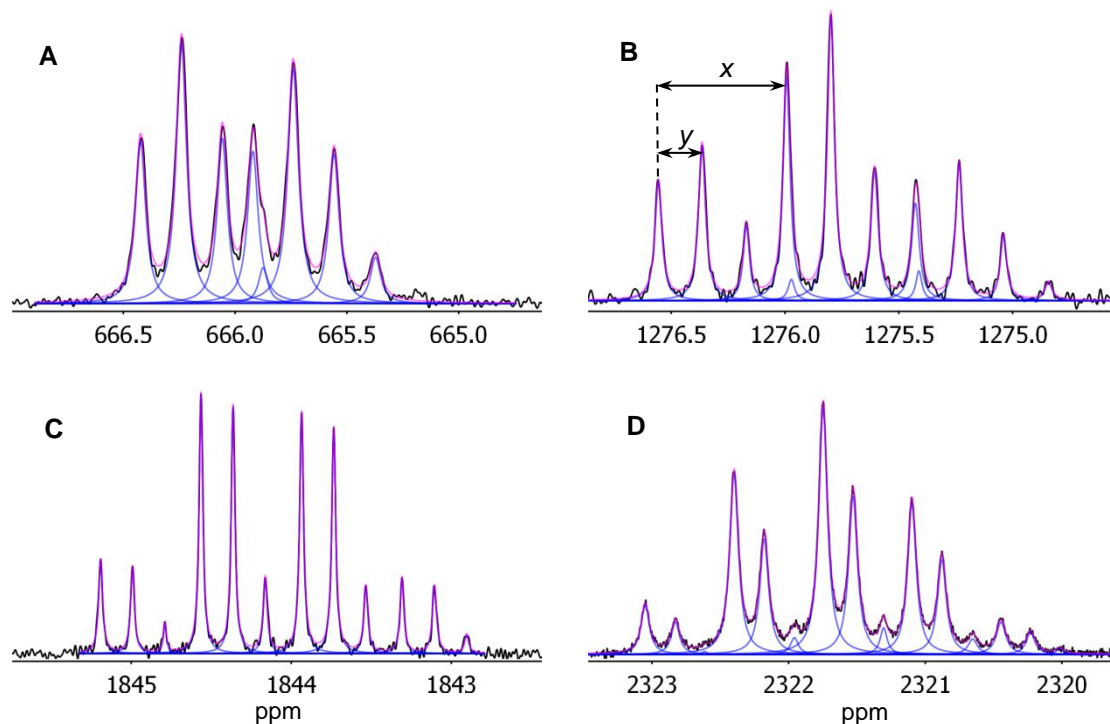
3 Isotope effects in ^{195}Pt NMR spectra of complexes

Figure 3.6 128.8 MHz ^{195}Pt NMR spectra of the complexes $[\text{PtCl}_5(\text{OH})]^{2-}$ (A), $\text{cis-}[\text{PtCl}_4(\text{OH})_2]^{2-}$ (B), $\text{fac-}[\text{PtCl}_3(\text{OH})_3]^{2-}$ (C) and $\text{trans-}[\text{PtCl}_2(\text{OH})_4]^{2-}$ (D) in an ^{18}O -enriched (45 %) alkaline aqueous solution at 293 K. Black lines are experimental spectra, while magenta lines show the fitted models and the blue lines represent the individual isotopologue/isotopomer signals. Separations labelled x and y show the relative magnitudes of respectively $^{16}/^{18}\text{O}$ and $^{35}/^{37}\text{Cl}$ isotope shifts in the spectra of $\text{cis-}[\text{PtCl}_4(\text{OH})_2]^{2-}$ as a general example.

signals of $\text{cis-}[\text{PtCl}_4(\text{OH})_2]^{2-}$ are labelled respectively x and y in the interest of clarity. Considering first the set of signals of the isotopologues $[\text{Pt}^{35/37}\text{Cl}_5(^{16/18}\text{OH})]^{2-}$, we can recognise two sets of Cl isotopologue signals; these are essentially identical, save a slightly greater intensity for the less shielded (more downfield) set. Following the reasoning of Koch *et al.*³⁸, these two sets of signals are assigned to the sets of $^{35/37}\text{Cl}$ isotopologues $[\text{Pt}^{35/37}\text{Cl}_5(^{16}\text{OH})]^{2-}$ and $[\text{Pt}^{35/37}\text{Cl}_5(^{18}\text{OH})]^{2-}$, the latter is expected to be the more shielded and this is also suggested by the slightly lower intensity of this set of signals; recall that the ratio of ^{16}O to ^{18}O in our sample is about 55 to 45. The excellent fit of a function consisting of the sum of two sets of five equally spaced Lorentzian peaks of equal width at half height to the experimental spectrum confirms this assignment in the sense that the relative peak areas assigned to each of these complexes correspond reasonably well to the expected abundances; these values are compared in Table 3.2. These abundances can be calculated in a manner similar to that described previously by multinomial probability theory and employing the

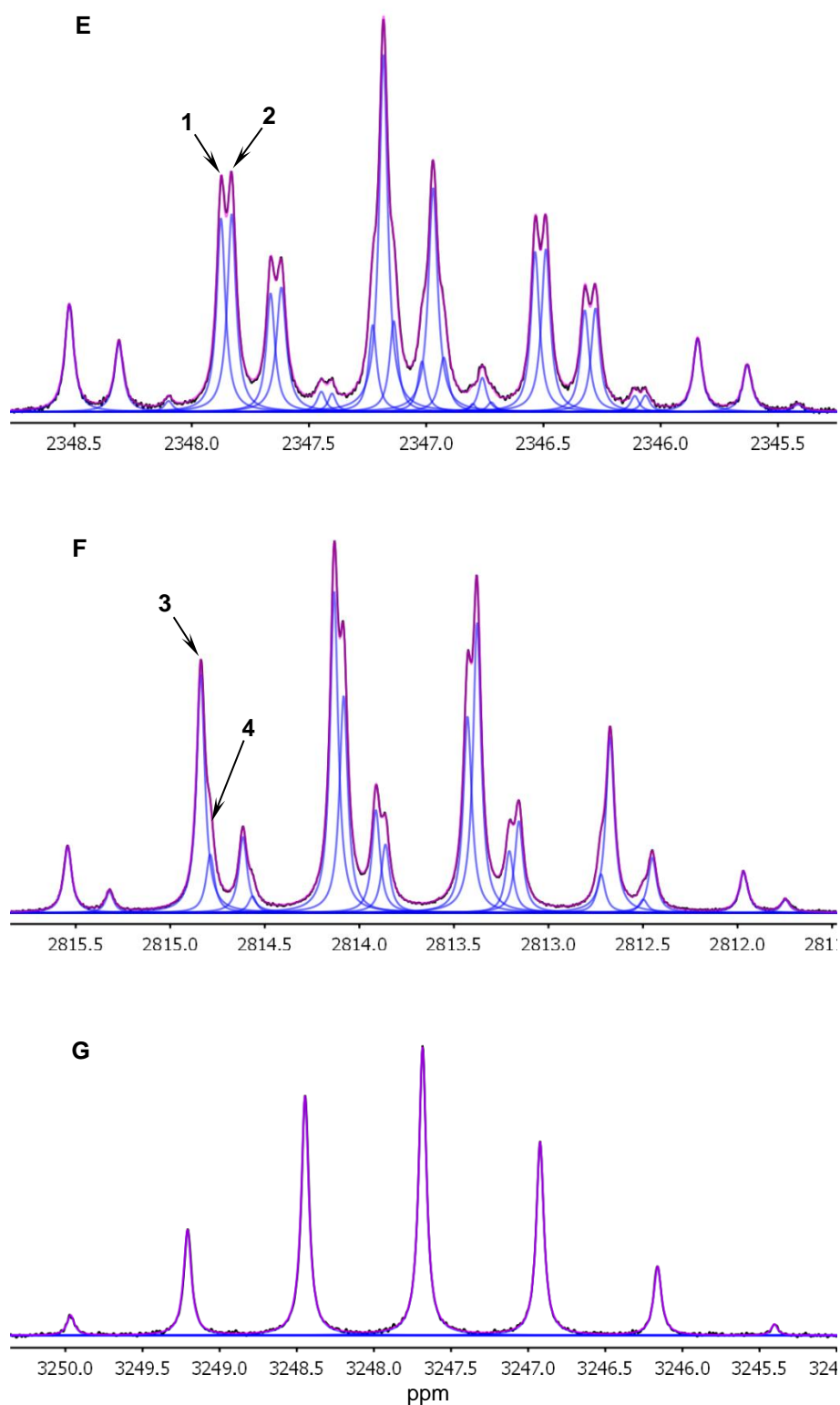
3 Isotope effects in ^{195}Pt NMR spectra of complexes

Figure 3.6 (continued) 128.8 MHz ^{195}Pt NMR spectra of the complexes $\text{cis-}[\text{PtCl}_2(\text{OH})_4]^{2-}$ (E), $[\text{PtCl}(\text{OH})_5]^{2-}$ (F) and $[\text{Pt}(\text{OH})_6]^{2-}$ (G) in an ^{18}O -enriched (45 %) alkaline aqueous solution of Na_2PtCl_6 at 293 K. Black lines are the experimental spectra, while magenta lines show the fitted models and blue lines the individual isotopologue/isotopomer signals.

3 Isotope effects in ^{195}Pt NMR spectra of complexes

known natural fractional abundances of the two Cl isotopes and the ratio of $^{16/18}\text{O}$ isotopes quoted above:

$$\rho(n_1, n_2, \dots, n_x) = \frac{\left(\sum_{i=1}^x n_i\right)!}{\prod_{i=1}^x (n_i)!} \left(\prod_{i=1}^x (\rho_i)^{n_i}\right) \quad (3.2)$$

where n_x is the number of x -isotopes in the particular isotopologue and ρ_x is the fractional (natural or enriched) abundance of this isotope.⁵⁹ The results of the fitting procedure suggest that the $^{35/37}\text{Cl}$ isotope shifts are essentially the same for the sets $[\text{Pt}^{35/37}\text{Cl}_5(^{16}\text{OH})]^{2-}$ and $[\text{Pt}^{35/37}\text{Cl}_5(^{18}\text{OH})]^{2-}$; in fact, we find this almost surprising in view of the extreme sensitivity of ^{195}Pt shielding to exceedingly small changes in bond displacements to atoms in the inner coordination sphere. Similar analyses pertain to the spectra of the complexes *cis*- $[\text{PtCl}_4(\text{OH})_2]^{2-}$ and *fac*- $[\text{PtCl}_3(\text{OH})_3]^{2-}$: the former consists of three sets of five uniformly spaced $^{35/37}\text{Cl}$ isotopologue signals and the latter four sets of four such $^{35/37}\text{Cl}$ isotopologue signals, each set resulting from complexes containing the same number of each of the two O isotopes. Comparing these spectra to those of the corresponding *aqua*-complexes reported by Koch *et al.* (e.g. compare Figures 1.7A and 3.6B), we note that our sets of isotopologue signals appear significantly less complex and also more symmetrical; this, of course, is a result of respectively the lack of $^{35/37}\text{Cl}$ isotopomer resolution in the spectra of the hydroxido-complexes (or, more precisely, the lack of resolution of isotopomers with different combinations of the two Cl isotopes coordinated *trans* to hydroxido-ligands) and the higher level of ^{18}O enrichment in these samples.

Turning now to the ^{195}Pt spectra of the stereoisomers *trans*- $[\text{PtCl}_2(\text{OH})_4]^{2-}$ and *cis*- $[\text{PtCl}_2(\text{OH})_4]^{2-}$ (Figure 3.6D and E), it is immediately evident that these sets are not equivalent with the latter set showing additional, partially resolved fine structure. This might seem surprising at first, considering the fact that in normal water the simple triple-line $^{35/37}\text{Cl}$ isotope-induced patterns of these stereoisomers are essentially indistinguishable. (See Figure 3.3.) Considering first the more shielded set of signals, those assigned to the isotopologues *trans*- $[\text{Pt}^{35/37}\text{Cl}_2(^{16/18}\text{OH})_4]^{2-}$, we note that this set consists of the expected five equivalent sets of three $^{35/37}\text{Cl}$ isotopomer signals, *trans*- $[\text{Pt}^{35/37}\text{Cl}_2(^{16}\text{OH})_{4-n}(^{18}\text{OH})_n]^{2-}$ where $n = 0-4$, with only the relative intensities of these five sets that differ; an analysis similar to that described

Table 3.2 Calculated abundances of isotopologues and percentage area contribution by corresponding resonance signals (determined from non-linear least-squares fitting procedure) for complexes $[\text{Pt}^{35/37}\text{Cl}_6_n(^{16/18}\text{OH})_n]^{2-}$, $n=0-6$, in ^{18}O -enriched sample coordination sphere.

Isotopologue/Isotopomer	Natural abundance	Percentage area (<i>fit</i>)
$[\text{Pt}^{35}\text{Cl}_5(^{16}\text{OH})]^{2-}$	13.49	13.27
$[\text{Pt}^{35}\text{Cl}_4(^{37}\text{Cl}(^{16}\text{OH}))]^{2-}$	21.86	21.55
$[\text{Pt}^{35}\text{Cl}_3(^{37}\text{Cl}_2(^{16}\text{OH}))]^{2-}$	14.16	13.39
$[\text{Pt}^{35}\text{Cl}_2(^{37}\text{Cl}_3(^{16}\text{OH}))]^{2-}$	4.59	2.60
$[\text{Pt}^{35}\text{Cl}^{37}\text{Cl}_4(^{16}\text{OH})]^{2-}$	0.74	<i>n.o.</i>
$[\text{Pt}^{37}\text{Cl}_5(^{16}\text{OH})]^{2-}$	0.04	<i>n.o.</i>
$[\text{Pt}^{35}\text{Cl}_5(^{18}\text{OH})]^{2-}$	11.10	13.02
$[\text{Pt}^{35}\text{Cl}_4(^{37}\text{Cl}(^{18}\text{OH}))]^{2-}$	17.96	20.21
$[\text{Pt}^{35}\text{Cl}_3(^{37}\text{Cl}_2(^{18}\text{OH}))]^{2-}$	11.64	12.09
$[\text{Pt}^{35}\text{Cl}_2(^{37}\text{Cl}_3(^{18}\text{OH}))]^{2-}$	3.77	3.86
$[\text{Pt}^{35}\text{Cl}^{37}\text{Cl}_4(^{18}\text{OH})]^{2-}$	0.61	<i>n.o.</i>
$[\text{Pt}^{37}\text{Cl}_5(^{18}\text{OH})]^{2-}$	0.04	<i>n.o.</i>
$cis\text{-}[\text{Pt}^{35}\text{Cl}_4(^{16}\text{OH})_2]^{2-}$	9.80	8.70
$cis\text{-}[\text{Pt}^{35}\text{Cl}_3(^{37}\text{Cl}(^{16}\text{OH})_2)]^{2-}$	12.71	11.46
$cis\text{-}[\text{Pt}^{35}\text{Cl}_2(^{37}\text{Cl}_2(^{16}\text{OH})_2)]^{2-}$	6.18	4.95
$cis\text{-}[\text{Pt}^{35}\text{Cl}^{37}\text{Cl}_3(^{16}\text{OH})_2]^{2-}$	1.33	1.46
$cis\text{-}[\text{Pt}^{37}\text{Cl}_4(^{16}\text{OH})_2]^{2-}$	0.11	<i>n.o.</i>
$cis\text{-}[\text{Pt}^{35}\text{Cl}_4(^{16}\text{OH})(^{18}\text{OH})]^{2-}$	16.11	16.56
$cis\text{-}[\text{Pt}^{35}\text{Cl}_3(^{37}\text{Cl}(^{16}\text{OH})(^{18}\text{OH}))]^{2-}$	20.88	21.40
$cis\text{-}[\text{Pt}^{35}\text{Cl}_2(^{37}\text{Cl}_2(^{16}\text{OH})(^{18}\text{OH}))]^{2-}$	10.15	10.04
$cis\text{-}[\text{Pt}^{35}\text{Cl}^{37}\text{Cl}_3(^{16}\text{OH})(^{18}\text{OH})]^{2-}$	2.19	1.89
$cis\text{-}[\text{Pt}^{37}\text{Cl}_4(^{16}\text{OH})(^{18}\text{OH})]^{2-}$	0.18	<i>n.o.</i>
$cis\text{-}[\text{Pt}^{35}\text{Cl}_4(^{18}\text{OH})_2]^{2-}$	6.62	7.84
$cis\text{-}[\text{Pt}^{35}\text{Cl}_3(^{37}\text{Cl}(^{18}\text{OH})_2)]^{2-}$	8.58	9.89
$cis\text{-}[\text{Pt}^{35}\text{Cl}_2(^{37}\text{Cl}_2(^{18}\text{OH})_2)]^{2-}$	4.17	4.39
$cis\text{-}[\text{Pt}^{35}\text{Cl}^{37}\text{Cl}_3(^{18}\text{OH})_2]^{2-}$	0.90	1.43
$cis\text{-}[\text{Pt}^{37}\text{Cl}_4(^{18}\text{OH})_2]^{2-}$		
$fac\text{-}[\text{Pt}^{35}\text{Cl}_3(^{16}\text{OH})_3]^{2-}$	7.13	6.57
$fac\text{-}[\text{Pt}^{35}\text{Cl}_2(^{37}\text{Cl}(^{16}\text{OH})_3)]^{2-}$	6.93	5.80
$fac\text{-}[\text{Pt}^{35}\text{Cl}^{37}\text{Cl}_2(^{16}\text{OH})_3]^{2-}$	2.24	1.58
$fac\text{-}[\text{Pt}^{37}\text{Cl}_3(^{16}\text{OH})_3]^{2-}$	0.24	<i>n.o.</i>
$fac\text{-}[\text{Pt}^{35}\text{Cl}_2(^{16}\text{OH})_2(^{18}\text{OH})]^{2-}$	17.57	17.11
$fac\text{-}[\text{Pt}^{35}\text{Cl}_2(^{37}\text{Cl}(^{16}\text{OH})_2(^{18}\text{OH}))]^{2-}$	17.07	16.06
$fac\text{-}[\text{Pt}^{35}\text{Cl}^{37}\text{Cl}_2(^{16}\text{OH})_2(^{18}\text{OH})]^{2-}$	5.53	5.27
$fac\text{-}[\text{Pt}^{37}\text{Cl}_3(^{16}\text{OH})_2(^{18}\text{OH})]^{2-}$	0.60	<i>n.o.</i>
$fac\text{-}[\text{Pt}^{35}\text{Cl}_3(^{16}\text{OH})(^{18}\text{OH})_2]^{2-}$	14.44	16.40
$fac\text{-}[\text{Pt}^{35}\text{Cl}_2(^{37}\text{Cl}(^{16}\text{OH})(^{18}\text{OH})_2)]^{2-}$	14.03	15.39
$fac\text{-}[\text{Pt}^{35}\text{Cl}^{37}\text{Cl}_2(^{16}\text{OH})(^{18}\text{OH})_2]^{2-}$	4.55	4.59
$fac\text{-}[\text{Pt}^{37}\text{Cl}_3(^{16}\text{OH})(^{18}\text{OH})_2]^{2-}$	0.49	<i>n.o.</i>
$fac\text{-}[\text{Pt}^{35}\text{Cl}_3(^{18}\text{OH})_3]^{2-}$	3.96	5.01
$fac\text{-}[\text{Pt}^{35}\text{Cl}_2(^{37}\text{Cl}(^{18}\text{OH})_3)]^{2-}$	3.84	4.87
$fac\text{-}[\text{Pt}^{35}\text{Cl}^{37}\text{Cl}_2(^{18}\text{OH})_3]^{2-}$	1.25	1.35
$fac\text{-}[\text{Pt}^{37}\text{Cl}_3(^{18}\text{OH})_3]^{2-}$	0.13	<i>n.o.</i>
$trans\text{-}[\text{Pt}^{35}\text{Cl}_2(^{16}\text{OH})_4]^{2-}$	5.18	4.11
$trans\text{-}[\text{Pt}^{35}\text{Cl}^{37}\text{Cl}(^{16}\text{OH})_4]^{2-}$	3.36	2.64
$trans\text{-}[\text{Pt}^{37}\text{Cl}_2(^{16}\text{OH})_4]^{2-}$	0.54	0.15
$trans\text{-}[\text{Pt}^{35}\text{Cl}_2(^{16}\text{OH})_3(^{18}\text{OH})]^{2-}$	17.02	15.88
$trans\text{-}[\text{Pt}^{35}\text{Cl}^{37}\text{Cl}(^{16}\text{OH})_3(^{18}\text{OH})]^{2-}$	11.03	10.17
$trans\text{-}[\text{Pt}^{37}\text{Cl}_2(^{16}\text{OH})_3(^{18}\text{OH})]^{2-}$	1.79	1.31
$trans\text{-}[\text{Pt}^{35}\text{Cl}_2(^{16}\text{OH})_2(^{18}\text{OH})_2]^{2-}$	20.99	21.59
$trans\text{-}[\text{Pt}^{35}\text{Cl}^{37}\text{Cl}(^{16}\text{OH})_2(^{18}\text{OH})_2]^{2-}$	13.60	14.04
$trans\text{-}[\text{Pt}^{37}\text{Cl}_2(^{16}\text{OH})_2(^{18}\text{OH})_2]^{2-}$	2.20	1.88
$trans\text{-}[\text{Pt}^{35}\text{Cl}_2(^{16}\text{OH})(^{18}\text{OH})_3]^{2-}$	11.50	13.00
$trans\text{-}[\text{Pt}^{35}\text{Cl}^{37}\text{Cl}(^{16}\text{OH})(^{18}\text{OH})_3]^{2-}$	7.45	8.39
$trans\text{-}[\text{Pt}^{37}\text{Cl}_2(^{16}\text{OH})(^{18}\text{OH})_3]^{2-}$	1.21	1.42
$trans\text{-}[\text{Pt}^{35}\text{Cl}_2(^{18}\text{OH})_4]^{2-}$	2.36	3.11
$trans\text{-}[\text{Pt}^{35}\text{Cl}^{37}\text{Cl}(^{18}\text{OH})_4]^{2-}$	1.53	1.93

Isotopologue/Isotopomer	Natural abundance	Percentage area (<i>fit</i>)	Isotopologue/Isotopomer	Natural abundance	Percentage area (<i>fit</i>)
<i>trans</i> -[Pt ³⁷ Cl ₂ (¹⁸ OH) ₄] ²⁻	0.25	0.39	[Pt ³⁷ Cl(¹⁶ OH) ₄ (¹⁸ OH)] ²⁻	4.01	3.59
<i>cis</i> -[Pt ³⁵ Cl ₂ (¹⁶ OH) ₄] ²⁻	5.18	4.51		1.00	0.75
<i>cis</i> -[Pt ³⁵ Cl ³⁷ Cl(¹⁶ OH) ₄] ²⁻	3.36	2.83	[Pt ³⁵ Cl(¹⁶ OH) ₃ (¹⁸ OH) ₂] ²⁻	15.25	14.50
<i>cis</i> -[Pt ³⁷ Cl ₂ (¹⁶ OH) ₄] ²⁻	0.54	0.42		10.17	10.09
<i>cis</i> -[Pt ³⁵ Cl ₂ (¹⁶ OH) ₃ (¹⁸ OH)] ²⁻	8.79	7.74	[Pt ³⁷ Cl(¹⁶ OH) ₃ (¹⁸ OH) ₂] ²⁻	4.94	4.65
	8.79	8.06		3.29	3.20
<i>cis</i> -[Pt ³⁵ Cl ³⁷ Cl(¹⁶ OH) ₃ (¹⁸ OH)] ²⁻	5.52	4.66	[Pt ³⁵ Cl(¹⁶ OH) ₂ (¹⁸ OH) ₃] ²⁻	8.36	9.24
	5.52	5.70		12.53	13.07
<i>cis</i> -[Pt ³⁷ Cl ₂ (¹⁶ OH) ₃ (¹⁸ OH)] ²⁻	0.90	0.79	[Pt ³⁷ Cl(¹⁶ OH) ₂ (¹⁸ OH) ₃] ²⁻	2.71	2.90
	0.90	0.66		4.06	4.27
<i>cis</i> -[Pt ³⁵ Cl ₂ (¹⁶ OH) ₂ (¹⁸ OH) ₂] ²⁻	3.50	3.29	[Pt ³⁵ Cl(¹⁶ OH)(¹⁸ OH) ₄] ²⁻	1.72	1.78
	13.99	14.20		6.86	8.32
	3.50	3.57	[Pt ³⁷ Cl(¹⁶ OH)(¹⁸ OH) ₄] ²⁻	0.56	0.64
<i>cis</i> -[Pt ³⁵ Cl ₂ (¹⁶ OH) ₂ (¹⁸ OH) ₂] ²⁻	2.27	1.95		2.22	2.63
	9.07	9.49	[Pt ³⁵ Cl(¹⁸ OH) ₅] ²⁻	1.41	1.98
	2.27	2.36	[Pt ³⁷ Cl(¹⁸ OH) ₅] ²⁻	0.46	0.61
<i>cis</i> -[Pt ³⁵ Cl ₂ (¹⁶ OH) ₂ (¹⁸ OH) ₂] ²⁻	0.37	0.24	[Pt(¹⁶ OH) ₆] ²⁻	2.74	2.10
	1.47	1.31	[Pt(¹⁶ OH) ₅ (¹⁸ OH)] ²⁻	13.49	11.53
	0.37	0.36	[Pt(¹⁶ OH) ₄ (¹⁸ OH) ₂] ²⁻	27.71	25.94
<i>cis</i> -[Pt ³⁵ Cl ₂ (¹⁶ OH)(¹⁸ OH) ₃] ²⁻	5.75	6.32	[Pt(¹⁶ OH) ₃ (¹⁸ OH) ₃] ²⁻	30.36	30.96
	5.75	6.69	[Pt(¹⁶ OH) ₂ (¹⁸ OH) ₄] ²⁻	18.71	20.86
<i>cis</i> -[Pt ³⁵ Cl ³⁷ Cl(¹⁶ OH)(¹⁸ OH) ₃] ²⁻	3.73	4.11	[Pt(¹⁶ OH)(¹⁸ OH) ₅] ²⁻	6.15	7.62
	3.73	4.15	[Pt(¹⁸ OH) ₆] ²⁻	0.84	0.99
<i>cis</i> -[Pt ³⁷ Cl ₂ (¹⁶ OH)(¹⁸ OH) ₃] ²⁻	0.61	0.61			
	0.61	0.64			
<i>cis</i> -[Pt ³⁵ Cl ₂ (¹⁸ OH) ₄] ²⁻	2.36	3.02			
<i>cis</i> -[Pt ³⁵ Cl ³⁷ Cl(¹⁸ OH) ₄] ²⁻	1.53	1.99			
<i>cis</i> -[Pt ³⁷ Cl ₂ (¹⁸ OH) ₄] ²⁻	0.25	0.33			
[Pt ³⁵ Cl(¹⁶ OH) ₅] ²⁻	3.76	3.02			
[Pt ³⁷ Cl(¹⁶ OH) ₅] ²⁻	1.22	0.94			
[Pt ³⁵ Cl(¹⁶ OH) ₄ (¹⁸ OH)] ²⁻	12.37	11.09			
	3.09	2.74			

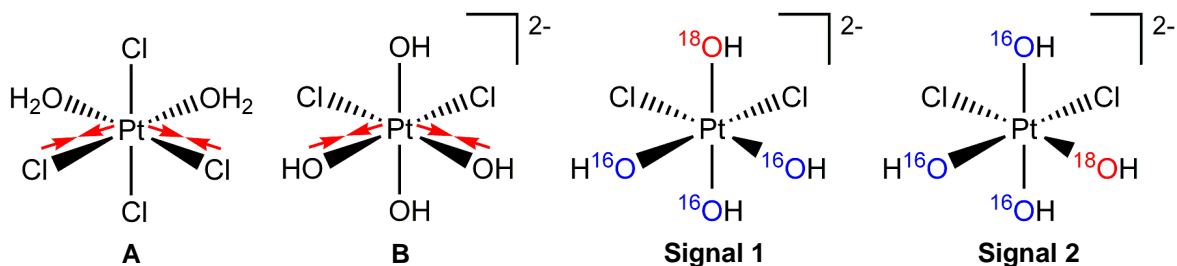
3 Isotope effects in ^{195}Pt NMR spectra of complexes

Figure 3.7 Molecular structures of $\text{cis-}[\text{PtCl}_4(\text{H}_2\text{O})_2]^0$ (A) and $\text{cis-}[\text{PtCl}_2(\text{OH})_4]^{2-}$ (B), showing qualitatively the expected analogous contraction of Pt-Cl and Pt-O bonds (red arrows); also, structures of isotopomers assigned to Signals 1 and 2 in Figure 3.6 are presented.

above for $[\text{Pt}^{35/37}\text{Cl}_5(^{16/18}\text{OH})]^{2-}$, $\text{cis-}[\text{Pt}^{35/37}\text{Cl}_4(^{16/18}\text{OH})_2]^{2-}$ and $\text{fac-}[\text{Pt}^{35/37}\text{Cl}_3(^{16/18}\text{OH})_3]^{2-}$ also performs well for this complex. (See Figure 3.6D and numerical results in Table 3.2; note, however, that due to substantial noise levels there are in some cases notable discrepancies between the experimental and statistically expected values, especially for isotopologues with low abundances.) The spectrum of the isotopologues $\text{cis-}[\text{Pt}^{35/37}\text{Cl}_2(^{16/18}\text{OH})_4]^{2-}$, on the other hand, is truly remarkable (Figure 3.6E); while the two outer sets certainly resemble those of the *trans*-stereoisomer [these should be the signals of isotopologue sets $\text{cis-}[\text{Pt}^{35/37}\text{Cl}_2(^{16}\text{OH})_4]^{2-}$ (downfield) and $\text{cis-}[\text{Pt}^{35/37}\text{Cl}_2(^{18}\text{OH})_4]^{2-}$ (upfield)], the $^{35/37}\text{Cl}$ isotopologue signals of their neighbouring sets are partially resolved to ‘doublets’ with a separation of about 6 Hz and those constituting the central set have broadened bases, suggestive of an unresolved triple-line structure. In fact, this spectrum is strongly reminiscent of that reported by Koch *et al.* for the $\text{cis-}[\text{Pt}^{35/37}\text{Cl}_2(\text{H}_2^{16/18}\text{O})_4]^{2-}$ isotopologues and it turns out that our spectrum can be understood within the same framework³⁸: these additional signals are the result of a measurable magnetic non-equivalence of ^{195}Pt nuclei in *isotopomers* differing only in the number of ^{18}O isotopes coordinated in the two sites *trans* to the chlorido-ligands.

For the set of $^{35/37}\text{Cl}$ isotopologues $\text{cis-}[\text{Pt}^{35/37}\text{Cl}_2(^{16}\text{OH})_3(^{18}\text{OH})]^{2-}$ there exists an equal probability of having two ^{16}O isotopes or one ^{16}O and one ^{18}O isotope in the sites *trans* to chlorido-ligands and, similarly, for the set $\text{cis-}[\text{Pt}^{35/37}\text{Cl}_2(^{16}\text{OH})(^{18}\text{OH})_3]^{2-}$ an equal probability of two ^{18}O isotopes or one ^{18}O and one ^{16}O isotope residing in these sites, resulting in the ‘doublet’ structure of these signals. In view of the greater *trans*-influence of hydroxido- compared to that of chlorido-ligand, we tentatively assign the more upfield (shielded) signal in the doublet $\text{cis-}[\text{Pt}^{35}\text{Cl}_2(^{16}\text{OH})_3(^{18}\text{OH})]^{2-}$ to the isotopomer in which one ^{18}O and one ^{16}O isotope is coordinated *trans* to chloride (Signal 1 in Figure 3.6E), while its downfield partner should result from the isotopomer in which two ^{16}O isotopes occupy these sites (Signal 2),

3 Isotope effects in ^{195}Pt NMR spectra of complexes

following a line of reasoning similar to that used by Koch *et al.* to rationalise the analogous problem of the shielding order of the isotopomers of $\text{cis-}[\text{Pt}^{35}\text{Cl}_3^{37}\text{Cl}(\text{H}_2^{16}\text{O})_2]$ (Figure 3.7).³⁸ As mentioned in the introduction to this section, these authors suggested that since chlorido-ligand has the greater *trans*-influence in these aqua-complexes, the Pt-Cl bond displacements opposite the two coordinated water molecules should be slightly contracted compared to those opposite chloride ions, resulting in an enhancement of the $^{16/18}\text{O}$ isotope shift resulting from isotopic substitution in these sites, which in turn produces the observed double-line pattern. Similar analyses should pertain to the other two $^{35/37}\text{Cl}$ isotopologues in this set and also to the more upfield set of isotopologues $\text{cis-}[\text{Pt}^{35/37}\text{Cl}_2(^{16}\text{OH})(^{18}\text{OH})_3]^{2-}$, the signals of which are also split: the more upfield partner in each ‘doublet’ is assigned to the isotopomer in which more ^{18}O isotopes are coordinated in the two sites *trans* to the chloride ions.

The central set of signals is assigned to the complexes $\text{cis-}[\text{Pt}^{35/37}\text{Cl}_2(^{16}\text{OH})_2(^{18}\text{OH})_2]^{2-}$; the least shielded, most intense triple-line structure is the Pt signals of the isotopologue $\text{cis-}[\text{Pt}^{35}\text{Cl}_2(^{16}\text{OH})_2(^{18}\text{OH})_2]^{2-}$ which, in this case, starts to resolve to the unique signals of the three isotopomers. Continuing our previous shielding hypothesis, we assign the central signal to the isotopomer in which one ^{18}O isotope and one ^{16}O isotope is coordinated opposite the chloride ions, the more downfield signal to the isotopomer with two ^{16}O isotopes and the most upfield signal to the isotopomer with two ^{18}O isotopes in these sites. This assignment can also explain the appearance of this unresolved set of peaks: the isotopomer assigned to the central peak has a *relative* statistical probability of four, while for those assigned to its neighbours this value is only one. This line of reasoning can be extended to the other two triple line structures in this set where only the chlorine isotope content differs. Interestingly, we note again that the $^{35/37}\text{Cl}$ content of these complexes does not seem to have an observable influence on the magnitude of resolution between these isotopomers; the separations between isotopomers of $\text{cis-}[\text{Pt}^{35}\text{Cl}_2(^{16}\text{OH})_3(^{18}\text{OH})]^{2-}$, $\text{cis-}[\text{Pt}^{35}\text{Cl}^{37}\text{Cl}(^{16}\text{OH})_3(^{18}\text{OH})]^{2-}$ and $\text{cis-}[\text{Pt}^{37}\text{Cl}_2(^{16}\text{OH})_3(^{18}\text{OH})]^{2-}$, for example, are identically about 6 Hz. The results of a line fitting procedure where the experimental spectrum was modelled as a sum of Lorentzian peaks, one for each of the isotopomers discussed above, are reported in Table 3.2 and the individual peaks are shown fitted to the spectrum in Figure 3.6E. The relative area contributions of most of these peaks can be seen to be in good agreement with the statistically expected abundances of the corresponding complexes which were calculated as described previously, confirming that this fine structure is indeed the result of a partial resolution of isotopomer signals; the shielding order of isotopomers, i.e. our exact assignment of isotopomer signals, however,

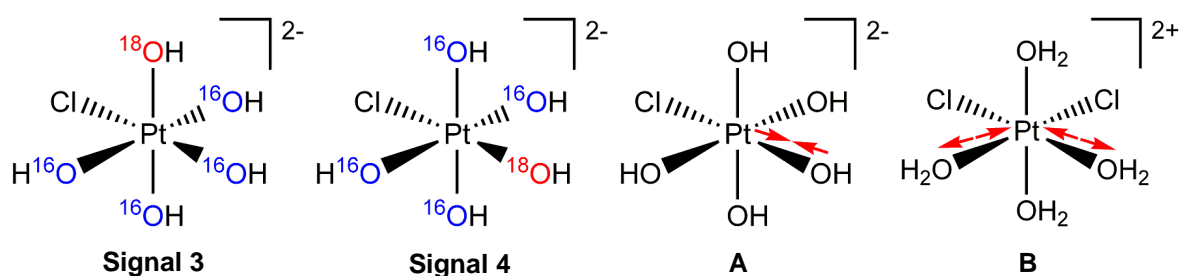
3 Isotope effects in ^{195}Pt NMR spectra of complexes

Figure 3.8 Molecular structures of isotopomers assigned to Signals 3 and 4 in Figure 3.6F; structures of $[\text{PtCl}(\text{OH})_5]^{2-}$ (A) and $\text{cis-}[\text{PtCl}_2(\text{H}_2\text{O})_4]^{2+}$ (B) showing expected bond contraction and extension as discussed in text.

cannot be evaluated from these results.

The set of signals assigned to the series of complexes $[\text{Pt}^{35/37}\text{Cl}(\text{OH})_5]^{2-}$, $n = 0-5$, clearly shows the expected six sets of $^{35/37}\text{Cl}$ isotopologues produced by the larger $^{16/18}\text{O}$ isotope effects, however, we also note some additional partially resolved fine structure for the four inner sets; these sets are assigned to the four pairs of $^{16/18}\text{O}$ -isotopologues $[\text{Pt}^{35/37}\text{Cl}(\text{OH})_5]^{2-}$ with $n = 1-4$ (Figure 3.6F). Since each of these isotopologues exist as two isotopomers of the type considered by Koch *et al.* (one in which an ^{18}O isotope is coordinated opposite the chloride ion and one in which a ^{16}O isotope occupies this site) and since the signals constituting these isotopologue pairs appear to consist identically of two closely separated signals of unequal intensity, it should be reasonable to suggest that this fine structure is also the result of magnetically non-equivalent isotopomers (Figure 3.8). This assignment is confirmed by a line fitting procedure similar to that performed for the signals of the complexes $\text{cis-}[\text{Pt}^{35/37}\text{Cl}_2(\text{OH})_4]^{2-}$, the results of which are also reported in Table 3.2. These results, however, also confirm our hypothesis regarding the shielding order of our $^{16/18}\text{O}$ isotopomers: the signal assigned to $[\text{Pt}^{35}\text{Cl}(\text{OH})_4(\text{OH})]^{2-}$, for example, clearly consists of two signals (Signals 3 and 4) with an integral ratio of 4:1, the more shielded partner also being the less intense, and so it follows that this signal should be assigned to the isotopomer of lower statistical abundance/probability in which an ^{18}O isotope is coordinated opposite the chloride ion (See Figure 3.8). A full assignment of the set of signals in Figure 3.6F is presented in the Appendix in the interest of completeness and as a general example.

We recall that Koch *et al.* have assigned their signals of isotopomers in the set of complexes $\text{cis-}[\text{Pt}^{35/37}\text{Cl}_2(\text{H}_2\text{O})_4]^{2+}$ according to this same trend, i.e. the Pt shielding of isotopomers increase as more ^{18}O isotopes are incorporated in the two sites *trans* to the chloride ions.³⁸ This is interesting in view of the *reversed* relative strengths of the *trans*-influence of chloride

3 Isotope effects in ^{195}Pt NMR spectra of complexes

ion and water molecules; we find it tempting to predict that since the two Pt-O bonds opposite the chloride ligands could reasonably be expected to be *elongated* rather than *contracted* relative to than those in the other two (*cis*) sites owing to the larger *trans*-influence of chlorido-ligands in these aqua-complexes, $^{16/18}\text{O}$ isotope effects in these *trans*-sites should be all but accentuated (enhanced) in a manner that would facilitate resolution of isotopomer signals (Figure 3.8B, compare also Figure 3.7B). Evidently these simple considerations are too limited to even qualitatively explain the very subtle effects that are at play in the ^{195}Pt shielding of stereoisomers of even these relatively simple complexes; perhaps more sophisticated models that also incorporate solvation effects could account for this apparent disparity.

Finally, we consider the most downfield set of signals, that of the isotopologues $[\text{Pt}(^{16/18}\text{OH})_6]^{2-}$. (Figure 3.6G) This set of signals is simple, yet beautifully resolved owing to the lack of $^{35/37}\text{Cl}$ isotope-effects and the narrow lines; one can readily identify all seven $^{16/18}\text{O}$ isotopologues. (The results of a fitting procedure are plotted in Figure 3.6 and tabulated in Table 3.2; also compare this spectrum to that of $[\text{Pt}^{35/37}\text{Cl}_6]^{2-}$ in Figure 3.3A.) These isotope-effects lead for the first time to the *unambiguous* assignment of this signal at ~3250 ppm to the hexahydroxido-complex; while chemical shift trend analysis certainly does allow for a rather convincing assignment of this single peak (in samples with a natural ^{18}O content none of the ^{18}O -containing isotopologues can be detected, at least not within a reasonable space of time), it is not a definite assignment in principle, especially in view of the pronounced sensitivity of ^{195}Pt shielding to solution composition and temperature and the possibility of other, even bridged complexes that could produce a similar single Pt signal. (One of the main disadvantages of chemical shift trend analysis is that signals of at least three of these complexes have to be measured in order to establish the trend.²⁴)

3 Isotope effects in ^{195}Pt NMR spectra of complexes

3.3 Temperature dependence of isotope-induced fine structure in ^{195}Pt NMR spectra

The 128.8 MHz ^{195}Pt signals of the complexes $[\text{Pt}^{35/37}\text{Cl}_6]^{2-}$ and $[\text{Pt}^{35/37}\text{Cl}(\text{OH})_5]^{2-}$ in aqueous solutions measured at various temperatures between 283 K and 308 K are compared in Figure 3.9. A significant change in the isotope-induced profile of the $[\text{Pt}^{35/37}\text{Cl}_6]^{2-}$ resonances is immediately evident as the temperature is increased; this phenomenon will be discussed shortly. For now, however, we consider the gradual downfield shift of this signal, averaging about 1 ppm per degree K, while the shift position of the ^{195}Pt signals of $[\text{PtCl}(\text{OH})_5]^{2-}$ hardly changes. A plot of the ^{195}Pt chemical shifts of these two complex anions (reported relative to that of $[\text{PtCl}_6]^{2-}$ in the external reference solution mentioned previously at 298 K) as a function of the temperature in Figure 3.10 shows that the slopes of the linear trends fitted to these two data sets are significantly different (about 1 and < 0.1 ppm/K respectively; these are the average *temperature coefficients* of the ^{195}Pt chemical shifts over this temperature range, $d\delta(^{195}\text{Pt})/dT$). In fact, these linear trends are reminiscent of the temperature effects observed by Jameson and co-workers for the ^{51}V chemical shift of the octahedral vanadium carbonyl complex $[\text{V}(\text{CO})_6]^-$ in solution.²¹ As mentioned earlier, these authors presented a theory within which to interpret the pronounced sensitivity of transition metal shielding in octahedral complexes to temperature and isotopic substitution in ligands based on the expansion of the nuclear shielding as a function of powers of the mean metal-to-ligand bond displacements: the observed temperature coefficients and mass dependence of shielding could be successfully accounted for by changes in the average metal-to-ligand bond displacements, or more precisely, the derivative of shielding with respect to these bond displacements, also taking into account Morse bond stretching anharmonicity and non-bonded interactions.²¹

In these cases it is important to note that we are referring to the *intrinsic* temperature coefficient of metal shielding that is produced by rotational and vibrational changes in the metal complex. The temperature coefficient of shielding of many nuclei, and especially the proton, in liquid samples is dominated by changes in intermolecular interactions and solution density. Transition metal nuclei situated at the centre of octahedral complexes, on the other hand, are surrounded by ligands, effectively ‘shielding’ the metal nucleus from intermolecular interaction, and so the temperature coefficient observed directly in solution is a good approximation of the desired intrinsic temperature coefficient which provides inform-

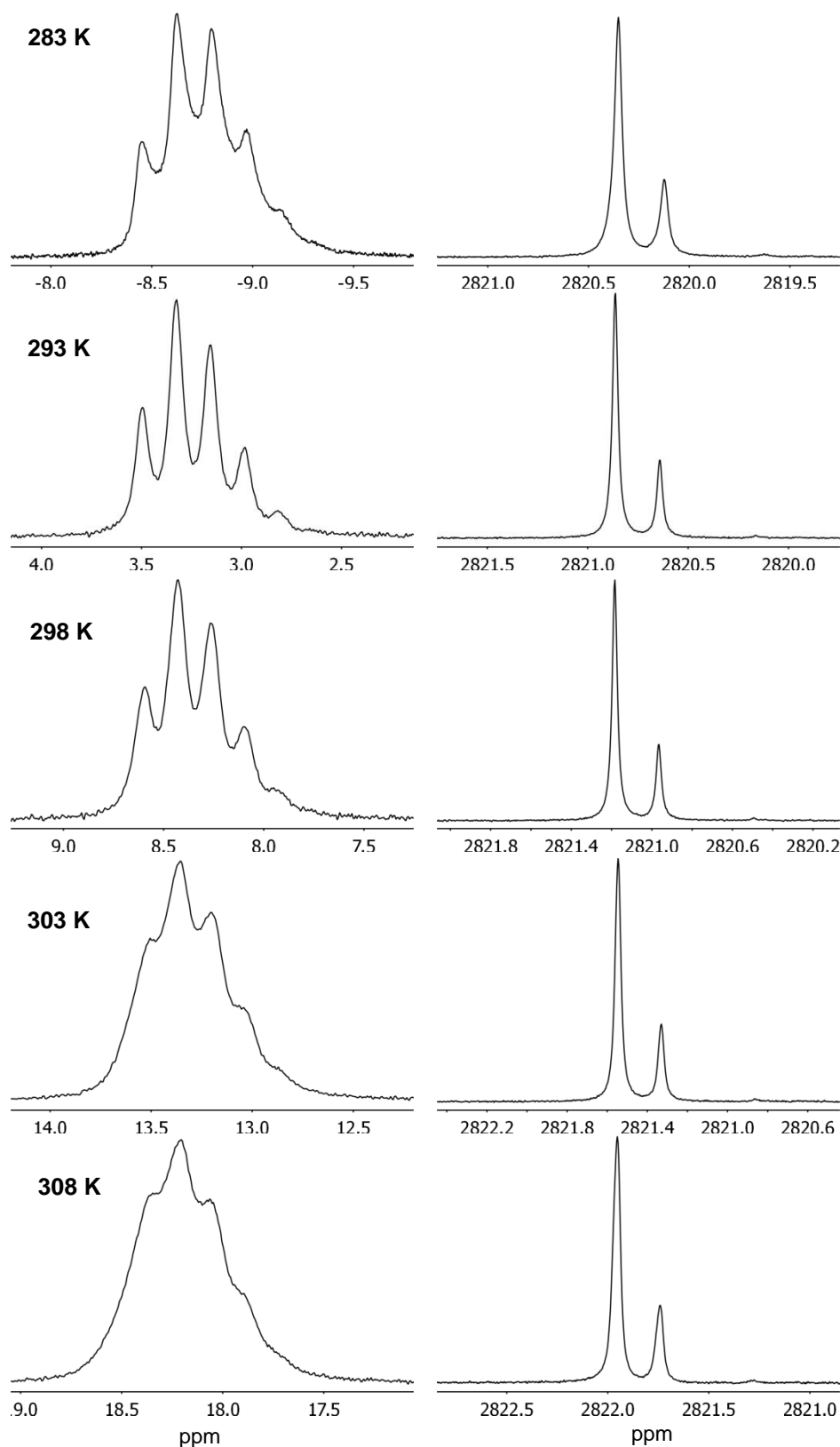
3 Isotope effects in ^{195}Pt NMR spectra of complexes

Figure 3.9 128.8 MHz ^{195}Pt NMR spectra of the sets of isotopologues $[\text{Pt}^{35/37}\text{Cl}_6]^{2-}$ (left column) and $[\text{Pt}^{35/37}\text{Cl}(\text{}^{16}\text{OH})_5]^{2-}$ (right column) in aqueous solutions of Na_2PtCl_6 (1 mol.dm $^{-3}$ perchloric acid and 4 mol.dm $^{-3}$ sodium hydroxide, ca. 30 % D_2^{16}O , respectively) collected at various temperatures between 283 and 308 K.

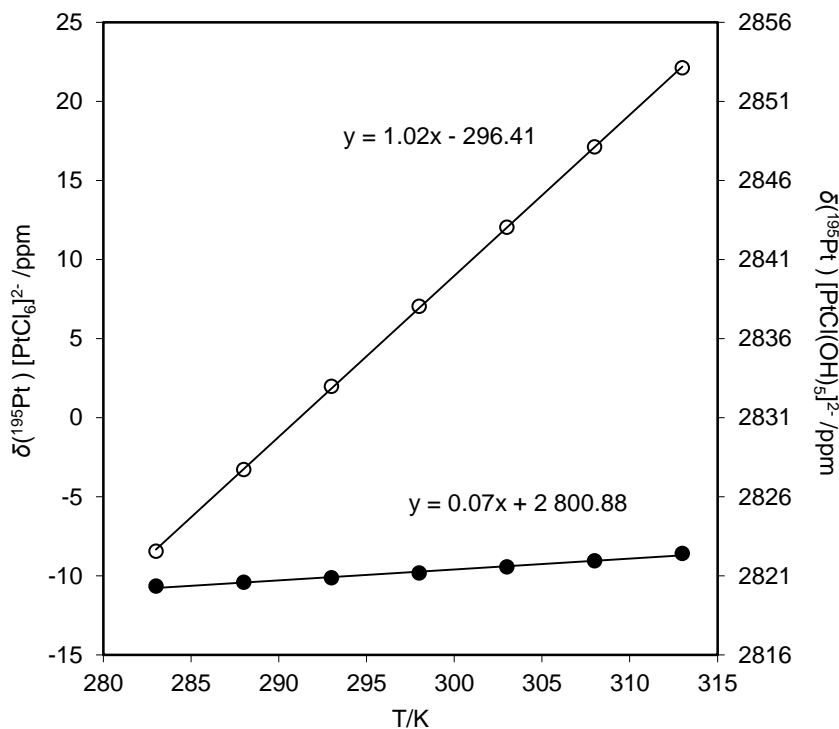
3 Isotope effects in ^{195}Pt NMR spectra of complexes

Figure 3.10 Plot of average ^{195}Pt chemical shifts of the complexes $[\text{PtCl}_6]^{2-}$ (open circles) and $[\text{PtCl}(\text{OH})_5]^{2-}$ (solid circles) in aqueous solutions as a function of temperature between 283 and 313 K with regression lines. (Note that the two chemical shift-axes have the same overall range)

ation on the sensitivity of magnetic shielding to changes in *rovibrationally averaged* bond displacements in the complex.²¹

Jameson *et al.* used experimental $^{12/13}\text{C}$ and $^{16/18}\text{O}$ isotope shifts in the ^{51}V NMR spectra of $[\text{V}(\text{CO})_6]^-$ along with calculated mean bond displacements to determine the sensitivity of ^{51}V shielding to bond extension, $(\partial\sigma^{\text{V}}/\partial\Delta r_{\text{VC}})_e$ and $(\partial\sigma^{\text{V}}/\partial\Delta R_{\text{CO}})_e$, and ultimately to estimate the temperature dependence of the ^{51}V chemical shift; this value was found to be in good agreement with that measured experimentally. (The subscript ‘e’ signifies that these derivatives are evaluated at the equilibrium bond length.) A similar analysis could be used to successfully recover the experimental temperature dependence of ^{59}Co shielding in $[\text{Co}(\text{CN})_6]^{3-}$, demonstrating the generality of this model of transition metal shielding in complexes in solution.²¹

Comparing the temperature dependence of ^{51}V shielding in various octahedral carbonyl-containing vanadium complexes, Jameson *et al.* observed a correlation between the ^{51}V shielding, or chemical shift, and its temperature coefficient: the temperature coefficient appeared to increase linearly with a decrease in ^{51}V shielding (increase in chemical shift, δ).

3 Isotope effects in ^{195}Pt NMR spectra of complexes

This observation was demonstrated to be consistent with a relatively simple electrostatic model of transition metal shielding in complexes that considers only changes in paramagnetic shielding by d electrons and, for the most part, neglects bond covalency effects. (See Bramley *et al.*⁶⁰) This so-called d^q model also predicts that isotope shifts should correlate with transition metal shielding in a similar linear fashion for a series of related complexes, where the dynamic properties (the mean bond length and its temperature coefficient) of the chemical bonds in question vary only slightly in the series, and this was found to describe the observed trend for $^{12/13}\text{C}$ isotope shifts in the ^{51}V NMR spectra of some of these carbonyl-containing complexes reasonably well. (Interestingly, *two-bond* $^{16/18}\text{O}$ isotope shifts were found to be much smaller for these carbonyl-complexes.)

We find that this latter prediction appears to be qualitatively consistent with the slightly larger absolute $^{35/37}\text{Cl}$ isotope shift of 28 Hz (0.22 ppm) in the ^{195}Pt NMR signal of $[\text{PtCl}(\text{OH})_5]^{2-}$ with chemical shift about 2820 ppm at 293 K compared to the 21 Hz (0.17 ppm) between the isotopologues of $[\text{PtCl}_6]^{2-}$ at about 3 ppm (note that this is the shift resulting from substitution of *one* ^{35}Cl isotope; Jameson *et al.* commonly refer to isotope shifts, but these are the frequency separations between the signals of the all ^{35}Cl and the all ^{37}Cl isotopologues, i.e. an *overall* isotope shift). The average $^{35/37}\text{Cl}$ and $^{16/18}\text{O}$ isotope shifts in the Pt signals of most of the hydroxido-complexes (all except *trans*- $[\text{PtCl}_4(\text{OH})_2]^{2-}$ and *mer*- $[\text{PtCl}_3(\text{OH})_3]^{2-}$) at 293 K are plotted in Figure 3.11 as a function of the average ^{195}Pt chemical shift; we note that both sets of data appear to be well approximated by linear trends with small positive slopes. However, this is certainly not the case regarding the predicted correlation between shielding and the temperature coefficient of shielding. The $[\text{PtCl}(\text{OH})_5]^{2-}$ complex, the Pt centre of which is deshielded relative to that of $[\text{PtCl}_6]^{2-}$ by nearly 3000 ppm, clearly displays a much smaller temperature coefficient to shielding in the temperature range 283 to 313 K. (See Figure 3.10; *ca.* -0.1 and -1 ppm/degree respectively.) In fact, while these data are not shown in Figure 3.10, we do find intermediate temperature coefficients for *cis*- $[\text{PtCl}_2(\text{OH})_4]^{2-}$ (-0.3 ppm/K at $\delta(^{195}\text{Pt}) \approx 2350$ ppm) and *fac*- $[\text{PtCl}_3(\text{OH})_3]^{2-}$ (-0.5 ppm/K at $\delta(^{195}\text{Pt}) \approx 1860$ ppm), suggestive of a complete reversed relationship in this series between the shielding and temperature coefficient from that expected from the d^q model.

These results are quite interesting, especially in view of the fact that both $^{35/37}\text{Cl}$ and $^{16/18}\text{O}$ isotope shifts follow the predicted trend rather closely, which implies that the assumptions of this model are well satisfied. It is felt that differences in dynamic properties between Pt-Cl

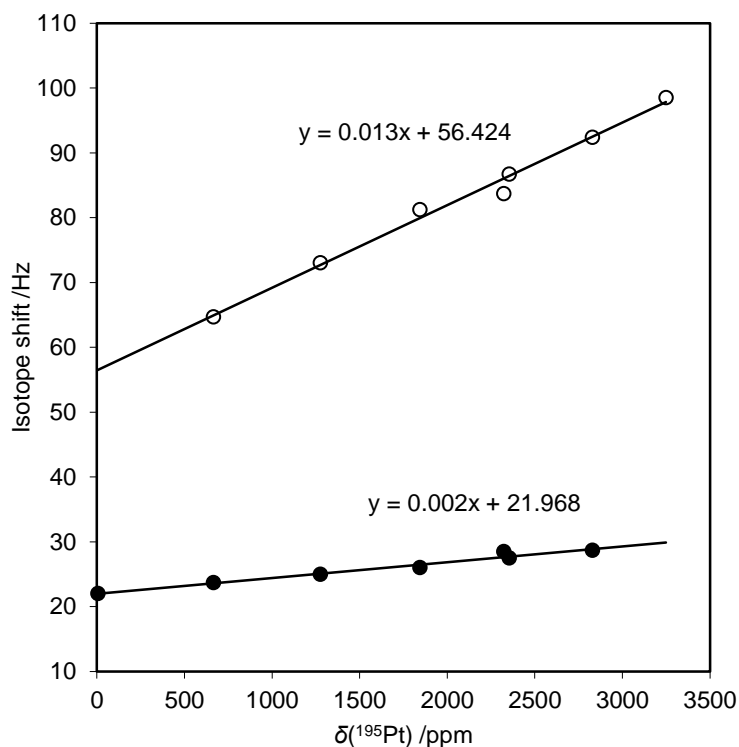
3 Isotope effects in ^{195}Pt NMR spectra of complexes

Figure 3.11 $^{35/37}\text{Cl}$ (solid circles) and $^{16/18}\text{O}$ (open circles) isotope shifts (in hertz, at 14.1 T field) in the ^{195}Pt NMR spectra of the complexes $[\text{PtCl}_{6-n}(\text{OH})_n]^{2-}$ in aqueous solutions at 293 K plotted as a function of the average ^{195}Pt chemical shift, $\delta(^{195}\text{Pt})$, of the corresponding complexes with regression lines.

and Pt-O bonds in these complexes may well be important (the temperature coefficient of shielding is dependent on *all* bonds to the metal): while the dynamic properties of these two bonds may vary only slowly among themselves through this series of complexes, e.g. the properties of all Pt-Cl bonds are quite similar in this series, this is unlikely to be the case when comparing Pt-Cl and Pt-O bonds. Jameson *et al.* concluded their work by suggesting that, although experimental data implies a correlation between paramagnetic shielding, σ^p , (which is for the most part the major contribution to changes in transition metal shielding with bond extension; i.e. $\partial\sigma^p/\partial\Delta r_{\text{ML}} \approx \partial\sigma/\partial\Delta r_{\text{ML}}$) and the derivative $\partial\sigma/\partial\Delta r_{\text{ML}}$, this correlation should be more complicated than the linear correlation predicted by the simple electrostatic d^q model.²¹ Still, we find the *reversed* relationship observed for our complexes intriguing.

Interestingly, studies of the related series aqua-complexes, $[\text{PtCl}_n(\text{H}_2\text{O})_{6-n}]^{4-n}$, $n = 2-5$, by Koch *et al.* shows that there does not appear to exist a simple relationship between the magnitudes of $^{35/37}\text{Cl}$ isotope shifts and the number of coordinated water molecules, hence essentially the ^{195}Pt chemical shift.³⁸ These authors also reported that the members of stereoisomer pairs in this series, having rather comparable ^{195}Pt shielding relative to the

3 Isotope effects in ^{195}Pt NMR spectra of complexes

overall chemical shift range for these complexes, have significantly different $^{35/37}\text{Cl}$ isotope shifts, the more deshielded stereoisomers having the *smaller* isotope shift throughout. We propose that this observation probably is a result of more abrupt variations in the dynamic properties of Pt-Cl bonds in this aqua-series (mean metal-to-ligand bond displacement and its temperature coefficient, $d\Delta r_{\text{ML}}/dT$); as a result the correlation between the electronic factors σ and $d\sigma/d\Delta r_{\text{ML}}$ cannot be observed directly. While ^{195}Pt shielding temperature coefficients have not been reported for these aqua-complexes, agreement with the trend predicted by the electrostatic d^q shielding model is not expected; here it is interesting to compare the effect of temperature on ^{199}Hg chemical shifts in the octahedral mercury(II) solvate $[\text{Hg}(\text{H}_2\text{O})_6]^{2+}$ recently reported by Maliarik and Persson.⁶¹ In these exceedingly labile complexes ('labile' in the sense that exchange of water molecules in the primary coordination sphere of the metal is extremely rapid) the Hg nuclear shielding *increases* as the temperature is increased, characteristic of a dominant intermolecular contribution to the observed temperature coefficient of shielding.²¹ This seems intuitively reasonable considering the ligands are themselves solvent molecules and are also likely to interact with the surrounding solvent via specific intermolecular interactions (hydrogen bonding), which may be expected to have an effect on Hg-O bond properties. In the series of aqua-complexes $[\text{PtCl}_n(\text{H}_2\text{O})_{6-n}]^{4-n}$ ($n = 2-5$) similar phenomena, or interactions, are likely to affect the ^{195}Pt shielding temperature coefficient; moreover, even though Pt-O bonds are expected to be considerably more kinetically inert in the related series of hydroxido-complexes, $[\text{PtCl}_{6-n}(\text{OH})_n]^{2-}$ ($n = 1-6$), it should not be inconceivable that similar contributions to the overall observed temperature coefficient of Pt shielding in these complexes by changes in intermolecular interactions could be important, and increasingly so as more hydroxide ions are introduced into the coordination sphere of the metal. (Note that, even in the series of mixed aqua-platinum complexes, the Pt-O bonds are certainly less labile compared to the Hg-O bonds in $[\text{Hg}(\text{H}_2\text{O})_6]^{2+}$ in aqueous solution, as evidenced by the exquisite $^{16/18}\text{O}$ -induced fine structure observed in the ^{195}Pt NMR signals of these platinum complexes; e.g. Figure 1.7.)

It is interesting to recall also that when attempting to compute the ^{195}Pt shielding tensors of some of these hydroxido-complexes by high-level DFT calculations, Burger *et al.*²⁶ found that agreement with experimental values deteriorated as the number of hydroxide ions in the coordination sphere was increased and this was suggested to be the result of inadequate modelling of interactions of especially these coordinated hydroxide ions with water molecules in the surrounding solvation spheres. It seems reasonable that if indeed such

3 Isotope effects in ^{195}Pt NMR spectra of complexes

intermolecular interactions have a significant effect on Pt shielding in these complexes, they should also assume an important part in the observed temperature coefficients of Pt shielding (that is, if the nature of these intermolecular interactions change with temperature; however, this is expected to be more than likely for these relatively weak interactions).

Considering now the changes in the ^{195}Pt spectra of the isotopologues $[\text{Pt}^{35/37}\text{Cl}_6]^{2-}$ in Figure 3.9, we see that as the temperature is increased, considerable loss of resolution between these signals results. A possible explanation for the loss of resolution may be based on changes in the statistical occupancies of vibrational energy levels of these complexes upon increasing the temperature. As mentioned earlier, NMR isotope shifts are the result of small differences in the magnetic shielding of the probe nuclei in isotopologues, which are produced by minute differences in the mean bond displacement between the probe nucleus and the nucleus of which the composition varies (various isotopes). These differences in bond displacement, in turn, are produced by small differences in the vibrational frequencies of the isotopologues (typically, bond *stretching* vibrations are the most important) and the effect of bond stretching anharmonicity. When the temperature is increased, successively higher vibrational energy levels become populated which, in addition to a decrease in the separation between these levels, is likely to be accompanied by a decrease in the *difference* between the vibrational frequencies of isotopologues, resulting in smaller differences in bond displacement and a reduction in the magnitude of the isotope shift (see Gombler⁶² and Osten and Jameson⁶³). Comparing also the spectra of the complexes $[\text{Pt}^{35/37}\text{Cl}(\text{}^{16}\text{OH})_5]^{2-}$, however, we notice that here the magnitude of the isotope shift hardly changes as the temperature is increased; in the context of the above theory based on changes in the occupancies of vibrational energy levels, this observation requires that the dynamic properties of the Pt-Cl bonds in these latter isotopologues be significantly different to those of the complexes $[\text{Pt}^{35/37}\text{Cl}_6]^{2-}$ in these aqueous solutions. While this requirement certainly does not seem unreasonable at first, we recall that the good linear correlation observed between the $^{35/37}\text{Cl}$ isotope shift and the metal chemical shift in these complexes suggests that the dynamic properties of these Pt-Cl bonds probably change only slowly in this series (Figure 3.11). At any rate, a fuller understanding of the importance of these dynamic differences will certainly require calculations of the vibrational energy level populations of these complexes and these are currently in progress; for now we note that, at least visually, the separation between the isotopologue signals of $[\text{Pt}^{35/37}\text{Cl}_6]^{2-}$ do appear to decrease at the higher temperatures.

3 Isotope effects in ^{195}Pt NMR spectra of complexes

While this ‘collapse’ of $^{35/37}\text{Cl}$ isotope shifts may well be responsible for loss of resolution in the ^{195}Pt signals of $[\text{PtCl}_6]^{2-}$ upon increasing the temperature, it is also quite possible that line-broadening of the individual isotopologue peaks could contribute. This is also suggested by the fact that the overall width of the overall width of the $[\text{Pt}^{35/37}\text{Cl}_6]^{2-}$ set of signals does not decrease, or ‘sharpen up’, at higher temperatures, as would be expected if indeed changes in the magnitude of $^{35/37}\text{Cl}$ isotope shifts were *solely* responsible for the observed loss of resolution. (See Figure 3.9; the ^{195}Pt signals of $[\text{Pt}^{35/37}\text{Cl}]^{2-}$ collected at 353 K is a single, broad peak with rather *Gaussian*, somewhat asymmetric peak shape.) As mentioned previously, Murray *et al.*³⁷ first reported these changes in the appearance of the ^{195}Pt NMR signals of $[\text{PtCl}_6]^{2-}$ and the aqua-complexes $[\text{PtCl}_5(\text{H}_2\text{O})]^-$ and *cis*- $[\text{PtCl}_4(\text{H}_2\text{O})_2]$ in aqueous solutions at temperatures exceeding a narrow range of *ca.* 10 degrees centred at 293 K. These authors also suggested that line broadening should be responsible, presumably due to the spin-rotation relaxation mechanism which is known to become more effective as the temperature is increased.³⁷ Similar observations were described by Koch and co-workers⁵³ in the ^{103}Rh NMR spectra of the series of rhodium complexes $[\text{RhCl}_n(\text{H}_2\text{O})_{6-n}]^{3-n}$, $n = 3-6$. Pesek and Mason¹⁸ have reported the longitudinal (T_1) relaxation times of $[\text{PtCl}_6]^{2-}$ in solutions of the sodium salt and di-acid in water at several temperatures and these data certainly suggest that this spin-rotation mechanism is important in the temperature range of interest. This possibility will be considered in greater detail in the next chapter; for now we note that the Pt line widths of the two $^{35/37}\text{Cl}$ isotopologues of $[\text{PtCl}(\text{OH})_5]^{2-}$ hardly change as the temperature is increased.

Finally, we consider the spectra collected at temperatures below 293 K and we note that while the spectra appear to suffer relatively little loss of isotopologue resolution at the lower temperatures, the spectra collected at 283 K certainly differ visually from those at 293 K. Closer inspection of these Pt signals reveals that isotopologue line widths appear to broaden only slightly and isotope shifts remain essentially unchanged, yet the isotopologue profiles of these peaks gradually change as the temperature is decreased. We note an interesting trend: as the temperature is decreased the signals of isotopologues containing more ^{37}Cl isotopes appear to increase in intensity relative to those containing fewer. This trend can also be recognised in the ^{195}Pt NMR spectra of $[\text{PtCl}_6]^{2-}$ in an acidic aqueous solution collected at various temperatures by Koch *et al.*³⁷ Attempting to model the set of signals collected at 283 K as a sum of Lorentzian peaks, however, reveals that the shapes of these individual isotopologue signals are certainly not symmetrical; in fact, they clearly slope to the upfield.

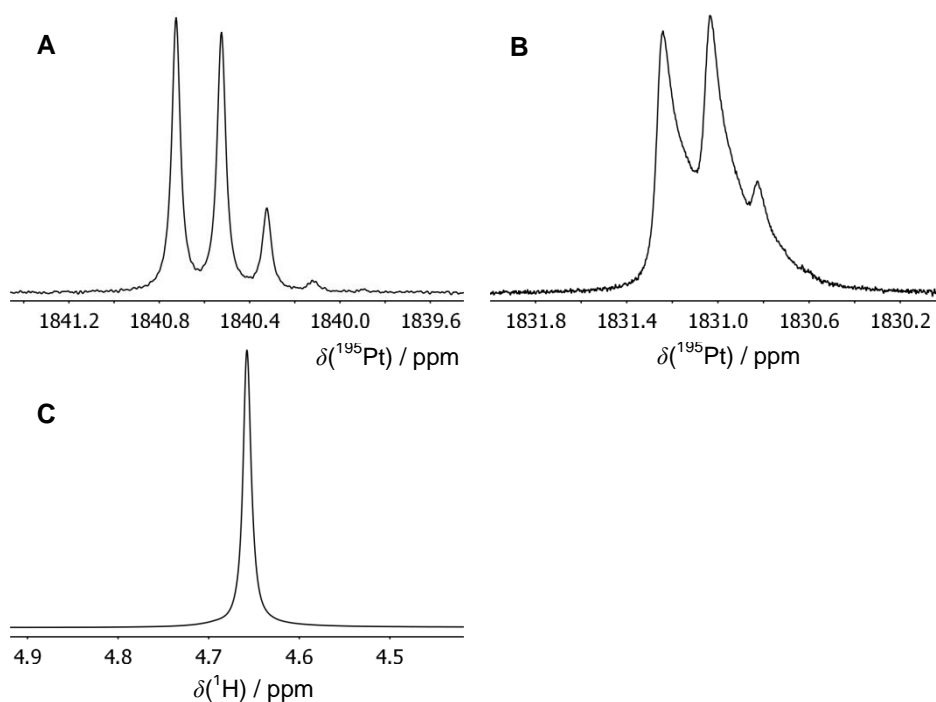
3 Isotope effects in ^{195}Pt NMR spectra of complexes

Figure 3.12 128.8 MHz ^{195}Pt NMR spectra of *fac*- $[\text{PtCl}_3(\text{OH})_3]^{2-}$ in an alkaline aqueous solution at 293 K (A) and 278 K (B) and 600 MHz ^1H signal of water (H_2O and HDO) in the same sample at 278 K (C).

While observations of this kind are commonly associated with poor magnetic field homogeneity, we find that under the exact same conditions the water ^1H signal, although slightly broadened (proton relaxation times are commonly reduced at lower temperatures), does not show this asymmetric sloping and has a perfectly normal Lorentzian shape. To demonstrate the generality of this phenomenon, we show the ^{195}Pt signals of the isotopologues *fac*- $[\text{Pt}^{35/37}\text{Cl}_3(^{16}\text{OH})_3]^{2-}$ collected at 278 K in Figure 3.12; also shown is the water ^1H signal for this same sample under the exact same conditions. In view of the extreme sensitivity of ^{195}Pt chemical shifts to temperature, we cooled this sample for several days prior to extensive thermal equilibration in the NMR probe at 278 K, yet this proved to have little, if any, effect on our spectra; in fact, the ^{195}Pt spectrum shown in Figure 3.12B (and the ^1H signal in C) was collected during this very experiment. It is interesting to note that the ^{195}Pt signals of $[\text{Pt}^{35/37}\text{Cl}(\text{OH})_5]^{2-}$ collected at 283 K do not seem to show this peculiar peak shape (Figure 3.9); since these complexes have a significantly smaller ^{195}Pt shielding temperature coefficient compared to that of the $[\text{Pt}^{35/37}\text{Cl}_6]^{2-}$ and *fac*- $[\text{Pt}^{35/37}\text{Cl}_3(^{16}\text{OH})_3]^{2-}$ complexes (note the *ca.* 10 ppm downfield shift for the latter on going from 298 to 278 K), suggesting that this phenomenon could well be related to thermal equilibration or inadequate temperature control.

4

¹⁹⁵Pt nuclear magnetic relaxation in complexes of the type $[\text{PtCl}_{6-n}(\text{OH})_n]^{2-}$, $n = 0-6$

4.1 Introduction

In general, once a nuclear spin system has been perturbed from thermal equilibrium in an NMR experiment, the spins return to equilibrium by an exchange of energy with their environment. This phenomenon is known as spin relaxation and can proceed via two fundamentally different types of processes. The first involves the interaction of a nuclear spin with its surroundings and these processes are known as spin-lattice or longitudinal relaxation mechanisms; the rate of exchange by these mechanisms is characterised by the spin-lattice relaxation time, commonly denoted T_1 . The second type of process involves interaction of the nuclear spin with other spins to which it is magnetically coupled and is correspondingly referred to as spin-spin relaxation or transverse relaxation, the rate of which is similarly characterised by a time T_2 . These spin-lattice and spin-spin relaxation rates are described by the well-known set of phenomenological equations once formulated by Bloch.⁶⁴ More rigorous and concise introductions to NMR relaxation can be found in a number of texts. (See, for example, Farrar and Becker⁶⁵, Bakhmutov⁶⁶ and Slichter.⁶⁷) Besides enabling modern multi-pulse NMR experiments, these relaxation processes are of particular interest since they are responsible for the broadening of nuclear spin energy levels which manifests as line broadening in NMR spectra. Since all processes, or relaxation mechanisms, contributing to spin-lattice relaxation similarly affect spin-spin relaxation, we note that the following condition holds: $T_1 \geq T_2$. Invoking also Heisenberg's Uncertainty Principle, it can be demonstrated that the width at half height of an NMR signal can be expressed by the following equation: $\nu_{1/2} = 1/\pi T_2$. In addition to this homogeneous broadening of the

4 ¹⁹⁵Pt nuclear magnetic relaxation in complexes

theoretically Lorentzian signal, inhomogeneity of the applied magnetic field over the sample cause spatially separated resonant nuclei to precess at (slightly) different frequencies, resulting in a *Gaussian* broadening contribution. Ideally this is to be prevented as far possible by proper shimming of the magnet before starting the experiment.⁶⁸

Spin interactions contributing to spin-lattice *and* spin-spin relaxation (i.e. which act to reduce relaxation times) produce transient magnetic fields at the probe nucleus that fluctuate at or near its Larmor frequency, ω_0 . These stochastic fluctuations are generally produced by thermal molecular tumbling and/or intramolecular rotations. The classic example of the dipolar (DD) relaxation mechanism is also the most frequently encountered in proton relaxation in solution: protons interact with magnetic dipoles, usually other protons, in their immediate vicinity and this interaction is modulated by rapid tumbling of the molecule in solution which in turn facilitates spin relaxation. The dipolar contributions to the observed spin-lattice and spin-spin relaxation rates are described by the equations of Bloembergen, Purcell and Pound⁶⁸ (note that these historic equations are only valid for a system of like spins, I , e.g. two protons, in the same molecule);

$$\begin{aligned} 1/T_1^{DD} &= \frac{2\gamma^4\hbar^2 I(I+1)}{5r^6} \left(\frac{\tau_c}{1+\omega^2\tau_c^2} + \frac{4\tau_c}{1+4\omega^2\tau_c^2} \right) \\ 1/T_2^{DD} &= \frac{\gamma^4\hbar^2 I(I+1)}{5r^6} \left(3\tau_c + \frac{5\tau_c}{1+\omega^2\tau_c^2} + \frac{2\tau_c}{1+4\omega^2\tau_c^2} \right) \end{aligned} \quad (4.1a)$$

we note that these rates are dependent on the Larmor frequency (ω) and magnetogyric ratio (γ) of the nuclei, the distance between them (r) and the rotational correlation time of the molecule, τ_c (which can be thought of as the time required for the molecule to rotate through one radian). In mobile liquids where $\omega_0\tau_c \ll 1$, a situation commonly referred to as the *extreme narrowing condition*, these equations are simplified in the sense that they become independent of the Larmor frequency resulting in the spin-lattice and spin-spin relaxation rates (henceforth denoted by R_1 and R_2 , respectively) becoming equal;

$$R_1^{DD} = R_2^{DD} = \frac{2\gamma^4\hbar^2 I(I+1)}{r^6} \tau_c \quad (4.1b)$$

Similar sets of equations describing the contributions to R_1 and R_2 by a number of other relatively common relaxation mechanisms have since been formulated and are readily

4 ¹⁹⁵Pt nuclear magnetic relaxation in complexes

available in a number of texts.⁶⁶ (Including heteronuclear and intermolecular dipolar relaxation.) These relaxation rate formulae generally take the form $1/T_i = R_i = CJ(\omega_0\tau_c)$ where C represents the strength of the spin interaction and J is commonly referred to as the spectral density function (the form changes for different relaxation mechanisms); moreover, the value of C is related to molecular structure characteristics while that of J depends on the characteristics of the molecular motion.⁶⁵ It follows that measurements of relaxation times can provide valuable information regarding molecular structure and motion and these relationships have been exploited in many studies. (See Bakhmutov⁶⁶, for example.) In general, a number of relaxation mechanisms may be simultaneously operative in many chemical systems and these contribute in an additive fashion to the observed relaxation rate. (Note that while the relaxation rates are additive, this implies that the relaxation times are not) Fortunately, these contributions can often be separated by experiments which exploit the unique temperature and frequency dependence of the different relaxation mechanisms. Under extreme narrowing conditions, for example, the dipolar mechanism is independent of frequency, unlike the chemical shift anisotropy (CSA) mechanism.⁶⁶ Consequently, the presence of a significant CSA relaxation contribution can be easily uncovered by measuring the T_1 relaxation time of the nucleus in question in two different magnetic fields. Nevertheless, one relaxation mechanism is often found to be dominant under a certain set of experimental conditions.^{65,66}

There has in the past been much interest in the spin relaxation mechanisms of spin one-half heavy metal nuclei (¹⁹⁵Pt, ¹⁹⁹Hg and ²⁰⁷Pb) in complexes in solution.⁶⁹ The first measurements of ¹⁹⁵Pt relaxation times date back some 40 years to the early work of Pregosin⁷⁰ and co-workers and that of Pesek and Mason.¹⁸ The latter authors were particularly interested in studying the electronic and structural properties of Pt complexes using the then new pulsed Fourier transform technique and their comprehensive work includes ¹⁹⁵Pt relaxation times (T_1 and T_2 times, both measured using sequential pulse techniques) for $[\text{PtCl}_4]^{2-}$ and $[\text{PtCl}_6]^{2-}$ salts in aqueous solutions at different temperatures and also in a number of solvents. These measurements suggested that dipolar relaxation mechanisms do not contribute substantially to ¹⁹⁵Pt relaxation in these complexes in solution (at least not at the moderate temperatures studied) and convincing evidence was presented for a dominant spin-rotation relaxation mechanism for both complexes at 9.75 MHz between about 294 and 345 K. This spin-rotation (SR) relaxation mechanism was first described by Ramsey⁷¹ and involves the interaction of the spin one-half resonant nucleus with magnetic

4 ¹⁹⁵Pt nuclear magnetic relaxation in complexes

moments produced by electrons in the rotating molecule; this interaction is modulated by collisions with other molecules which results in changes in the angular momentum of the molecule, thus enabling nuclear relaxation.^{65,66} Early theoretical treatments of this theory by Hubbard⁷² and others⁷³ can be simplified for spherical top molecules undergoing isotropic reorientation and with the probe nucleus at the centre of spherical symmetry in the following relaxation rate equation,

$$R_1^{SR} = R_2^{SR} = \frac{8\pi^2 I k T}{\hbar^2} C_{\text{eff}}^2 \tau_J \quad (4.2)$$

in which I is the molecular moment of inertia, T the temperature, C_{eff} is the effective spin-rotation vector (which in this special case reduces to a scalar with magnitude in Hertz units) and τ_J is the angular momentum correlation time, which essentially describes the time that a molecule maintains a certain state of angular momentum after suffering a collision, hence the alternative ‘angular momentum memory time’.⁷² The spin-rotation mechanism can be particularly effective for nuclei with large chemical shift ranges (paramagnetic shielded) situated in small, rapidly rotating molecules and becomes increasingly more effective as the temperature is increased. This unique temperature dependence of spin-rotation relaxation compared to that of virtually all other mechanisms is a result of the dependence of this mechanism on angular momentum; most other relaxation mechanisms are dependent only on molecular reorientational correlation times (τ_c).⁶⁵ This phenomenon may be understood as follows: as the temperature is increased, the rotational velocity of the molecule increases, which results in a greater angular momentum. Note, however, that molecular collisions also become more frequent under these conditions, complicating this simple line of reasoning; several models describing the rotational motions of colliding molecules have been devised (see Hubbard⁷² and Steele⁷⁵ for small-step and Gordon⁷⁶ and McClung⁷⁷ for extended diffusion models).

Interestingly, Pesek and Mason¹⁸ also reported large discrepancies to the extent of two orders of magnitude between the ¹⁹⁵Pt T_1 and T_2 values measured for respectively $[\text{PtCl}_4]^{2-}$ and $[\text{PtCl}_6]^{2-}$ in water at 299 K; similar observations were reported for these complexes in the presence of different counter-ions and also in a number of different solvents. Since both complexes contain magnetically quadrupolar Cl nuclei (nuclei with spin $I \geq 1$, nuclei with a non-spherical charge distribution; both ³⁵Cl and ³⁷Cl isotopes are quadrupolar nuclei with $I =$

4 ¹⁹⁵Pt nuclear magnetic relaxation in complexes

3/2) and since none of the commonly encountered relaxation mechanisms can account for a discrepancy of this magnitude, at least not in the extreme narrowing regime which was thought to be prevalent, the possibility of a scalar coupling relaxation mechanism was considered. This scalar coupling (SC) mechanism is enabled by simultaneous Fermi contact of the resonant spin one-half nucleus, I , and a rapidly relaxing nucleus, S , (typically a quadrupolar nucleus) with the electrons constituting the chemical bond between them. (Note that while this is most often the case, in theory this mechanism can also operate between two dipolar nuclei; moreover, several quadrupolar nuclei can contribute to relaxation by this mechanism and, finally, there have even been investigations of intermolecular scalar relaxation in hydrated ions by Laaksonen *et al.*⁷⁸) This spin interaction is modulated by rapid spin relaxation of these S nuclei, which in turn produce magnetic field fluctuations at the resonant nucleus, driving the scalar relaxation. (These are the fast ‘flip-flop’ motions of the S nuclei between spin states during the NMR experiment often encountered in the literature.) This mechanism is often referred to as scalar relaxation of the second kind (SRSK); an alternative mechanism, scalar relaxation of the first kind (SRFK), exists in which the spin interaction is modulated by internal molecular motions, often chemical exchange of the S nucleus (i.e. spin coupling between the two nuclei is time dependent). In general, the contributions to the spin-lattice and spin-spin relaxation rates of I by both scalar coupling mechanisms can be adequately described by the following set of equations (see Abragam⁷⁹),

$$\begin{aligned} R_1^{SC} &= \frac{8\pi^2 J_{IS}^2}{3} S(S+1) \left(\frac{\tau_S}{1 + (\omega_I - \omega_S)^2 \tau_S^2} \right) \\ R_2^{SC} &= \frac{4\pi^2 J_{IS}^2}{3} S(S+1) \left(\tau_S + \frac{\tau_S}{1 + (\omega_I - \omega_S)^2 \tau_S^2} \right) \end{aligned} \quad (4.3)$$

where J_{IS} is the spin-spin coupling constant in hertz, S is the spin of the quadrupolar nucleus and τ_S is the T_1 relaxation time of the S nucleus or the mean lifetime of the chemical bond, depending on whether SRSK or SRFK is considered. It is interesting to note also that this is the same spin coupling which often manifests as ‘multiplets’ in proton NMR spectra; in the present case, however, the rapid modulation of coupling during the period of data acquisition results in disappearance of these multiplet structures and a single resonance peak is observed for the I nucleus. Scalar coupling relaxation can be very effective in strongly coupled systems where $J_{IS} \gg 1/\tau_S$ (we note that the magnitude of J_{IS} increases as the mass of these nuclei increase); it is also clear from the above set of equations that under these conditions $R_2^I > R_1^I$.

4 ¹⁹⁵Pt nuclear magnetic relaxation in complexes

Pesek and Mason, however, abandoned the possibility that scalar relaxation could be responsible for the discrepancies observed between the ¹⁹⁵Pt T_1 and T_2 times of their complexes at 299 K after observing similar discrepancies even for complexes containing no quadrupolar nuclei directly associated with Pt; the authors did not attempt alternative explanations for this phenomenon.¹⁸ The temperature dependence of the contributions of the SC mechanisms to R_1 and R_2 will depend on the relative magnitudes of $(\omega_I - \omega_S)$ and τ_S and the behaviour of the latter with temperature.⁸⁰

The chemical shift anisotropy (CSA) mediated relaxation mechanism mentioned previously has been implicated in the spin relaxation of a number of spin one-half heavy metal nuclei in complexes of lower symmetry in solution.^{70,81,82} This mechanism is enabled by shielding anisotropy of the resonant nucleus in the applied magnetic field, i.e. the shielding is dependent on the orientation of the molecule in the applied field. Rapid molecular reorientation results in stochastic fluctuations of the field strength at the resonant nucleus which in turn allows for spin relaxation.⁶⁵ The following equations give the contributions to the relaxation rates by this mechanism for the case of isotropic molecular reorientation

$$\begin{aligned} R_1^{CSA} &= \frac{1}{5} \gamma^2 B_0^2 (\Delta\sigma)^2 \frac{2\tau_c}{1 + \omega^2 \tau_c^2} \\ R_2^{CSA} &= \frac{1}{90} \gamma^2 B_0^2 (\Delta\sigma)^2 \left(\frac{6\tau_c}{1 + \omega^2 \tau_c^2} + 8\tau_c \right) \end{aligned} \quad (4.4)$$

where γ_I is the gyromagnetic ratio, B_0 is the applied field strength, $\Delta\sigma$ is the chemical shift anisotropy and τ_c is the rotational correlation time of the molecule. Under extreme narrowing conditions the contributions become frequency independent and can be expressed by the following set of equations. Interestingly, even under these conditions the contributions are not equal, with $R_1/R_2 = 6/7$.

$$\begin{aligned} R_1^{CSA} &= \frac{2}{15} \gamma^2 B_0^2 (\Delta\sigma)^2 \tau_c \\ R_2^{CSA} &= \frac{7}{45} \gamma^2 B_0^2 (\Delta\sigma)^2 \tau_c \end{aligned} \quad (4.5)$$

The most characteristic feature of CSA mediated relaxation in the extreme narrowing region, however, is the dependence of both contributions on the strength of the applied magnetic

4 ^{195}Pt nuclear magnetic relaxation in complexes

field; this mechanism becomes increasingly more effective at higher fields. The importance of the CSA mechanism in ^{195}Pt relaxation of square planar platinum complexes at higher magnetic fields was demonstrated by Lallemand *et al.*⁸³ and Dechter and Kowalewski.⁸⁴ Moreover, this mechanism has been reported to be dominant in ^{199}Hg relaxation in linear mercury compounds even at relatively low fields.⁸² Finally, it has been demonstrated that ion pairing can produce substantial transient chemical shift anisotropy at heavy metal nuclei in complexes in solution, leading to relaxation of these nuclei by the CSA mechanism (e.g. see study of ^{207}Pb relaxation in aqueous solution of $\text{Pb}(\text{ClO}_4)_2$ and theoretical work by Schwartz)⁸².

^{195}Pt NMR T_1 and T_2 data for the complexes $[\text{Pt}^{35/37}\text{Cl}_6]^{2-}$ in an aqueous solution in the temperature range 298 to 353 K are reported here; these data were collected at 9.4 and 14.1 T fields. The importance of a number of the more common relaxation mechanisms to the ^{195}Pt spin relaxation in complexes are evaluated in an attempt to rationalise the differing effect of temperature on the signals of the $[\text{PtCl}_6]^{2-}$ and $[\text{PtCl}(\text{OH})_5]^{2-}$ complexes, as reported in the previous section (Figure 3.9).

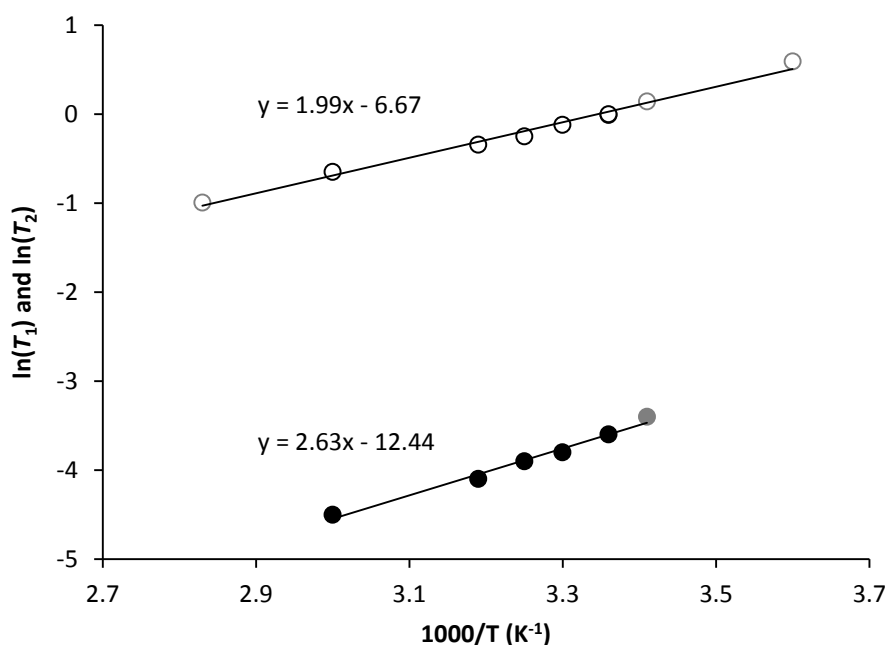
4.2 Results and discussion

The ¹⁹⁵Pt T_1 and T_2 relaxation times measured for $[\text{PtCl}_6]^{2-}$ in a 0.1 mol.dm⁻³ solution of the disodium salt in D₂O (1 mol.dm⁻³ HClO₄) at different temperatures at 9.4 and 14.1 T are collected in Table 4.1. These data are plotted in Figure 4.1 in the usual logarithmic fashion as a function of the inverse absolute temperature. Time constraints prohibited the measurement of these relaxation times in replicate (each of the relaxation time experiments required at least 10 hours of instrument time, save thermal equilibration of samples in the probe and pulse optimisations at each temperature) and as a result no actual evaluation of the errors associated with these measurements is possible; it is reassuring, however, that exponential fits to our relaxation data were always good (see data and fits in Figures 2.1A and B, for example) and it is particularly gratifying that the ¹⁹⁵Pt T_2 measurement of 39 ms at 293 K is in good agreement with the T_2 of 32 ms derived from the line widths of the $[\text{Pt}^{35}\text{Cl}_{6-n}^{37}\text{Cl}_n]^{2-}$ ($n = 0-6$) isotopologue Pt signals at this temperature.

Comparison of our ¹⁹⁵Pt relaxation time measurements for this complex at 298 K with those of Pesek and Mason¹⁸ at 299 K and in a 2.35 T field reveals that our T_1 measurement of 0.990 s is significantly shorter than the 1.35 s measured by these authors; conversely, our T_2 measurement of 27 ms is considerably *greater* than their 5.2 ms. While it might be tempting to ascribe these discrepancies to differences in sample concentrations and solvent (our sample consisted about 90 % D₂O by volume, the sample of Pesek and Mason was mostly H₂O), these authors demonstrated rather convincingly that their relaxation time measurements for this complex were largely independent of concentration and counter ion and essentially identical in D₂O and normal water. Pesek and Mason similarly reported that their ¹⁹⁵Pt T_2 measurements at 299 K could be recovered quite satisfactorily from the line widths of the corresponding resonance signals. (Note that this was reported to be the case for a variety of octahedral Pt(IV) and square planar Pt(II) complexes.) Upon closer investigation of the data reported by these authors we note that an observed ¹⁹⁵Pt line width of 78 Hz was tabulated for the solution of Na₂PtCl₆ dissolved in water; consulting also the work of Sadler *et al.*¹⁹ (these authors report ¹⁹⁵Pt resonance signals for $[\text{PtCl}_6]^{2-}$ in aqueous solutions at 1.4, 4.7 and 9.4 T), it becomes apparent that the large width reported by Pesek and Mason was indeed the *overall* width and not the width of the signals of the individual isotopologues $[\text{Pt}^{35}\text{Cl}_{6-n}^{37}\text{Cl}_n]^{2-}$; in fact, these isotopologues signals could not be resolved at 2.35 T (see also previous section; this issue was also addressed by Kidd⁸⁵ in *NMR and the Periodic Table*, 1979).

4 ^{195}Pt nuclear magnetic relaxation in complexes**Table 4.1** ^{195}Pt T_1 and T_2 relaxation time data for $[\text{Pt}^{35/37}\text{Cl}_6]^{2-}$ complexes in aqueous solution at various temperatures; measurements in italics were performed at 14.1 T

T/K	T_1 /s	T_2 /ms
278	<i>1.806</i>	
293	<i>1.155</i>	32
298	<i>0.998</i>	
	0.990	27
303	0.884	23
308	0.779	20
313	0.708	17
333	0.522	11
353	<i>0.371</i>	

**Figure 4.1** Logarithmic plots of the ^{195}Pt T_1 (open circles) and T_2 (solid circles) relaxation times of the $[\text{PtCl}_6]^{2-}$ complexes as a function of the inverse absolute temperature measured in aqueous perchloric acid solution. Grey data points were acquired at 14.1 T; black points at 9.4 T. (Linear trends have been fitted to both data sets)

Confidence in our relaxation time measurements was increased by recent work by Pregosin and co-workers who report rather comparable ^{195}Pt relaxation times for $[\text{PtCl}_6]^{2-}$ ($T_1 = 890$ ms in D_2O at 299 K).²⁷ It is interesting to note also that the above consideration of isotope effects reveals an important limitation of our relaxation time measurements, namely that we are not able to measure the ^{195}Pt relaxation times of individual isotopologues $[\text{Pt}^{35}\text{Cl}_{6-n}^{37}\text{Cl}_n]^{2-}$; i.e. we assume that these complexes have the same ^{195}Pt relaxation times. While this assumption

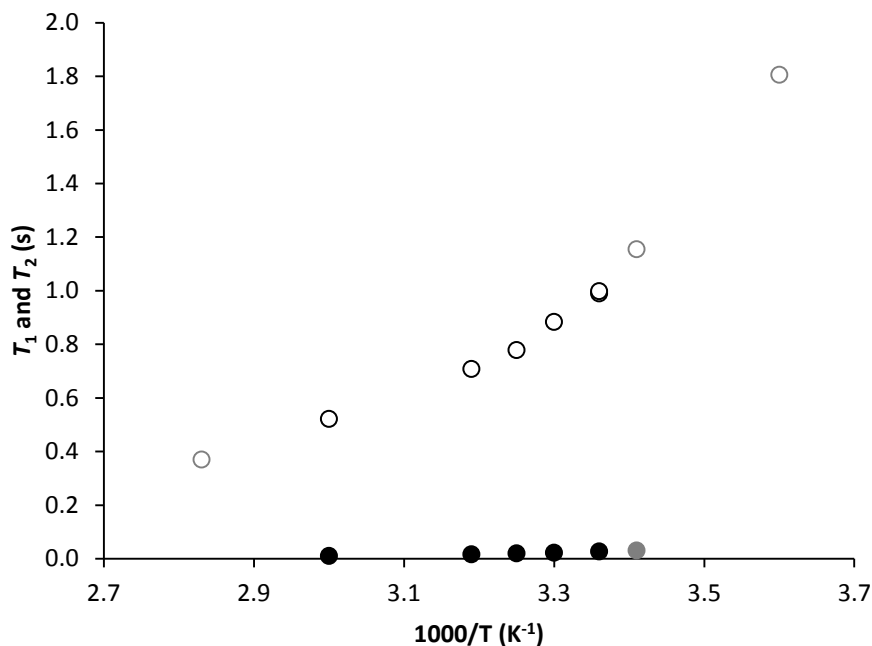
4 ^{195}Pt nuclear magnetic relaxation in complexes

Figure 4.2 ^{195}Pt NMR T_1 (open circles) and T_2 (solid circles) relaxation times of $[\text{PtCl}_6]^{2-}$ in aqueous perchloric acid solution as a function of inverse absolute temperature; grey data points were acquired at 14.1 T, black points at 9.4 T.

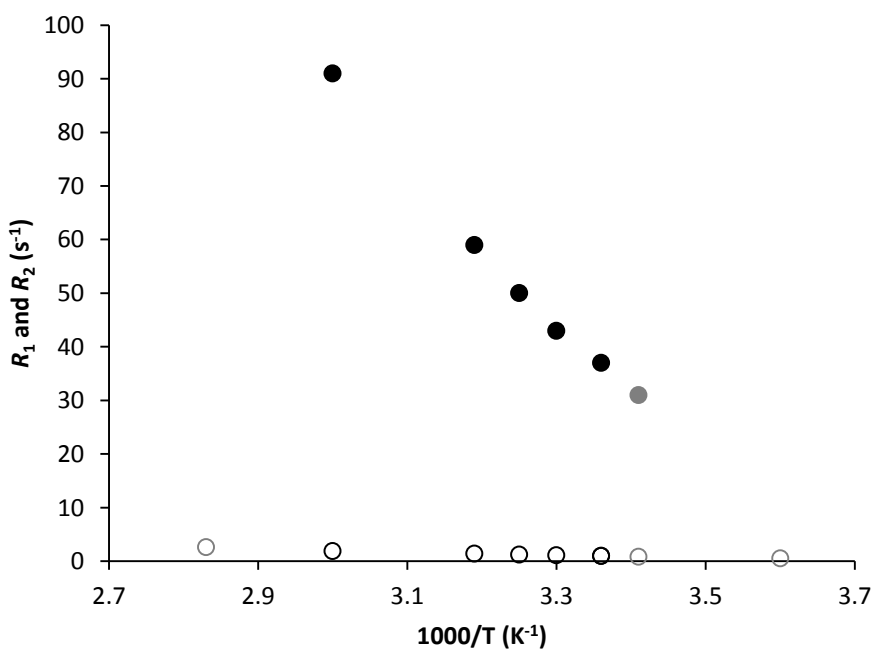


Figure 4.3 ^{195}Pt R_1 (open circles) and R_2 (solid circles) relaxation rates of $[\text{PtCl}_6]^{2-}$ in aqueous perchloric acid solution as a function of inverse absolute temperature; grey data points were acquired at 14.1 T, black points at 9.4 T.

4 ¹⁹⁵Pt nuclear magnetic relaxation in complexes

certainly appears to be reasonable at lower temperatures on account of the similar line widths of the signals of these isotopologues, the collapse of spectral fine structure at temperatures above about 298 K unfortunately does not allow for such estimates. As mentioned previously, however, the results of both our T_1 and T_2 experiments were reasonably well approximated by mono-exponential functions at all temperatures studied, which suggest equal or at least very comparable relaxation times.

A survey of the literature reveals that relatively few ¹⁹⁵Pt NMR relaxation data have been reported for octahedral Pt(IV) complexes in solution; in fact, the work of Pesek and Mason¹⁸ appears to be the most comprehensive, even when considering the relatively often studied $[\text{PtCl}_6]^{2-}$ complex. While the above considerations are not meant to detract from the pioneering work by these authors, some of the transverse relaxation time measurements certainly do seem peculiar; in fact, Kidd (a contemporary) suggested that their line width measurements be disregarded.⁸⁵ Even though our ¹⁹⁵Pt relaxation studies are not as expansive as that of Pesek and Mason, we do feel that our measurements of T_1 and T_2 times for $[\text{PtCl}_6]^{2-}$ at different temperatures should afford some insight into the mechanisms by which these nuclei relax in our complexes and shed some light on the different temperature dependence of the ¹⁹⁵Pt spectra of the $[\text{Pt}^{35/37}\text{Cl}_6]^{2-}$ and $[\text{Pt}^{35/37}\text{Cl}(\text{OH})_5]^{2-}$ complexes reported previously.

Figure 4.1 clearly shows two important trends: firstly, both the T_1 and T_2 measurements decrease as the temperature is increased and, secondly, the T_2 measurements are consistently at least one order of magnitude smaller than the T_1 measurements. While the former trend certainly is consistent with the spin-rotation mechanism mentioned earlier, the possibility of significant contributions by other mechanisms cannot be disregarded, especially in view of the fact that this relaxation mechanism cannot account for the large discrepancies between our T_1 and T_2 measurements, at least not in the presumed extreme narrowing motional regime. As mentioned previously, Pesek and Mason suggested that the intermolecular DD mechanism does not contribute significantly to the ¹⁹⁵Pt R_1 relaxation rates of $[\text{PtCl}_4]^{2-}$ and $[\text{PtCl}_6]^{2-}$ in aqueous solutions; this contention was based on their observations that these rates did not change significantly upon isotopic substitution of protons for deuterons (i.e. the rates were identical for these complexes in normal water and D₂O). The deuterium nucleus has a significantly smaller gyromagnetic ratio compared to that of the proton and so it follows from Equations 4.1b (the equations describing *intermolecular* DD relaxation are quite similar⁶⁵) that if indeed the intermolecular DD mechanism was important, this substitution should be

4 ¹⁹⁵Pt nuclear magnetic relaxation in complexes

accompanied by a noticeable increase in the ¹⁹⁵Pt T_1 time. (Note that while quadrupolar nuclei can also act in this capacity, the low gyromagnetic ratios of the two chlorine isotopes obviate contributions by these nuclei, even in the Pt coordination sphere, to the ¹⁹⁵Pt relaxation rate by this DD mechanism.) This conclusion certainly seems reasonable, especially for the octahedral complex when also considering the dependence of this mechanism on the internuclear separation, r_{IS} ; ligands effectively surround these ¹⁹⁵Pt nuclei and could be expected to prevent dipolar nuclei in solvent molecules from entering into close proximity, thus greatly reducing the efficiency of this intermolecular mechanism since this rate contribution is inversely proportional to r^6 . In this context it is also interesting to note that Dechter and Kowalewski⁸⁴ have demonstrated that the DD mechanism is of little importance even in ¹⁹⁵Pt relaxation of the square planar [Pt(acac)₂] complex (using NOE measurements); we could reasonably expect greater accessibility to the metal nucleus in this complex when compared to the octahedral [PtCl₆]²⁻ complex and for the former we have dipolar protons chemically bonded in the ligands themselves (in the vicinity of metal nucleus). In fact, while the intramolecular DD relaxation mechanism is very often the dominant mechanism for proton relaxation in many organic molecules in solution, we note that this mechanism is rather inefficient when comparing the T_1 relaxation times of these protons (typically 5 s and longer) to that observed for our ¹⁹⁵Pt nuclei (about 1 s). At any rate, Dechter and Kowalewski⁸⁴ were able to determine that the CSA mediated mechanism is dominant for ¹⁹⁵Pt relaxation in this [Pt(acac)₂] complex in toluene-*d*₈ at fields greater than 9.4 T and even at relatively high temperatures (the efficiency of this mechanism decreases as the temperature is increased).

The shielding anisotropy at the Pt centres of our octahedral complexes can certainly be expected to be much smaller, especially for the highly symmetrical [PtCl₆]²⁻ complex and it follows that the contribution by this CSA mechanism to ¹⁹⁵Pt relaxation should be negligible.⁶⁹ As mentioned previously, however, the contributions by the CSA mechanism to the R_1 and R_2 rates are not equal, to the effect of $T_1/T_2 = 7/6$; this trait does bear some resemblance to our situation. To this end, we have measured the ¹⁹⁵Pt T_1 of [PtCl₆]²⁻ in our aqueous sample at 9.4 and 14.1 T; we find that at 298K these measurements are essentially identical. (990 ms at 9.4 T and 998 ms at 14.1 T) Given also the peculiar temperature dependence of our relaxation time measurements and the fact that at 298 K we observe a significant discrepancy between T_1 and T_2 , we retire the possibility that CSA mediated

4 ^{195}Pt nuclear magnetic relaxation in complexes

relaxation contributes substantially to the ^{195}Pt relaxation of the $[\text{PtCl}_6]^{2-}$ complex at these temperatures and fields.

We have mentioned previously that the scalar coupling (SC) relaxation mechanism can also affect T_1 and T_2 times differently; since our complexes contain rapidly relaxing quadrupolar chlorine isotopes directly coordinated to Pt, a consideration of the possibility of a significant SC contribution to the ^{195}Pt relaxation of our complexes seems a logical next step. In fact, Pesek and Mason have also considered this mechanism, but abandoned the possibility after noting similar discrepancies between the relaxation times of Pt complexes containing no directly bonded quadrupolar nuclei.¹⁸ Nonetheless, the scalar coupling mechanism has been implicated in a number of relaxation studies, including that of ^{119}Sn for tin tetrachloride⁷⁴; moreover, Koch *et al.* have questioned the importance of the SC mechanism in ^{195}Pt and ^{103}Rh relaxation of complexes of the type $[\text{PtCl}_n(\text{H}_2\text{O})_{6-n}]^{4-n}$ ($n = 4-6$) and $[\text{RhCl}_n(\text{H}_2\text{O})_{6-n}]^{3-n}$ ($n = 3-6$) in aqueous solutions^{37,53}; we feel that this warrants consideration of this mechanism for our closely related complexes. Proper evaluation of the SC mechanism is, arguably, not a trivial matter, however, since its contributions to the relaxation rates are dependent on the spin-spin coupling (J -coupling) between the resonant nucleus and the rapidly relaxing/exchanging nuclei and the spin relaxation times or exchange rates of these nuclei, depending on whether scalar relaxation of the second (SRSK) or first kind (SRFK) is considered, and these quantities are often not known or difficult to determine.⁶⁵ (See Equation 4.3.) This is certainly also the case for our complexes as no time averaged spin-spin coupling between ^{195}Pt and either of the chlorine isotopes ($^{35/37}\text{Cl}$) can be measured directly from our ^{195}Pt spectra (see, for example, work by Szymanski and co-workers⁸⁶) and since the relaxation times of these chlorine nuclei are exceedingly short, resulting in extremely broad $^{35/37}\text{Cl}$ signals (typically several kHz⁸⁰) which are not ideal for relaxation time measurements by standard pulse techniques.

Even though the magnitude of spin-spin coupling between two nuclei is generally dependent on molecular properties, e.g. bond characteristics and stereo-conformations, these J values certainly increase as a function of the atomic number (mass) of the nuclei considered. (As mentioned previously, this is a result of increasing Fermi-contact of these nuclei with the bond electrons.) It follows that we can reasonably expect relatively large one-bond spin coupling between ^{195}Pt and the $^{35/37}\text{Cl}$ isotopes ($^1J(^{195}\text{Pt}-^{31}\text{P})$) often reach several thousand hertz, however, our coupling constants are likely to be smaller on account of the rather

4 ¹⁹⁵Pt nuclear magnetic relaxation in complexes

different bond covalency characteristics) and these could, in principle, facilitate large SC relaxation contributions. However, while ^{35/37}Cl relaxation/exchange rates in our complexes can potentially be very large, this should be all but offset by even larger frequency differences between ¹⁹⁵Pt and ^{35/37}Cl at these high fields; ($\omega_{\text{Pt}} - \omega_{\text{Cl}} \approx 50$ MHz at 9.4 T. We conclude that SC relaxation probably does not contribute substantially to ¹⁹⁵Pt spin-lattice relaxation in these complexes. This is also suggested by the fact that ¹⁹⁵Pt T_1 measurements for $[\text{PtCl}_6]^{2-}$ at 9.4 T and 14.1 T are essentially identical; if indeed SC relaxation was dominant, we would expect a *ca.* 50 fold increase in ¹⁹⁵Pt T_1 at the higher field. (Note from Equation 4.3 in the introduction that SC relaxation is field dependent since the frequency difference is field dependent.) In this context, it is also interesting to note that Koch *et al.* have reported that intermolecular chloride exchange in the $[\text{PtCl}_6]^{2-}$ coordination sphere is slow on the NMR timescale, which certainly should preclude SRFK contributions to ¹⁹⁵Pt R_1 for this complex.³⁷ (This work employed isotopic enrichment techniques.)

Still, we are especially interested here in the SC contribution to the ¹⁹⁵Pt *transverse* relaxation; we note that for this contribution an additional term enters the relaxation rate expression and this additional term is directly proportional to τ_s , the spin relaxation time (T_1^S) or residence time (τ_e) of the strongly coupled *S* nuclei. The temperature dependence of this term is clearly dependent on the behaviour of T_1^S and τ_e . Considering first SRFK, and recalling that at least *intermolecular* chloride ion exchange is relatively slow, we expect relatively large τ_e values for this complex. However, it would also not be unreasonable to expect that these τ_e should decrease as the temperature is increased (on account of increasing chemical exchange rates), resulting in decreasing SRFK contributions at higher temperatures. In fact, we observe the exact opposite: the $T_2(^{195}\text{Pt})$ certainly decrease (i.e. R_2 increases) at higher temperatures; and so we are content with the assumption that SRFK is not responsible for the large discrepancies between ¹⁹⁵Pt T_1 and T_2 of $[\text{PtCl}_6]^{2-}$ in our samples (a similar argument pertains to SRFK driven by *intramolecular* chloride exchange).

For SRSK, on the other hand, the relaxation times of the quadrupolar chlorine isotopes are governed by the quadrupolar relaxation mechanism, which decreases in efficiency as the temperature is increased in a similar fashion to intramolecular DD relaxation.⁶⁶ (Most often, proton lines ‘sharpen up’ at higher temperatures.) This is of course the result of a similar direct proportionality of the efficiency of these mechanisms to the rotational correlation time, τ_c , of the molecule: the quadrupolar relaxation mechanism is mediated by interaction of the

4 ¹⁹⁵Pt nuclear magnetic relaxation in complexes

magnetic quadrupole with the electric field gradient (EFG) at the quadrupolar nucleus (usually oriented along the chemical bond); as the molecule reorients, the orientation of the EFG changes which, in an external magnetic field, produces magnetic field fluctuations at the quadrupolar nucleus (thus effecting spin relaxation; see also formulae in Bakhmutov⁶⁶). Here it is also pertinent to draw attention to the dependence of quadrupolar relaxation on the symmetry of the environment of the quadrupolar nucleus (enters as asymmetry parameter, η): the solution T_1 relaxation time of the ³⁵Cl isotope in the approximately tetrahedral ClO₄⁻ ion has been measured as 270 ms, while in HCl this value is reduced to only 0.8 ms.⁶⁶ Assuming that SRSK relaxation is solely responsible for the measured discrepancy between the ¹⁹⁵Pt T_1 and T_2 relaxation times of [Pt^{35/37}Cl₆]²⁻ at 298 K ($R_2 - R_1 \approx 37 \text{ s}^{-1}$), for example, and assuming an equal ³⁵Cl and ³⁷Cl $T_1 = T_2$ relaxation time of 10^{-6} s for chlorine in a low-symmetry environment (see Farrar and Becker⁶⁵, Bakhmutov⁶⁶), we can calculate the required average $|^1J(^{195}\text{Pt}-^{35/37}\text{Cl})|$ coupling as *ca.* 100 Hz, assuming also that the contributions of the six chlorine nuclei are equal and completely additive; this value certainly does not seem unreasonable. (Rearrange Equation 4.3.)

While this simple calculation suggests that SRSK may well be important in ¹⁹⁵Pt relaxation of our complexes, we note that there is, however, no theoretical basis for the assumption that the quadrupolar relaxation times of the two chlorine isotopes should be exactly equal; the quadrupole moments of these nuclei differ by a factor of about 1.6 and these enter into the quadrupolar relaxation rate equations⁸⁷: in similar EFGs with the same symmetry, this should result in at least two-fold difference in quadrupolar relaxation times which, in turn, should produce a similar difference in the SRSK contributions of these isotopes to ¹⁹⁵Pt relaxation. If indeed the ¹⁹⁵Pt R_2 rates of the [PtCl₆]²⁻ isotopologues were dominated by SRSK relaxation, it follows that we could reasonably expect the ¹⁹⁵Pt signals of these isotopologues to have different line widths throughout the temperature range encompassing the region of extreme narrowing. While these signals overlap considerably at higher temperatures, we find that at 293 and even 298 K this certainly does not appear to be the case: these sets of isotopologue signals can be approximated very well by a sum of uniformly spaced Lorentzian peaks of *equal* width. Since we are at this stage unable to accurately measure the relaxation times of the individual isotopologues [Pt^{35/37}Cl₆]²⁻, especially at higher temperatures, we have to be content with this somewhat inconclusive picture of the role of the SC mechanism in the ¹⁹⁵Pt relaxation of our complexes; we estimate that the SC mechanism probably does not contribute substantially to ¹⁹⁵Pt relaxation of the [PtCl₆]²⁻ isotopologues.

4 ^{195}Pt nuclear magnetic relaxation in complexes

Finally, we consider the spin-rotation (SR) relaxation mechanism. We have mentioned that this mechanism has been reported by Pesek and Mason¹⁸ to be dominant in the ^{195}Pt longitudinal relaxation of $[\text{PtCl}_6]^{2-}$ in aqueous solutions, and our results in Figure 4.1 certainly appear to corroborate this notion: both the ^{195}Pt T_1 and T_2 measurements for $[\text{Pt}^{35/37}\text{Cl}_6]^{2-}$ in our aqueous samples decrease as the temperature is increased and these logarithmic plots are linear and approximately parallel, suggesting a common dominant relaxation mechanism (though, admittedly, the significance of the observed deviation from parallelism is difficult to evaluate as the uncertainty of these data are not known exactly). Still, we find the large discrepancies between the T_1 and T_2 data over this entire temperature range intriguing, especially since this observation cannot be accounted for by the SR mechanism, at least not under extreme narrowing conditions; we conclude that this apparent disparity probably is the result of our assumptions regarding the motional regime of these ^{195}Pt nuclei.⁶⁶ At least visually, these aqueous solutions certainly appear rather more viscous compared to pure water, owing probably to the high salt concentrations. Indeed, measuring also the ^1H relaxation times of water (H_2O and HDO signal) in these samples reveal that even at 333 K the proton T_1 relaxation times are significantly longer than the T_2 (ca. 3 s and 0.5 s, respectively). These protons are relaxed by a DD relaxation mechanism which is known to produce T_1/T_2 discrepancies outside the region of extreme narrowing, i.e. long τ_c .⁶⁵ (While this ‘extreme narrowing’ correlation time range will obviously not be identical for protons and our ^{195}Pt nuclei on account of their different magnetic resonance frequencies, these should be at least of the same order of magnitude.) Interestingly, a survey of the literature reveals that while formulae describing the SR contribution to the longitudinal relaxation rate under extreme narrowing conditions are readily available,^{72,66} there appears to be very little information regarding the treatment of the region of reduced mobility.⁶⁵

It is well known from the theory of intramolecular DD relaxation that in this latter motional regime the relaxation rates become frequency dependent; the T_1 relaxation times of protons relaxed by this mechanism increase as the field strength is increased (in viscous solutions, of course). While this DD mechanism is probably not of significant importance for our ^{195}Pt nuclei, we find it interesting to recall that our ^{195}Pt T_1 measurements for the complexes $[\text{Pt}^{35/37}\text{Cl}_6]^{2-}$ at 9.4 and 14.1 T are essentially identical at 298 K (990 and 998 ms, respectively). Moreover, contrary to the theory of the DD relaxation mechanisms, our ^{195}Pt relaxation time measurements do not appear to converge at higher temperatures; the slopes of logarithmic plots of these relaxation times certainly have the same sign (Figure 4.1). Finally,

4 ¹⁹⁵Pt nuclear magnetic relaxation in complexes

one could reasonably suggest that the observed differences between our T_1 and T_2 measurements should be the result of relaxation contributions by residual dissolved oxygen (or other paramagnetic impurities) in our solutions. While this is often the case, one would certainly expect a decreasing efficiency for these intermolecular mechanisms as the temperature is increased, yet even at 333 K our T_1 and T_2 measurements do not seem to converge (Figure 4.1).

We have previously demonstrated that while the ¹⁹⁵Pt signals of the isotopologues $[\text{Pt}^{35/37}\text{Cl}_6]^{2-}$ can only be resolved at temperatures below about 303 K and that this loss of resolution should be at least partly due to line-broadening of the individual isotopologue signals, the signals of the isotopologues $[\text{Pt}^{35/37}\text{Cl}(\text{}^{16}\text{OH})_5]^{2-}$ in alkaline aqueous solutions are considerably more resistant to these higher temperatures, being well resolved even at 313 K. In view of the fact that the hydroxido-ligands in these latter complexes are likely to engage in hydrogen-bonding interactions with water molecules in the solvation spheres surrounding these complexes in aqueous solutions,²⁶ this observation appears intuitively consistent with a dominant SR relaxation mechanism; specific intermolecular interactions of this type are thought to reduce the rotational velocity (or increase the rotational correlation time, τ_c) of molecules in solution, which in turn could reasonably be expected to reduce SR relaxation contributions.⁶⁵ (i.e. the spin-rotation interaction is moderated by a ‘quenching’ of rotational motion due to intermolecular interactions, as explained by Ramsey⁷¹) This reasoning becomes more apparent when substituting in the SR relaxation rate formula the well-known Hubbard relationship (assuming small-step diffusive rotational motion), $\tau_c\tau_J = I/6kT$, where τ_J is again the angular momentum correlation time and I the rotational moment of inertia of the molecule.⁶⁵ We obtain the following expression, where C_{eff} is the nuclear spin-rotation tensor:

$$R_1^{SR} = \frac{4\pi^2 I^2 C_{\text{eff}}^2}{3\hbar^2 \tau_c} \quad (4.6)$$

Note that while we expect this SR relaxation rate equation to be a good approximation for our relatively small and approximately spherical octahedral Pt complexes, evaluation of the validity of the often-used Hubbard relationship is arguably more complicated; for now we note that the molecular diffusion model of Gordon suggests a similar inverse relationship between τ_c and τ_J , reproducing at least the general form of this modified SR relaxation rate

4 ¹⁹⁵Pt nuclear magnetic relaxation in complexes

equation.⁷⁶ (The Hubbard relationship is sometimes routinely substituted in the SR equation.⁶⁶)

However, the *strength* of the spin-rotation interaction is dependent on the electron distribution in the molecule. It is pertinent to draw attention here to the intimate connection between the nuclear spin-rotation tensor, C_{eff} (which, in the special case of a nucleus situated at the centre of a spherical molecule, reduces to a scalar quantity), and the paramagnetic term of the magnetic shielding tensor^{65,88}: electron distributions producing large chemical shifts (large paramagnetic shielding/screening) will also result in the nucleus experiencing large spin-rotation components.⁶⁵ Flygare and Goodisman⁸⁹ have devised a simple equation for estimating the chemical shielding of a nucleus if the spin-rotation tensor is known (this spin-rotation tensor can often be determined by molecular-beam measurements for small molecules),

$$\sigma = \sigma_{\text{FA}} + \frac{1}{2} \frac{M}{m} \frac{C_{\text{eff}}}{B} \frac{1}{g_k} \quad (4.7)$$

where σ_{FA} is the nuclear shielding in the free atom, M and m are respectively the proton and electron mass, g_k is the nuclear g -factor and $B = \hbar/4\pi I$, the spectroscopic rotational constant.⁷⁴ In view of the fact that the ¹⁹⁵Pt centres of the $[\text{Pt}^{35/37}\text{Cl}_6]^{2-}$ isotopologues are more shielded relative to those of $[\text{Pt}^{35/37}\text{Cl}(\text{}^{16}\text{OH})_5]^{2-}$ by nearly 3000 ppm and noting that the second term on the right-hand side of Equation 4.7 will be *negative* (as this term accounts for the paramagnetic shielding contribution), one could expect a much larger C_{eff} value (i.e. a stronger interaction) for the latter set, assuming that the average rotational moment of inertia of these complexes are similar. At any rate, it is the product $C_{\text{eff}} \cdot I$ which enters the SR relaxation rate formula, and this quantity is certainly larger for the complexes $[\text{Pt}^{35/37}\text{Cl}(\text{}^{16}\text{OH})_5]^{2-}$. (The average rotational moment of inertia of $[\text{Pt}^{35/37}\text{Cl}_6]^{2-}$ should be greater, on account of the larger number of heavier ligands.) It follows from Equation 4.6 that, if the rotational correlation times of these two sets of complexes $[\text{Pt}^{35/37}\text{Cl}_6]^{2-}$ and $[\text{Pt}^{35/37}\text{Cl}(\text{}^{16}\text{OH})_5]^{2-}$ were similar in solution, the SR contribution to ¹⁹⁵Pt relaxation should also be *larger* for members of the latter set; i.e. considering only differences in the electron distributions in these two sets of complexes, we expect a shorter relaxation time for this latter set, which is the reverse of that expected previously when considering only differences in molecular motion.

4 ¹⁹⁵Pt nuclear magnetic relaxation in complexes

When measuring the ¹⁹⁵Pt T_1 relaxation times of these complexes in aqueous solutions at 293 K (9.4 T field), we find that the 1.155 s measured for the set $[\text{Pt}^{35/37}\text{Cl}_6]^{2-}$ is indeed longer than that of the $[\text{Pt}^{35/37}\text{Cl}(\text{}^{16}\text{OH})_5]^{2-}$ pair at only 582 ms. Interestingly, the reversed is true of the T_2 measurements at these same temperature and field: the ¹⁹⁵Pt T_2 of 32 ms measured for the complexes $[\text{Pt}^{35/37}\text{Cl}_6]^{2-}$ is somewhat *shorter* than the 39 ms of $[\text{Pt}^{35/37}\text{Cl}(\text{}^{16}\text{OH})_5]^{2-}$. These short T_2 measurements are in qualitative agreement with the narrower line widths of the ¹⁹⁵Pt resonance signals of the complexes $[\text{Pt}^{35/37}\text{Cl}(\text{}^{16}\text{OH})_5]^{2-}$ compared to those of $[\text{Pt}^{35/37}\text{Cl}_6]^{2-}$ at 293 K, as can be seen in Figure 3.3A and G. It is important to note that, while the T_2 measurements are much smaller than the T_1 , it is the former which govern the line widths of the resonance signals, as discussed previously. Moreover, direct comparison of relaxation times can often be misleading, since it is the relaxation *rate* contributions which are additive.⁶⁵ Taking the reciprocal of these time measurements, we find that the R_1 relaxation rates of these two sets of complexes are in fact quite comparable, with the difference between the R_2 rates being about seven times greater than that between the R_1 rates (*ca.* 5.6 and 0.8 s⁻¹, respectively) Since the relaxation times of these two sets of isotopologues were measured in different aqueous solutions, the $[\text{Pt}^{35/37}\text{Cl}_6]^{2-}$ complexes in 1 mol.dm⁻³ perchloric acid and the $[\text{Pt}^{35/37}\text{Cl}(\text{}^{16}\text{OH})_5]^{2-}$ pair in 4 mol.dm⁻³ sodium hydroxide, and since the errors associated with these measurements are not known (measurements were not performed in replicate as they are quite time-consuming at *ca.* 12 hours for each measurement, excluding thermal equilibration and pulse width optimisation which may require several hours), it may be argued that these can be of only limited value.

In view of this possibility, we decided to measure also the ¹⁹⁵Pt T_1 and T_2 relaxation times of the set of isotopologues $[\text{Pt}^{35/37}\text{Cl}_5(\text{H}_2\text{}^{16}\text{O})]^{1-}$, which is also present in the perchloric acid solution and forms by displacement of a chlorido-ligand from the coordination sphere by a water molecule;²³ these *aqua*-complexes are also likely to engage in intermolecular hydrogen-bonding interactions with water molecules (Figure 4.4) and their Pt centres are less shielded by approximately 500 ppm relative to those of the $[\text{Pt}^{35/37}\text{Cl}_6]^{2-}$ isotopologues. By a similar line of reasoning, then, we expect a greater spin-rotation interaction (C_{eff}) with the Pt nuclei of the complexes $[\text{Pt}^{35/37}\text{Cl}_5(\text{H}_2\text{}^{16}\text{O})]^{1-}$ compared to those of $[\text{Pt}^{35/37}\text{Cl}_6]^{2-}$, but also a reduction in the efficiency of the SR relaxation mechanism due to an increased rotational correlation time (τ_c); i.e. a situation similar to that expected for $[\text{Pt}^{35/37}\text{Cl}(\text{}^{16}\text{OH})_5]^{2-}$. Indeed, we find that the relaxation times follow the same trend: at 296 ms the ¹⁹⁵Pt T_1 of the set

4 ^{195}Pt nuclear magnetic relaxation in complexes

Figure 4.4 Molecular model showing an optimised structure of a so-called ‘microsolvated cluster’ $[\text{PtCl}_5(\text{H}_2\text{O})]^{1-} \cdot 2\text{H}_2\text{O}$ (where blue sphere represents the Pt atom, green spheres Cl and red and white spheres respectively O and H), used as a basis for DFT computation of the ^{195}Pt shielding tensor, showing hydrogen bonding interactions (dotted lines). Image reproduced from Davis *et al.*⁴⁹

$[\text{Pt}^{35/37}\text{Cl}_5(\text{H}_2^{16}\text{O})]^{1-}$ is shorter than that of $[\text{Pt}^{35/37}\text{Cl}_6]^{2-}$ (990 ms) at the same temperature (298 K), while the T_2 of 35 ms is again *longer* than that of $[\text{Pt}^{35/37}\text{Cl}_6]^{2-}$ at only 27 ms.

These two sets of measurements are certainly intriguing, but it is difficult to evaluate the importance of the SR relaxation mechanism at this stage, especially since the ^{195}Pt nuclei in our samples are probably not in the extreme-narrowing motional regime. In fact, since time constraints have not allowed for the measurement of the relaxation times of the complexes $[\text{Pt}^{35/37}\text{Cl}(\text{OH})]^{2-}$ and $[\text{Pt}^{35/37}\text{Cl}_5(\text{H}_2^{16}\text{O})]^{1-}$ over a range of temperatures, as performed for $[\text{Pt}^{35/37}\text{Cl}_6]^{2-}$, the possibility of other important relaxation mechanism cannot be excluded. For example, proton and deuteron exchange rates in these aqua- and hydroxido-complexes are likely to be very rapid and it should not be unreasonable to suggest that these could contribute to the ^{195}Pt relaxation rates by a scalar coupling mechanism.⁶¹ (We thank Dr Alan Kenwright for this suggestion.) It also seems quite likely that displacement of chlorido-ligands should introduce greater ^{195}Pt shielding anisotropy, which could enable relaxation by the CSA mechanism. Moreover, while we have considered the SC mechanism and have suggested that it probably does not contribute substantially to ^{195}Pt relaxation in $[\text{Pt}^{35/37}\text{Cl}_6]^{2-}$, the significantly greater transverse relaxation rates of these complexes lead us inevitably to reconsider this possibility, especially in view of the fact that the T_2 relaxation times of the $[\text{Pt}^{35/37}\text{Cl}_6]^{2-}$ complexes, containing a larger number of quadrupolar chlorine nuclei, are shorter in both sets of measurements. (We note that since the SRSK rate contribution is essentially directly proportional to the relaxation time(s) of the quadrupolar or rapidly relaxing coupled nuclei when the resonance frequency difference is large, $\omega_I - \omega_S \gg 1/T_S$, as is the case here, it is also *inversely* proportional to the rotational correlation time of the molecule.) We conclude that, in the absence of detailed information on the motional characteristics of these complexes in solution, it is difficult to determine unambiguously the

4 ¹⁹⁵Pt nuclear magnetic relaxation in complexes

reason(s) for the observed trend in the relaxation time measurements and, more importantly, the difference in the sensitivity of the of the line widths of the signals of $[\text{Pt}^{35/37}\text{Cl}_6]^{2-}$ and $[\text{Pt}^{35/37}\text{Cl}(\text{}^{16}\text{OH})_5]^{2-}$; however, we anticipate that this latter phenomenon should result from differences in the activation energy of reorientational motion of these complexes in solution.

We have recently performed preliminary ¹⁹⁵Pt pulsed gradient spin-echo (PGSE) translational diffusion measurements for some of these complexes in aqueous solutions. These measurements can provide valuable information regarding the mobility of molecules in solution and can, in some cases, also be used to estimate the average sizes, or *hydrodynamic radii*, of molecules or aggregates. While PGSE experiments are often used to study the motion of especially ¹H nuclei (these are the well-known DOSY experiments), to our knowledge only one study has been reported in which ¹⁹⁵Pt was used as diffusion probe. We have mentioned that Pregosin *et al.*²⁷ have recently studied ion pairing of $[\text{PtCl}_6]^{2-}$ in solutions of Na_2PtCl_6 and H_2PtCl_6 in water and methanol; these workers employed ¹⁹⁵Pt PGSE diffusion measurements and the known viscosities of these solvents to estimate the hydrodynamic radii of the platinum complexes which, in turn, provided information on ion pair formation. ($\{\text{Na}^+[\text{PtCl}_6]^{2-}\}$ ion pairing was found to be prevalent in methanol, but not in water) The determination of hydrodynamic radii from diffusion coefficients (D) measured by PGSE sequences (these diffusion coefficients should be referenced to that of a suitable reference compound) typically involves rearranging the Stokes-Einstein equation

$$D = \frac{kT}{n\pi r_s \eta} \quad (4.8)$$

where k is the Boltzmann constant, r_s is the hydrodynamic radius of the *spherical* particle, η is the solution viscosity and n takes values 4 or 6 for the slip or stick boundary conditions, respectively. (The slip value is suggested to be a good approximation when considering larger molecules where the solvent can essentially be considered a featureless continuum.) It has been demonstrated that this methodology can also provide insights regarding intermolecular hydrogen-bonding interactions in solution since these are expected to produce changes in the observed hydrodynamic radii of molecules, which in turn should manifest as changes in diffusion coefficients.⁹⁰ Within this hydrodynamic continuum model (translational and rotational diffusion coefficients proportional to solution viscosity) the rotational correlation time, τ_c , of a spherical molecule can be expressed by the Stokes-Einstein-Debye equation:

4 ^{195}Pt nuclear magnetic relaxation in complexes

$$\tau_c = \frac{4\pi r_s^3 \eta}{3kT} \quad (4.9)$$

While it has been suggested that theories linking the translational and rotational motions of molecules in solution are not sufficiently developed to allow for their precise correlation,⁹¹ the above approximations should provide some insight into the *relative* differences in the motional characteristics of our octahedral platinum complexes, especially where these are present in the *same* solution (complexes experience same solution viscosity). Finally, we find that our ^{195}Pt PGSE diffusion measurements are complicated primarily by the short ^{195}Pt transverse relaxation times of these complexes; significant sensitivity losses occur during these PGSE sequences, even for sequences which do not incorporate convection compensation pulses, necessitating the acquisition of a large number of transient scans for each gradient strength increment which ultimately results in long experiment times (typically 12 hours or more per measurement, see also Pregosin *et al.*²⁷). This work is currently in progress and will be presented at a later stage.

5

Conclusions

^{195}Pt magnetic shielding in complexes of this metal is extremely sensitive to changes in the Pt coordination sphere. Isotopic substitution in the octahedral $[\text{PtCl}_6]^{2-}$ complex in solution, for example, results in an upfield shift of the ^{195}Pt resonance of *ca.* 0.17 ppm per ^{37}Cl isotope incorporated into the coordination sphere of the metal, producing a characteristic fine structure in the ^{195}Pt NMR signal in samples with a natural chlorine isotope distribution at 293 K; the ^{195}Pt shielding in this complex also shows a large temperature dependence, with the signals shifting downfield by about 1 ppm/K as the temperature is increased. Remarkably, Koch and co-workers³⁷ have found that in the ^{195}Pt spectra of some mixed-ligand complexes of the type $[\text{PtCl}_n(\text{H}_2\text{O})_{6-n}]^{4-n}$ ($n = 2-5$), $^{35/37}\text{Cl}$ isotopic substitution at sites *trans* to coordinated water molecules produce slightly larger isotope shifts compared to substitution *trans* to chlorido-ligands, i.e. the signals of certain sets of isotopomers are partially resolved, producing additional fine structure. Similar observations were reported for $^{16/18}\text{O}$ isotope shifts in the Pt signals of the complex *cis*- $[\text{PtCl}_2(\text{H}_2\text{O})_4]^{2+}$, where introduction of an ^{18}O isotope *trans* to a chlorido-ligand produced a slightly different isotope shift than *trans* to a water molecule.³⁸

In this study it was decided to investigate isotope shifts in the ^{195}Pt signals of the related series of octahedral hydroxido-complexes $[\text{PtCl}_{6-n}(\text{OH})_n]^{2-}$ ($n = 1-6$) in aqueous solutions; it is found that in many ways these are quite similar to those of their protonated analogues: substitution of a chlorido-ligand by hydroxide ion results in a large downfield shift of the ^{195}Pt resonance signal (*ca.* 600 ppm, to be compared with the ~500 ppm per water molecule in the aqua-series) and the signals of stereoisomers are well separated (*ca.* 20 ppm shielding difference). However, a number of interesting differences have also been found which we

5 Conclusions

have sought to interpret. While the signals of $^{35/37}\text{Cl}$ -isotopologues are generally well-resolved in the ^{195}Pt spectra of these hydroxido-complexes, it is found that *isotopomers* of the type mentioned above appear to have equivalent shifts, giving rise to a single resonance signal (i.e. isotopic substitution *trans* to a hydroxido-ligand results in the same isotope shift as that resulting from substitution *trans* to a chlorido-ligand). Moreover, the order of ^{195}Pt shielding is reversed in all stereoisomer pairs compared to that in the corresponding aqua-complexes, e.g. the Pt centre of the *cis*- $[\text{PtCl}_2(\text{H}_2\text{O})_4]^{2+}$ complex is more shielded than that of the *trans*-stereoisomer, while in the case of the *cis/trans*- $[\text{PtCl}_2(\text{OH})_4]^{2-}$ stereoisomer pair the *trans*-stereoisomer is the more shielded. It is also found that while the magnitude of $^{35/37}\text{Cl}$ isotope shifts in the signals of the *cis/trans*- $[\text{PtCl}_2(\text{OH})_4]^{2-}$ stereoisomers are essentially identical and comparable to those reported for the *cis*- $[\text{PtCl}_2(\text{H}_2\text{O})_4]^{2+}$ complex, they are significantly larger than the $^{35/37}\text{Cl}$ isotope shifts reported for *trans*- $[\text{PtCl}_2(\text{H}_2\text{O})_4]^{2+}$. A simple rationalisation of these phenomena was presented, based on the differing relative strengths of the *trans*-influences of the three ligands and the likely effects of these on metal-to-ligand bond displacements in these complexes.

The ^{195}Pt signals of the complexes *cis*- $[\text{PtCl}_2(\text{OH})_4]^{2-}$ and $[\text{PtCl}(\text{OH})_5]^{2-}$ in an ^{18}O -enriched sample show remarkable fine structure; in addition to the large $^{16/18}\text{O}$ isotope shifts producing a multiplication of the $^{35/37}\text{Cl}$ isotope-induced signal profiles, additional fine structure is observed which is similar to that reported by Koch *et al.*³⁸ for the complex *cis*- $[\text{PtCl}_2(\text{H}_2\text{O})_4]^{2+}$; these additional signals result from a magnetic non-equivalence of the Pt centres of isotopomers differing only in the combination of $^{16/18}\text{O}$ isotopes coordinated opposite chlorido-ligands. We find that, in these complexes, $^{16/18}\text{O}$ substitution *trans* to a chlorido-ligand produces a larger isotope shift than *trans* to a hydroxido-ligand, consistent with a shorter Pt-O bond expected in the former site. The proposed assignment of signals was confirmed by the excellent agreement between the calculated abundances of the various complexes and the relative area contributions of the corresponding signals, obtained by a line-fitting procedure. The $^{16/18}\text{O}$ isotope shifts have also been observed in the ^{195}Pt resonance signal of the complex $[\text{Pt}(\text{OH})_6]^{2-}$ in this ^{18}O -enriched sample and allow for the unambiguous assignment of these signals (which, in samples having a natural ^{18}O content, is the single peak of the all- ^{16}O isotopologue).

The effect of temperature on the $^{35/37}\text{Cl}$ isotope-induced profiles of the ^{195}Pt signals of the complexes $[\text{PtCl}_6]^{2-}$ and $[\text{PtCl}(\text{OH})_5]^{2-}$ in aqueous solution was investigated in the range 283-

5 Conclusions

308 K. While the spectral fine structure of the $[\text{PtCl}_6]^{2-}$ signal deteriorates significantly as the temperature is increased above about 303 K, the two isotopologue signals of the $[\text{PtCl}(\text{OH})_5]^{2-}$ complex remain essentially unaffected. ^{195}Pt relaxation time measurements for $[\text{PtCl}_6]^{2-}$ at various temperatures confirm that broadening of the resonance signals in this set occur as the temperature is increased, i.e. this line-broadening is at least *partially* responsible for the observed loss of resolution between the signals of the isotopologues $[\text{Pt}^{35/37}\text{Cl}_6]^{2-}$. The relaxation data appear to be consistent with the spin-rotation relaxation mechanism, which is thought to be important in these complexes.

Moreover, the temperature coefficient of ^{195}Pt shielding in the $[\text{PtCl}_6]^{2-}$ (*ca.* 1 ppm/K) is about one order of magnitude *greater* than that of $[\text{PtCl}(\text{OH})_5]^{2-}$, the Pt centre of which is less shielded by nearly 3000 ppm; this observation is interesting in that it appears to be at variance with a simple electrostatic model of magnetic shielding discussed by Jameson and co-workers.²¹ Possible explanations for the observed differences in the temperature dependence of the signals of the two complexes have been considered in some detail and these show considerable scope for future work.

References

1. D. Jollie, *Platinum 2010*, Johnson Matthey PLC, Royston, UK, 2010.
2. F. L. Bernardis, R. A. Grant and D. C. Sherrington, *React. Funct. Polym.*, 2005, **65** (3), 205.
3. E. Benguerel, G. P. Demopoulos and G. B. Harris, *Hydrometallurgy*, 1996, **40**, 135.
4. R. J. Warr, A. N. Westra, K. J. Bell, J. Chartes, R. Ellis, C. Tong, T. G. Simmance, A. Gadzhieva, A. J. Blake, P. Tasker and M. Schröder, *Chem. Eur. J.*, 2009, **15**, 4836.
5. T. M. Buslaeva and S. A. Simanova, *Russ. J. Coord. Chem.*, 1999, **25**, 151.
6. C. M. Davidson and R. F. Jameson, *Trans. Faraday Soc.*, 1965, **61**, 133.
7. W. Leavason and D. Pletcher, *Platinum Metals Rev.*, 1993, **37**, 17.
8. B. Shelimov, J. -F. Lambert, M. Che and B. Didillon, *J. Am. Chem. Soc.*, 1999, **121**, 545.
9. W. A. Spieker, J. Liu, J. T. Miller, A. J. Kropf and J. R. Regalbuto, *Appl. Catal. A: General*, **232**, 219.
10. B. Shelimov, J. -F. Lambert, M. Che and B. Didillon, *J. Mol. Catal. A: Chem.*, 2000, **158**, 91.
11. T. Slotte, PhD Dissertation, *Adsorption of Platinum- and Rhodium-complexes on Modified γ -Al₂O₃ Surfaces*, University of Oulu, 2000. See also references herein.
12. J. R. Anderson, *Structure of Metallic Catalysts*, Academic Press, New York, 1975.
13. P. S. Pregosin, *Coord. Chem. Rev.*, 1982, **44**, 247.
14. W. G. Proctor and F. C. Yu, *Phys. Rev.*, 1951, **80**, 20.
15. J. R. L. Priqueler, I. A. Butler and F. D. Rochon, *Appl. Spectrosc. Rev.*, 2006, **41**, 185.

16. B. M. Still, P. G. A. Kumar, J. R. Aldrich-Wright and W. S. Price, *Chem. Soc. Rev.*, 2007, **36**, 665.
17. A. von Zelewsky, *Helv. Chim. Acta*, 1968, **51**, 803.
18. J. J. Pesek and W. R. Mason, *J. Magn. Reson.*, 1977, **25**, 519.
19. I. M. Ismail, S. J. S. Kerrison and P. J. Sadler, *Chem. Soc., Chem. Commun.*, 1980, 1175.
20. C. J. Jameson and A. K. Jameson, *J. Chem. Phys.*, 1986, **85**, 5484.
21. C. J. Jameson, D. Rehder and M. Hoch, *J. Am. Chem. Soc.*, 1987, **109**, 2589.
22. C. Carr, P. L. Goggin and R. J. Goodfellow, *Inorg. Chim. Acta*, 1984, **81**, L25.
23. J. Kramer and K. R. Koch, *Inorg. Chem.*, 2006, **45**, 7843.
24. J. Kramer and K. R. Koch, *Inorg. Chem.*, 2007, **46**, 7466.
25. P. Murray and K. R. Koch, *J. Coord. Chem.*, 2010, **63**, 2561.
26. K. R. Koch, M. R. Burger, J. Kramer and A. N. Westra, *Dalton Trans.*, 2006, 3277.
27. D. Nama, P. G. A. Kumar and P. S. Pregosin, *Magn. Reson. Chem.*, 2005, **43**, 246.
28. M. Sterzel and J. Autschbach, *Inorg. Chem.*, 2006, **45**, 3316; L. A. Truflandier, K. Sutter and J. Autschbach, *Inorg. Chem.*, 2011, **50**, 1723.
29. L. A. Truflandier and J. Autschbach, *J. Am. Chem. Soc.*, 2010, **132**, 3472.
30. E. Penka Fowe, P. Belser, C. Daul and H. Chermette, *Phys. Chem. Chem. Phys.*, 2005, **7**, 1732.
31. T. M. Gilbert and T. Ziegler, *J. Phys. Chem. A*, 1999, **103**, 7535.
32. M. Kaupp, O. L. Malkina, V. G. Malkin and P. Pyykkö, *Chem. Eur. J.*, 1998, **4**, 118.
33. R. R. Dean and J. C. Green, *J. Chem. Soc. A*, 1968, 3047.
34. A. Pidcock, R. E. Richards and L. M. Venanzi, *J. Chem. Soc. A*, 1968, 1970.

35. N. F. Ramsey, *Phys. Rev.*, 1950, **78**, 699.
36. M. R. Burger, J. Kramer, H. Chermette and K. R. Koch, *Magn. Reson. Chem.*, 2010, **48**, S38.
37. W. J. Gerber, P. Murray and K. R. Koch, *Dalton Trans.*, 2008, 4113. See also Supplementary Information to this paper.
38. P. Murray, W. J. Gerber and K. R. Koch, *Dalton Trans.*, 2012, **41**, 10533.
39. H. Batiz-Hernandez and R. A. Bernheim, *Progr. NMR. Spectrosc.*, 1967, **3**, 63 and references herein.
40. M. Alei and W. E. Wageman, *J. Chem. Phys.*, 1978, **68**, 783.
41. N. M. Sergeyev, N. D. Sergeyeva and W. T. Raynes, *Chem. Phys. Lett.*, 1994, **221**, 385.
42. P. C. Lauterbur, *J. Chem. Phys.*, 1965, **42**, 799.
43. J. Jokisaari and K. Raisanen, *Mol. Phys.*, 1978, **36**, 113.
44. M. R. Bendall and D. M. Doddrell, *Aust. J. Chem.*, 1978, **31**, 1141.
45. N. F. Ramsey, *Phys. Rev.*, 1952, **87**, 1075.
46. H. -J. Osten and C. J. Jameson, *J. Chem. Phys.*, 1985, **82**, 4595.
47. C. J. Jameson, *J. Chem. Phys.*, 1977, **11**, 4983.
48. J. F. Stanton and L. S. Bartell, *J. Chem. Phys.*, 1985, **89**, 2544.
49. J. C. Davis, M. Bühl and K. R. Koch, *J. Chem. Theory Comput.*, 2012, **8**, 1344.
50. S. K. Wolff, T. Ziegler, E. van Lenthe and E. J. Baerends, *J. Chem. Phys.*, 1999, **110**, 7689.
51. M. J. Frisch, G. W. Trucks, H. B. Schlegel, G. E. Scuseria, M. A. Robb, J. R. Cheeseman, G. Scalmani, V. Barone, B. Mennucci, G. A. Petersson, H. Nakatsuji, M. Caricato, X. Li, H. P. Hratchian, A. F. Izmaylov, J. Bloino, G. Zheng, J. L.

- Sonnenberg, M. Hada, M. Ehara, K. Toyota, R. Fukuda, J. Hasegawa, M. Ishida, T. Nakajima, Y. Honda, O. Kitoa, H. Nakai, T. Vreven, J. A. Montgomery Jr., J. E. Peralta, F. Ogliaro, M. Bearpark, J. J. Heyd, E. Brothers, K. N. Kudin, V. N. Staroverov, R. Kobayashi, J. Normand, K. Raghavachari, A. Rendell, J. C. Burant, S. S. Iyengar, J. Tomasi, M. Cossi, N. Rega, J. M. Millam, M. Klene, J. E. Knox, J. B. Cross, V. Bakken, C. Adamo, J. Jaramillo, R. Gomperts, R. E. Stratmann, O. Yazyev, A. J. Austin, R. Cammi, C. Pomelli, J. W. Ochterski, R. L. Martin, K. Morokuma, V. G. Zakrzewski, G. A. Voth, P. Salvador, J. J. Dannenberg, S. Dapprich, A. D. Daniels, Ö. Farkas, J. B. Foresman, J. V. Ortiz, J. Cioslowski, D. J. Fox; *Gaussian 09*, revision A. 1; Gaussian, Inc., Wallington, CT, 2009.
52. P. K. Sajith and C. H. Suresh, *J. Organomet. Chem.*, 2011, **696**, 2086.
53. T. E. Geswindt, W. J. Gerber, D. J. Brand and K. R. Koch, *Anal. Chim. Acta*, 2012, **730**, 93.
54. (a) L. E. Cox and D. G. Peters, *Inorg. Chem.*, 1970, **9**, 1927; (b) G. Bandel, M. Müllner and M. Trömel, *Z. anorg. allg. Chem.*, 1979, **453**, 5.
55. S. M. Cohen and T. H. Brown, *J. Chem. Phys.*, 1974, **61**, 2985.
56. J. C. Davis, PhD thesis, University of Stellenbosch and University of St. Andrews, to be submitted 2013.
57. R. E. Wasylshen and N. Burford, *Can. J. Chem.*, 1987, **65**, 2707.
58. D. B. Chesnut, *Chem. Phys.*, 1986, **110**, 415; D. B. Chesnut and C. K. Foley, *J. Chem. Phys.*, 1986, **85**, 2814.
59. M. S. Holt, W. L. Wilson and J. H. Nelson, *Chem. Rev.*, 1989, **89**, 11.
60. R. Bramley, M. Brorson, A. M. Sargeson and C. E. Schäffer, *J. Am. Chem. Soc.*, 1985, **107**, 2780.
61. M. Maliarik and I. Persson, *Magn. Reson. Chem.*, 2005, **43**, 835.
62. W. Gombler, *J. Am. Chem. Soc.*, 1982, **104**, 6616.
63. H. -J. Osten and C. J. Jameson, *J. Chem. Phys.*, 1985, **82**, 4595.

64. F. Bloch, *Phys. Rev.*, 1946, **70**, 460.
65. T. C. Farrar and E. D. Becker, *Pulse and Fourier Transform NMR*, Academic Press, New York, 1971.
66. V. I. Bakhmutov, *Practical NMR Relaxation for Chemists*, John Wiley & Sons Ltd, Chichester, U.K., 2004.
67. C. P. Slichter, *Principles of Magnetic Resonance*, Harper, New York, 1963.
68. N. Bloembergen, E. M. Purcell and R. V. Pound, *Phys. Rev.*, 1948, **73**, 679.
69. I. M. Ismail, S. J. S. Kerrison and P. J. Sadler, *Polyhedron*, 1982, **1**, 57.
70. W. Freeman, P. S. Pregosin, S. N. Sze and L. M. Venanzi, 1976, *J. Mag. Reson.*, **22**, 473.
71. N. F. Ramsey, *Am. Sci.*, 1961, **49**, 509.
72. P. S. Hubbard, *Phys. Rev.*, 1963, **131**, 1155.
73. J. S. Bilcharski, *Acta Phys. Polon.*, 1963, **24**, 817; M. Bloom, F. B. Bridges and W. N. Hardy, *Can. J. Phys.*, 1967, **45**, 3533.
74. A. Laaksonen and R. E. Wasylshen, *J. Am. Chem. Soc.*, 1995, **117**, 392.
75. W. A. Steele, *J. Chem. Phys.*, 1963, **38**, 2404.
76. R. G. Gordon, *J. Chem. Phys.*, 1965, **42**, 3658.
77. R. E. D. McClung, *J. Chem. Phys.*, 1969, **51**, 3842.
78. A. Laaksonen, J. Kowalewski and B. Jönsson, *Chem. Phys. Lett.*, **89**, 412.
79. A. Abragam, *Principles of Magnetic Resonance*, Oxford University Press, London, 1961.
80. T.C. Farrar, S.J. Druck, R.R. Shoup and E.D. Becker, *J. Am. Chem. Soc.*, 1972, **94**, 699.
81. J. J. Dechter, O. R. Polanco and J. Kowalewski, *J. Mag. Reson.*, 1985, **65**, 395.

82. R. M. Hawk and R. R. Sharp, *J. Chem. Phys.*, 1974, **60**, 1522; R. N. Schwartz, *J. Mag. Reson.*, 1976, **24**, 205.
83. J. Y. Lallemand, J. Soulié and J. C. Chottard, *J.C.S. Chem. Comm.*, 1980, 437.
84. J. J. Dechter and J. Kowalewski, *J. Mag. Reson.*, 1984, **59**, 146.
85. R. G. Kidd, In *NMR and the Periodic Table*, R. K. Harris and B. E. Mann (eds.), Academic Press, London, 1978.
86. P. Bernatowicz, S. Szymański and B. Wrackmeyer, *J. Phys. Chem. A*, 2001, **105**, 6414.
87. M. Gee, R. E. Wasylshen and A. Laaksonen, *J. Phys. Chem. A*, 1999, **103**, 10805.
88. W. H. Flygare, *J. Chem. Phys.*, 1964, **41**, 793; W. H. Flygare, *Chem. Rev.*, 1974, **74**, 653.
89. W. H. Flygare and J. Goodisman, *J. Chem. Phys.*, 1968, **49**, 3122.
90. E. J. Cabrita and S. Berger, *Magn. Reson. Chem.*, 2001, **39**, S142.
91. W. S. Price, H. Ide and Y. Arata, *J. Chem. Phys.*, 2000, **113**, 3686.

Appendix

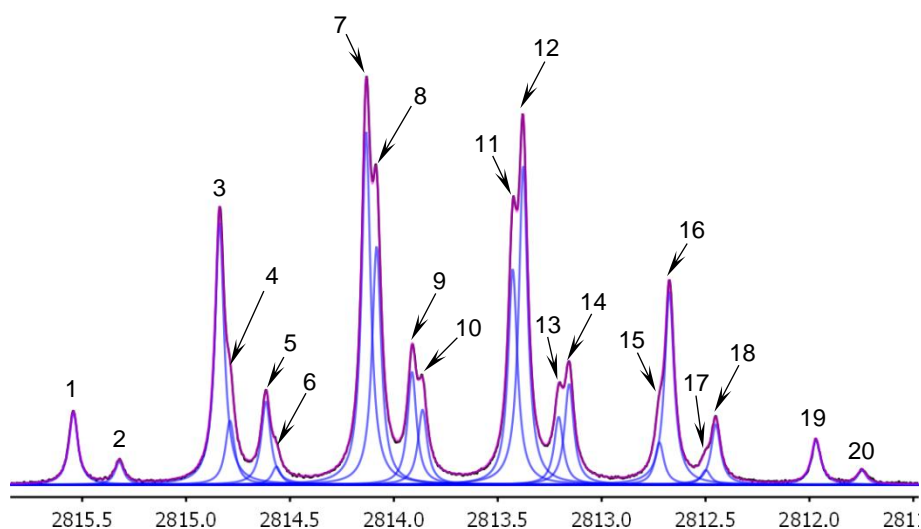
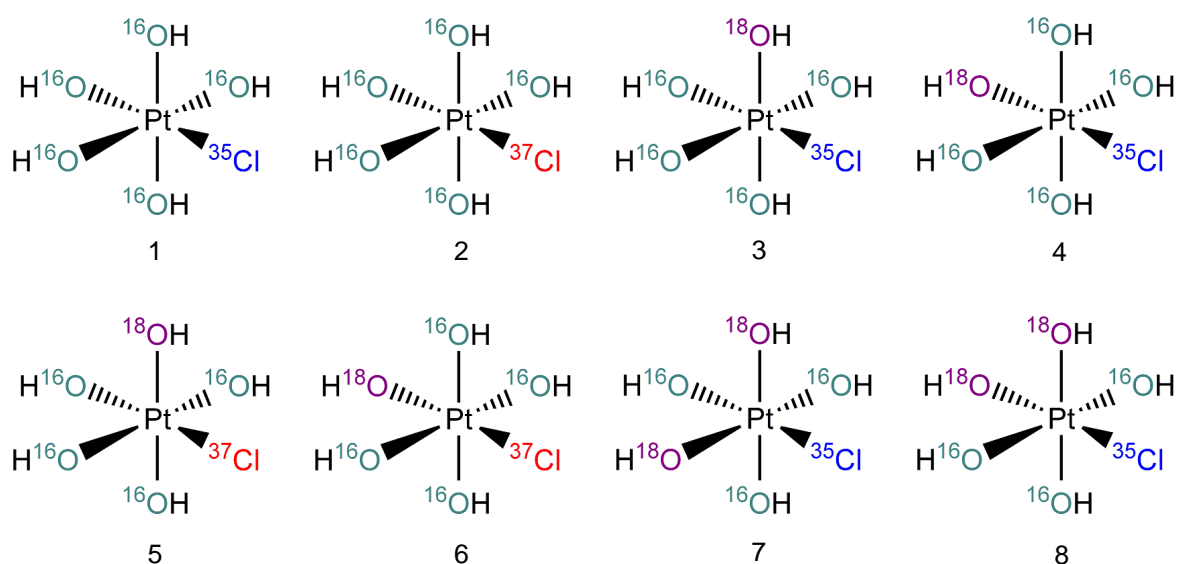
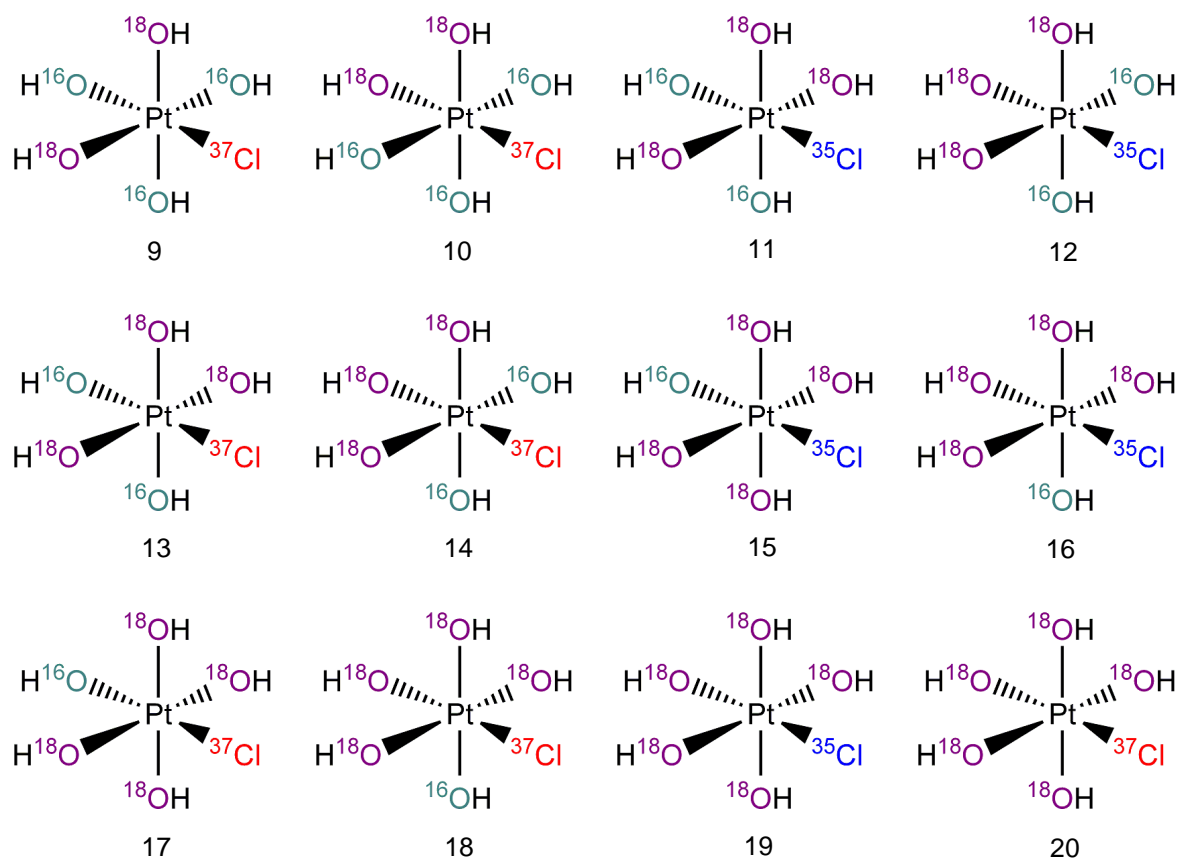
Full assignment of selected spectra

Figure S1 128.8 MHz ^{195}Pt NMR spectrum of the complexes $[\text{Pt}^{35/37}\text{Cl}^{16/18}\text{OH}_5]^{2-}$ in an ^{18}O -enriched (45 %) alkaline aqueous solution of Na_2PtCl_6 at 293 K. Black lines connect the experimental data, while magenta lines show the fitted model function and blue lines the individual isotopologue/isotopomer signals.





Note that in all structures shown above charges have been omitted in the interest of clarity; the charge on all isotopologues/isotopomers is 2- as given in the formula in the caption to Figure S1.